Itedale Namro Redwan

Design and the Synthesis of Potential Aminoacyl-tRNA Synthetase Inhibitors

Faculty of Science

ISBN 978-91-628-8445-1
Printed by Ineko

2012

Design and the Synthesis of Potential Aminoacyl-tRNA Synthetase Inhibitors

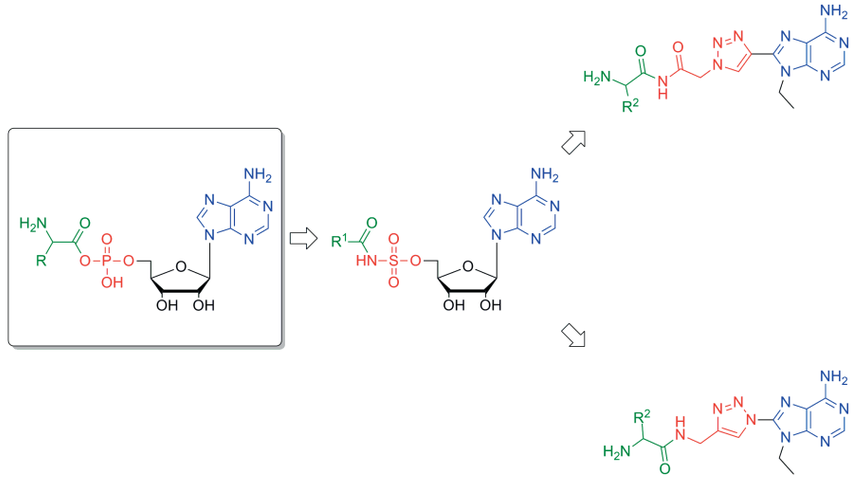

Itedale Namro Redwan

Ph.D. thesis
Department of Chemistry and Molecular Biology
University of Gothenburg

UNIVERSITY OF GOTHENBURG

Design and Synthesis of Potential Aminoacyl-tRNA Synthetase Inhibitors

ITEDALE NAMRO REDWAN

UNIVERSITY OF GOTHENBURG

Department of Chemistry and Molecular Biology
University of Gothenburg
2012

DOCTORAL THESIS

Submitted for fulfilment of the requirements for the degree of
Doctor of Philosophy in Chemistry

Design and Synthesis of Potential Aminoacyl-tRNA Synthetase Inhibitors

ITEDALE NAMRO REDWAN

Cover illustration: From left to right, the general structure for the aminoacyl-AMPs (in box), the general structure for the sulfamoyl-based analogues of the aminoacyl-AMPs and the designed ribose-free purine-based aminoacyl-AMP analogues (Chapter 7.2, Paper III).

ISBN: 978-91-628-8445-1
http://hdl.handle.net/2077/28794

Department of Chemistry and Molecular Biology
SE-412 96 Göteborg
Sweden

Printed by Ineko AB
Kållered, 2012

To My Family

Abstract

Aminoacyl-tRNA synthetases (aaRSs) are essential enzymes present in all living organisms, their catalytic activity is involved in the translation of the genetic code into functional proteins and they are potential targets for anti-infective agents. The first step in the biosynthetic pathway catalysed by aaRSs consists of activation of the corresponding amino acid by the reaction with ATP to form an aminoacyl-adenylate (aa-AMP), the key intermediate in the biosynthesis of proteins. As a result stable, analogues of aa-AMP have been identified as potential and valuable lead compounds for the development of potential aaRS inhibitors.

This thesis describes the design and synthesis of potential aaRSs inhibitors. The studies involve the development of a novel solution-phase synthetic route to non-hydrolysable sulfamoyl-based aa-AMP analogues. Synthesis includes the development of a protective group strategy that utilises global deprotection under neutral conditions to minimise by-product formation. Optimal reaction conditions for the coupling of different amino acids to the sulfamoyl moiety have also been investigated.

A solid-phase synthetic route leading to non-hydrolysable sulfamoyl-based aa-AMP analogues has also been developed. The novel synthetic route enables the possibility for rapid parallel synthesis of structurally diverse compounds in quantities sufficient for biological evaluation.

Molecular modelling techniques have been used to gain understanding about the structure–activity relationship of the inhibitors of aaRSs based on non-hydrolysable aa-AMP analogues. A model ligand adopting the putative bioactive conformation was identified based on X-ray data and conformational searches. Novel phosphate bioisosteres of aa-AMP have been designed using the derived model.

Molecular docking techniques were used for the design of ribose-free purine-based aa-AMP bioisosteres. The designed compounds were synthesised and evaluated biologically in an assay using aaRS isolated from *Escherichia coli.*

A novel mild method for the activation and recycling of a tritylated solid-phase resin has also been developed. Recycling of recovered resin after the completion of a reaction is considered beneficial since it minimises the associated costs and is environmentally friendly. The method was used for the attachment of primary and secondary alcohols, halogen-containing alcohols and anilines to trityl resin.

Keywords: Aminoacyl-tRNA Synthetases, Aminoacyl-AMP, Bioisosteres, Amino Acids, Solution-Phase Chemistry, Protective Groups, Solid-Phase Chemistry, Molecular Modelling, Biological Evaluation

List of Publications

This thesis is based on the following publications, which are referred to in the text by the Roman numerals **I-IV**.

I: **Investigation, Optimisation and Synthesis of Sulfamoyloxy-linked Aminoacyl-AMP Analogues.** Itedale Namro Redwan, Thomas Ljungdahl and Morten Grøtli. *Tetrahedron*, **2012**, *68*, 1507-1514.

II: **Development of a Solid-Phase Method for the Synthesis of 5′-*O*-[*N*-(Acyl)sulfamoyl]Adenosine Derivatives.** Itedale Namro Redwan, Hanna Jacobson Ingemyr, Thomas Ljungdahl, Christopher P. Lawson and Morten Grøtli. Submitted.

III: **Design, Synthesis and Biological Evaluation of Ribose-Free Isosteres of Aminoacyl-AMP.** Itedale Namro Redwan, David Bliman, Andrés Palencia Carrilero, Stephen Cusack and Morten Grøtli. Manuscript.

IV: **A Mild and Efficient Method for Activation and Recycling of Trityl Resin.** Itedale Namro Redwan and Morten Grøtli.
Submitted.

Paper **I** is reprinted with kind permission from the publisher.

The Authors' Contribution to Papers I-IV

I: Contributed to the formulation of the research problem, performed all experimental work, interpreted the results, and wrote the manuscript.

II: Contributed to the formulation of the research problem, performed or supervised all experimental work, interpreted the results, and wrote the manuscript.

III: Contributed to the formulation of the research problem, the experimental work, interpretation of the results and writing of the manuscript.

IV: Contributed to the formulation of the research problem, performed all experimental work, interpreted the results, and wrote the manuscript.

List of Abbreviations

Aa-AMP	Aminoacyl-adenosine-5′-monophosphate
AaRS	Aminoacyl-tRNA synthetase
Ac	Acetyl
ADP	Adenosine-5′-diphosphate
ADME	Absorption, Distribution, Metabolism and Excretion
AMP	Adenosine-5′-monophosphate
Ar	Aryl
ATP	Adenosine-5′-triphosphate
aq	Aqueous
BEMP	2-*tert*-Butylimino-2-diethylamino-1,3-dimethylperhydro-1,2,3-diazaphosphorine
Boc	*tert*-Butyloxycarbonyl
Bn	Benzyl
Bu	Butyl
t-Bu	*tert*-Butyl
Bz	Benzoyl
Cbz	Benzyloxycarbonyl
CDI	Carbonyldiimidazole
Dab	Diaminobutyric- acid
DBU	1,8-Diazabicyclo[5.4.0]undec-7-ene
DCC	*N*,*N*′-Dicyclohexylcarbodiimide
DCE	1,2-Dichloroethane
DCM	Dichloromethane
DCU	*N*,*N*′-Dicyclohexylurea
DEAD	Diethyl azodicarboxylate
DIC	*N*,*N*′-Diisopropylcarbodiimide
DIPEA	Diisopropylethylamine
DMAP	4-Dimethylaminopyridine
DMF	Dimethylformamide
DMSO	Dimethylsulfoxide
DNA	Deoxyribonucleic acid
DVB	Divinylbenzene
EDC	3-(Ethyliminomethyleneamino)-*N*,*N*′-dimethyl-propan-1-amine
Et	Ethyl
equiv	Equivalent(s)
Fmoc	9-Fluorenylmethoxycarbonyl
GPCR	G-protein coupled receptor
h	Hours

HATU	*O*-(7-Azabenzotriazole-1-yl) 1,1,3,3-tetramethyluronium hexafluorophosphate
HBTU	*O*-(Benzotriazole-1-yl) 1,1,3,3-tetramethyluronium hexafluorophosphate
HOAt	1-Hydroxy-7-azabenzotriazole
HOBt	1-Hydroxy-1-*H*-benzotriazole
HPLC	High performance liquid chromatography
HRMS	High resolution mass spectrometry
Hse	Homoserine
IBI	Intermediate-based inhibitor
IIDQ	*N*-Isobutoxycarbonyl-2-isobutoxy-1,2-dihydroquinoline
IR	Infrared
ITC	Isothermal titration calorimetry
ISTD	Internal standard
LC/MS	Liquid chromatography/mass spectrometry
LeuRS	Leucyl-tRNA synthetase
Me	Methyl
MW	Microwave(s)
NMR	Nuclear magnetic resonance
Np	4-Nitrophenyl
on	Overnight
OPLS	Optimised potentials for liquid simulations
Orn	Ornithine
PDB ID	Protein data bank identity
PEG	Poly(ethylene glycol)
Pfp	Pentafluorophenyl
Pg	Protecting group
Ph	Phenyl
POEPOP	Polyoxyethylene-polyoxypropylene
ppm	Parts per million
i-Pr	Isopropyl
PS	Polystyrene
PyAOP	[(7-Azabenzotriazol-1-yl)oxy]tripyrrolidinophosphonium hexafluorophosphate
PyBOP	[(Benzotriazol-1-yl)oxy]tripyrrolidinophosphonium hexafluorophosphate
PyBrOP	Bromotripyrrolidino phosphonium hexafluorophosphate
RNA	Ribonucleic acid
tRNA	Transfer ribonucleic acid
rt	Room temperature
SAR	Structure–activity relationship
soln	Solution
SPOCC	Superpermeable organic combinatorial chemistry resin

SPOS	Solid-phase organic synthesis
SSR	Solid supported reagents
Su	Succinimide
t	Time
TATU	*O*-(7-Azabenzotriazole-1-yl) 1,1,3,3-tetramethyluronium tetrafluoroborate
TBAF	Tetrabutylammonium fluoride
TBDMS	*tert*-Butyldimethylsilyl
TBTU	*O*-(Benzotriazole-1-yl) 1,1,3,3-tetramethyluronium tetrafluoroborate
TEOTFB	Triethyloxonium tetrafluoroborate
TFA	Trifluoroacetic acid
THF	Tetrahydrofuran
TIPS	Triisopropylsilyl
TLC	Thin layer chromatography
TMOF	Trimethylortoformate
TMS	Trimethylsilyl
Tol	Toluene
Tr	Trityl = triphenylmethyl
TsOH	*p*-Toluenesulfonic acid
UV	Ultraviolet
wt	Weight

Table of Contents

1

General Introduction

Since ancient times, humans have used medicines such as herbs and natural substances to treat illnesses. The use of more sophisticated medicines was initiated by the discovery of the antibiotic penicillin in 1928 by Alexander Fleming. In modern times, scientists have tried to improve upon what nature already started by developing pure and novel synthetic therapeutic agents using drug discovery. What is drug discovery? Drug discovery is the discovery of a substance that can be used for recovery from disease or relief of symptoms or to modify natural processes in the body. The role for the medicinal chemist in drug discovery involves the synthesis of and/or selection of suitable compounds for biological evaluation. If the compounds are found to be active, they could serve as so called lead compounds. A lead compound is a chemical structure that shows activity and selectivity towards a specific pharmacological or biological target. The derived lead compound is then used to gain understanding of the structure–activity relationships (SARs) of structurally similar compounds considering their *in vivo* and *in vitro* activity and safety.

Medicinal chemists involved in drug discovery are typically part of a team of people with different expertise. Consequently the understanding of other disciplines is necessary for the possibility to contribution to avoid problems related to absorption, distribution, metabolism and excretion (ADME) properties, evaluate results and move the project forward. Drug discovery programs include identification and validation of specific targets such as G-protein coupled receptors (GPCRs), ligand-gated ion channels or enzymes. One example of a group of enzymes identified as important drug targets is the aminoacyl-tRNA synthetases (aaRSs).

Enzymes are biological catalysts. By interacting with substrates they catalyse chemical reactions involved in the biosynthesis of many important cellular products. The aaRSs constitute an especially important group of enzymes due to their role in protein synthesis. In the mid-1950s, Francis Crick described in his “Adaptor Hypothesis” the necessity of these “activating enzymes” to provide a connection between the nucleic acids and the amino acid sequence of proteins.[1] AaRSs have a central role in the most exciting fields of biology and chemistry in addition to being identified as important targets for the development of potential drugs for human diseases.

2

Aims of the Thesis

The overall aim of the work presented in this thesis was to design and synthesise potential aaRS inhibitors. The aminoacyl-AMP (aa-AMP) is the key intermediate in the translation of the genetic code; thus, stable aa-AMP analogues have been identified as potential and valuable lead compounds for the development of aaRS inhibitors.
The specific objectives of the thesis were:

- To develop a solution-phase synthetic strategy for the preparation of sulfamoyl-based aa-AMP analogues. Such compounds have up to now been difficult or even impossible to prepare using current synthetic strategies.

- To develop a solid-phase based synthetic route leading to non-hydrolysable sulfamoyl-based aa-AMP analogues. A solid-phase synthetic route would allow parallel synthesis of structurally different compounds such as sulfamoyl-based aa-AMP analogues in quantities sufficient for biological screening.

- To use computational tools for the evaluation of the usefulness of various phosphate bioisosteres in the design of non-hydrolysable aa-AMP analogues.

- To design, synthesise and evaluate novel ribose-free purine-based mimetics of aa-AMP as potential aaRS inhibitors.

3

Background

3.1 Aminoacyl-tRNA Synthetases

Aminoacyl-tRNA synthetases (aaRSs) are essential enzymes present in all living organisms and their catalytic activity is involved in the translation of the genetic code into functional proteins.[2-6] These enzymes catalyse a two-step process involving the attachment of a specific amino acid to the corresponding (cognate) tRNA resulting in the formation of aminoacyl-tRNAs. AaRSs are also known to associate in higher order complexes with proteins involved in processes other than translation such as splicing, apoptosis, viral assembly and regulation of transcription and translation (**Figure 1**).[7,8]

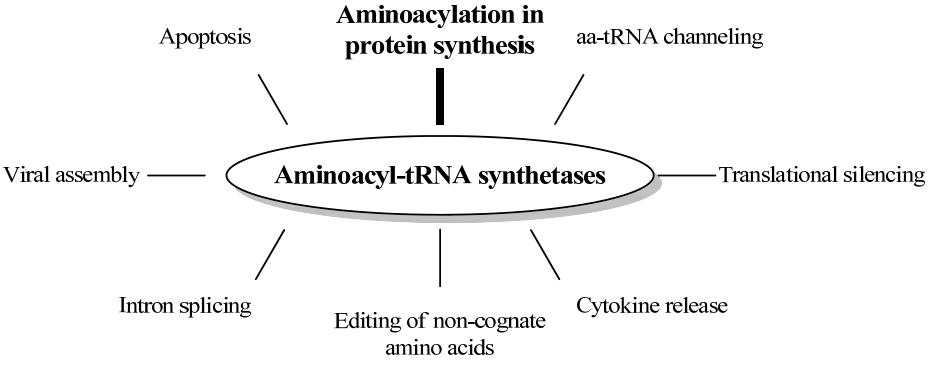

Figure 1. Representation of the function of aaRSs in several different cellular tasks beyond translation.

There are 20 different aaRSs, one for each endogenous amino acid (see **Appendix A**). The first step catalysed by all aaRSs consists of activation of their corresponding amino acid to form an aminoacyl-adenylate (aa-AMP, **1**) by the reaction with ATP (**Scheme 1**). In the second step the activated amino acid migrates to the 2′ end (**2**) or 3′ end (**3**) of the adenosine of the cognate tRNA to form the aminoacyl-tRNA which later directs the placement of the amino acid within a growing polypeptide chain.

The aaRSs are divided into two classes based on structural and mechanistic features. For class I enzymes, the aminoacyl group of aa-AMP (**1**) is transferred initially to the 2′-OH of the terminal adenylate in tRNA and is then moved to the 3′-OH by a transesterification, while for class II, the aminoacyl group is transferred directly to the 3′-OH.[9,10]

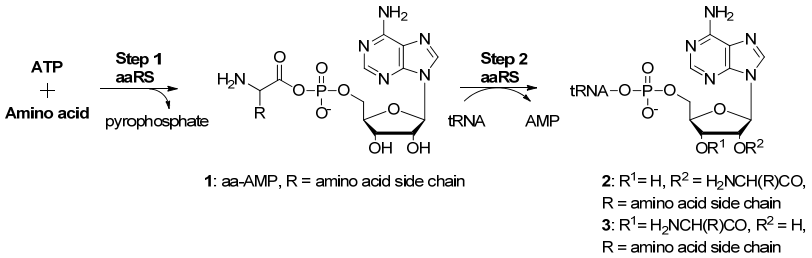

Scheme 1. AaRS catalyses the ATP-dependent esterification of tRNA with the cognate amino acids. The aa-AMP (**1**) is the key intermediate for the synthesis and is used as a lead compound for the development of intermediate-based inhibitors of aaRSs.

To ensure formation of the correct aminoacyl-tRNA and thereby enhance translation reliability, several aaRSs have an editing (proofreading) capability, the ability of the aaRSs to correct or prevent incorrect aminoacylations of tRNA.[11-14]

3.1.1 Aminoacyl-tRNA Synthetases as Drug Targets

AaRSs have been linked to several different human diseases (**Figure 2**).[6,8,15,16] Multiprotein complexes in which aaRSs are included have been implicated in the cause of cancer,[16,17] neuronal diseases,[18,19] diabetes,[20,21] and autoimmune diseases[22]. Mutations in the genes for aaRSs have also been associated with neuronal diseases and diabetes. Furthermore, cancer can also be related to abnormal aaRSs regulation. Autoantibodies against different aaRSs (also referred to as anti-tRNA synthetase antibodies) have been found in approximately 30% of all autoimmune patients.[6] A defect in the amino acid editing mechanism that can be catalysed by some aaRSs can be a potential cause of neuronal diseases.[6]

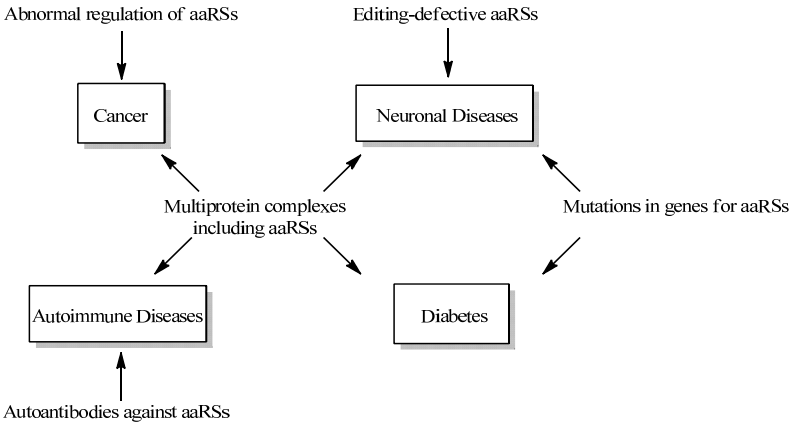

Figure 2. Map showing the linkage between aaRSs to various human diseases.

The pivotal role of aaRSs in protein synthesis has also made these enzymes interesting anti-infective drug targets.[15,23-26] Lymphatic filariasis is a prime example of a neglected parasitic tropical disease caused by *Wuchereria bancrofti*, *Brugia malayi* and *Brugia timori*.[27-29] It is a complex human nematode disease that affects more than 120 million persons worldwide for which the aaRSs have been validated as drug targets.[30] Moreover, an increased understanding of the editing mechanism for aaRSs has also contributed to the development of anti-infectives.[14] The key to their usefulness is finding compounds that distinguish between human and pathogen synthetases. Despite common features regarding the catalytic chemistry (**Scheme 1**), these enzymes display wide evolutionary divergence between prokaryotic and eukaryotic enzymes which should make it possible to develop selective drugs. Thus, analogues based on the structures of the substrates and intermediates of the aminoacylation reactions catalysed by these enzymes could potentially make valuable "leads" for the development of anti-infectives (**Scheme 1**).[15,23-26] Synthetically derived intermediate-based aaRSs inhibitors are discussed in below.

3.1.2 Natural Products as Inhibitors of Aminoacyl-tRNA Synthetases

Several different aaRS inhibitors have been isolated from natural sources (**Figure 3**). Most aaRS inhibitors act by competitive binding to the active site where the cognate amino acid normally would bind. Pseudomonic acid (**4**, inhibits isoleucyl-tRNA synthetases), also known as mupirocin, shows 8000-fold selectivity for pathogen synthetases over its mammalian counterpart in bacterial infections (such as *Staphylococcus aureus* and *Haemophilus influenzae*).[23,25,26,31]

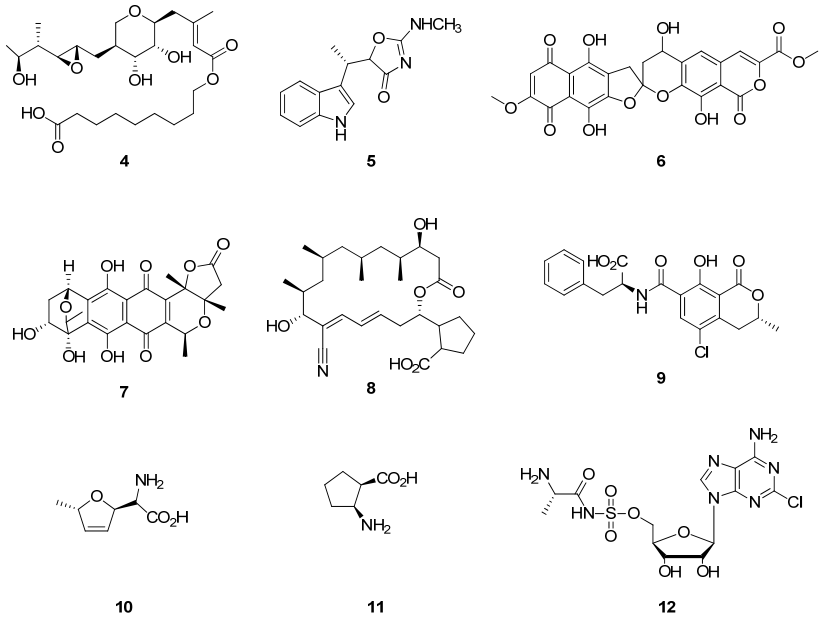

Figure 3. Structures of natural products acting as aaRS inhibitors.

The structure of **4** reveals the presence of a hydrolysable ester and an epoxide moiety that interacts with functional groups in the enzyme, resulting in the desired inhibition (**Figure 3**).[32] Due to the instability *in vivo*, the use of **4** has been limited to topical infections and is commercially available under the name Bactroban™. Other examples of isolated natural products as aaRS inhibitors are indolmycin (**5**, inhibits tryptophanyl-tRNA synthetases),[33] purpuromycin (**6**, inhibits all tRNA synthetases),[34] granaticin (**7**, inhibits leucinyl-tRNA synthetases),[35] borrelidin (**8**, inhibits threonyl-tRNA synthetases),[36] ochratoxin A (**9**, inhibits phenylalanyl-tRNA synthetases),[37] furanomycin (**10**, inhibits isoleucyl-tRNA synthetases),[38,39] cispentacin (**11**, inhibits prolyl-tRNA synthetases)[40] and ascamycin (**12**, inhibits phenylalanyl-tRNA synthetases).[25,41,42] The natural products illustrated in **Figure 3** show that molecules having diverse structural features are able to inhibit aaRSs. Unfortunately, several of these compounds have poor selectivity for pathogen synthetases and/or low potency.[23,25,26,31]

3.1.3 Miscellaneous Inhibitors of Aminoacyl-tRNA Synthetases

Miscellaneous inhibitors of aaRSs, not related to IBIs, such as compounds **13**–**16** (**Figure 4**) have been described in the literature.[26,43]

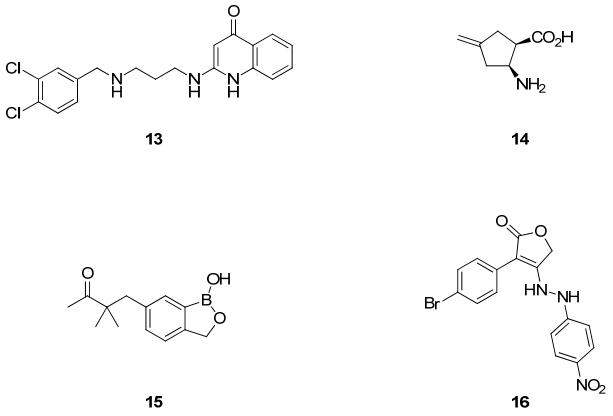

Figure 4. Structures for novel synthetically derived aaRSs inhibitors.

A high throughput screening (HTS) campaign to search for competitive inhibitors of methionyl-tRNA synthetase (*Staphylococcus aureus*) led to the identification of quinolone derivatives such as **13**.[43] Like in the case of the natural product inhibitors, compound **14** has no structural relationship with the IBIs. It is derived via modification of the natural product inhibitor cispentacin (**11**) and has also been found to be a potent aaRS inhibitor. The benzoxaborole derivative **15** has been used to investigate the inhibition of leucinyl-tRNA synthetases in the development of antitrypanosomal (sleeping sickness) drugs by trapping tRNA in the editing site.[14,44] Compound **16** has shown activity towards tyrosinyl-tRNA synthetases.[25,45]

3.1.4 Reaction Intermediate-Based Inhibitors of Aminoacyl-tRNA Synthetases

Modifications of the aminoacyl-adenylate **1** (**Scheme 1**) have been extensively investigated for the purpose of improving chemical stability, tight binding and pathogen selectivity.[46] Many of the modifications were made in the linker region since the mixed anhydride acylphosphate bond of the intermediate is readily susceptible to hydrolysis. Such intermediate based inhibitors (IBIs) are typically analogues of **1**, in which the hydrolysable phosphoanhydride linkage has been replaced with non-hydrolysable groups (**Figure 5**).[15,23,25,26,31,47,48]

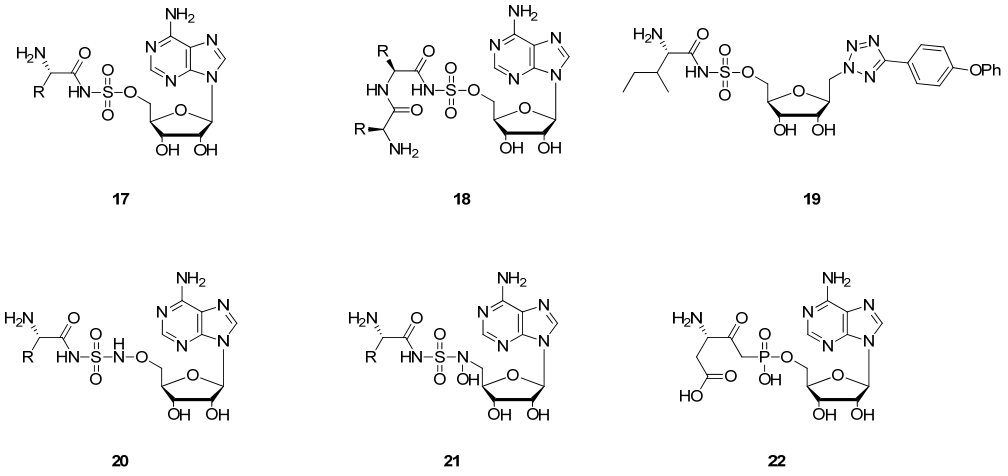

Figure 5. Structures of reaction intermediate-based aaRS inhibitors. In structures **17**, **18**, **20** and **21**, R can be any amino acid side chain.

3.2 Phosphate Isosteres

The phosphate group plays an important role in many biological processes, such as the ATP-dependent esterification of tRNA by the cognate amino acids (**Scheme 1**).[9,10] In the search for compounds intended to mimic the phosphate-binding interactions to a specific target, it is appropriate to include a phosphate group in the potential inhibitor. Utilisation of the phosphate moiety as part of an inhibitor is severely limited by the enzymatic liability and poor cellular bioavailability of this highly charged recognition element (**Figure 6**). Many phosphate mimetics, such as methylenephosphonates (e.g. **23** and **33**), retain the tetrahedral phosphorus atom. Others exclude the tetrahedral phosphate group and use instead groups based on the combination of one or more carboxylate groups (e.g. **28**) or isosteres of carboxylates (e.g. **24–27**, and **29**) that generally reduce the overall molecular charge. Some examples of phosphate isosteres are shown in **Figure 6**.[25,49-52] Fragments **23**–**28** are examples of phosphate isosteres mimicking phosphotyrosine.[51] The squaric monoamide moiety **29** was evaluated as a phosphate isostere in nucleotides.[51] Furthermore, the boranophosphate **30** has been used as a phosphate mimetic in oligonucleotides.[49] As discussed in section *3.1.4*, the most potent IBIs of aaRSs are typically analogues of **1**, in which the hydrolysable phosphoanhydride group has been replaced with non-hydrolysable groups such as in structures **17** and **31–33**.[24,47,53,54]

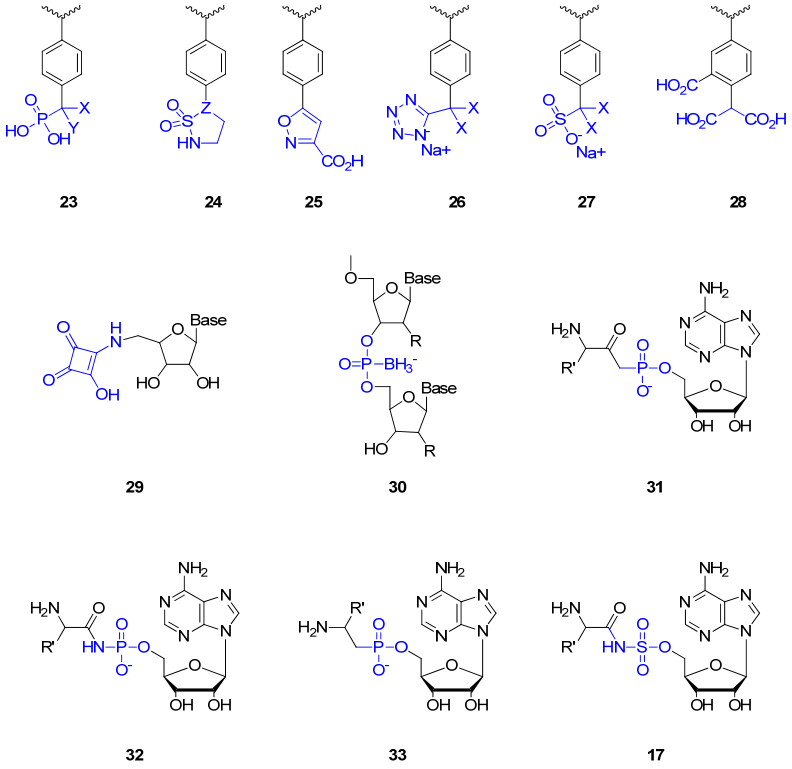

Figure 6. Examples of phosphate isosteres (blue) found in the literature. For compound **23**, X = F and Y = F or H; compound **24**, Z = C or N; compounds **26** and **27**, X = F or H; compound **30**, R = H or OH, **31**, **32**, **33** and **17**, R′= any amino acid side chain.

3.3 Protective Groups in Organic Synthesis

In organic synthesis, synthetic targets are often structurally complex molecules. Thus, obtaining such targets may involve several reaction steps, and each transformation has to occur selectively at the desired reaction site in multifunctional compounds. The presence of different functional groups may require careful planning of each step, and the use of protective groups often becomes essential. A protective group is placed on the desired functionality to prevent it from reacting and is then removed after the desired chemical transformation. The protective group itself has to fulfil several requirements such as: i) being able to react selectively in good yield to give the protected substrate; ii) it has to withstand the planned reaction conditions; iii) it has to be removed in good yield without interfering with other functional groups present in the molecule; and iv) the protective group should not introduce any additional reaction sites.[55,56]

3.3.1 Hydroxyl Protective Groups

Hydroxyl groups are common functional groups that are found in many different biological and synthetically interesting compounds such as nucleosides, carbohydrates and steroids.[55] Since the hydroxyl group is incompatible with several different reaction conditions such as oxidation, acylation and halogenation, protection is necessary. The protection of hydroxyl groups as alkyl or silyl ethers are most common in organic synthesis (**Figure 7**). The alkyl ethers are generally introduced under basic conditions and require catalytic hydrogenation or sodium in ammonia for the removal. Silyl ethers are also usually introduced under basic conditions and typically removed using a fluoride source such as tetrabutylammonium fluoride (TBAF). The silyl protective groups are generally more stable the more sterically hindered they are. Benzoates and acetates are the most common ester derivatives. The protected ester derivatives are generally formed by acylation using acid chlorides and anhydrides and are hydrolysed using a base such as sodium hydroxide. The benzoate ester can also be removed using catalytic hydrogenation.[55,56]

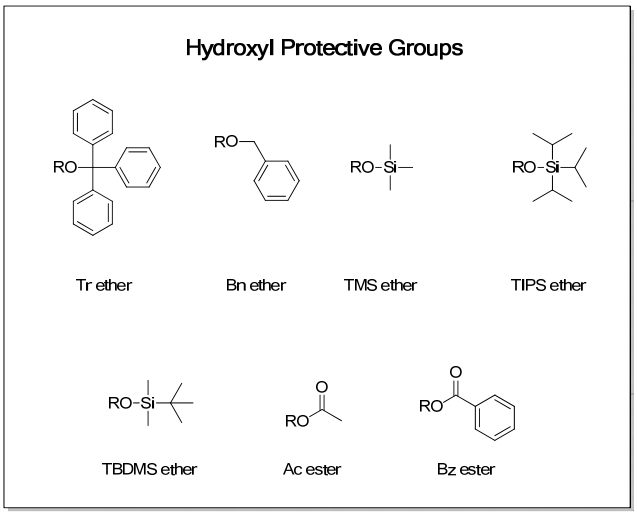

Figure 7. Examples of hydroxyl protective groups.

3.3.2 1,2-Diol Protective Groups

1,2-Diols are common functionalities in nucleosides and carbohydrates that can be masked as acetals under acidic conditions and deprotected by acid hydrolysis (**Figure 8**). The benzylidene acetal can also be removed by hydrogenolysis.[55,56]

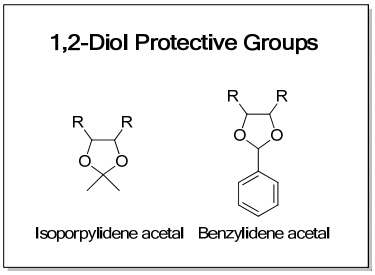

Figure 8. Examples of 1,2-diol protective groups.

3.3.3 Amine Protective Groups

Amines are found in many biologically important compounds such as peptides and proteins. The benzyloxycarbonyl group (Cbz) was the first modern amine protective group developed by Bergmann and Zervas.[57] Primary and secondary amines need to be protected due to their nucleophilic properties which can cause undesired side-reactions. **Figure 9** illustrates examples of the most commonly used amine protective groups. Carbamates are common protective groups and the protection is generally introduced by acylation using carbamoyl chlorides or anhydrides. The Cbz carbamate can be removed by hydrogenation or acidic conditions using e.g. AcOH or HBr. Boc carbamates are generally removed under acidic conditions (e.g. using TFA). Fmoc carbamates represent one of few examples of protective groups which can be removed using mild bases such as piperidine (20%). Benzyl groups can be removed from amines by catalytic hydrogenation. Furthermore, the trityl group (**Figure 7**) can also be used as an amine protective group and is typically introduced under basic conditions and removed under acidic conditions (e.g. using TFA) or by catalytic hydrogenation.[55,56]

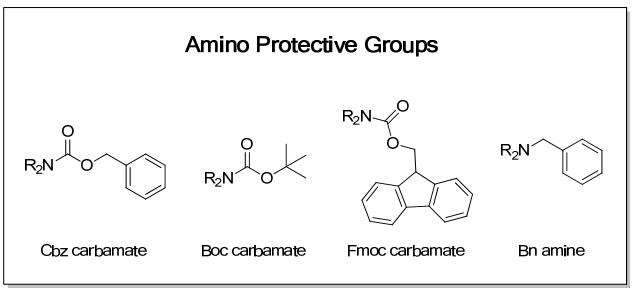

Figure 9. Examples of amino protective groups.

3.4 Amino Acid Coupling Reagents

Amide bonds are found in many biologically important compounds such as peptides and proteins.[58,59] The formation of an amide bond is an essential reaction in organic synthesis and results from bond reaction between a carboxylic acid and an amine. For the reaction to be efficient the carboxylic acid needs to be activated towards a nucleophilic attack by the amine (**Scheme 2**).[60-62]

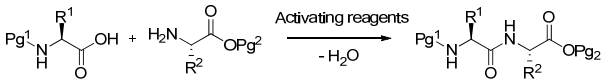

Scheme 2. General example of the amide bond formation. R^1 and R^2 = any amino acid side chains. Pg^1 and Pg^2 = protective groups.

Activation of the carboxylic acid can be accomplished by formation of the corresponding acyl halide, symmetric anhydrides, mixed anhydrides or a good leaving group such as a reactive ester. The acyl halide method is especially useful for sterically hindered substrates but is rarely used because of the potential unwanted side-reactions including racemisation.[60,61,63] Several activated esters are commercially available e.g. pentafluorophenyl esters (Pfp) and succinate esters (Su). The activated ester is obtained by reacting the carboxylic acid with e.g. pentafluorophenol prior to amine treatment. This activation can also be performed in one pot by addition of the coupling reagent such as ammonium or phosphonium salts to a mixture of the carboxylic acid and the amine.[60] A relevant problem due the activation of carboxylic acids using coupling reagents is the occurrence of racemisation and other side-reactions such as diketopiperazine formation.[64] Racemisation can occur via elimination of the α-proton, through a reversible β-elimination and/or via an oxazolone intermediate.[65] The most important mechanism is racemisation through the 5(*4H*)-oxazolone intermediate (**Scheme 3**).[60,66]

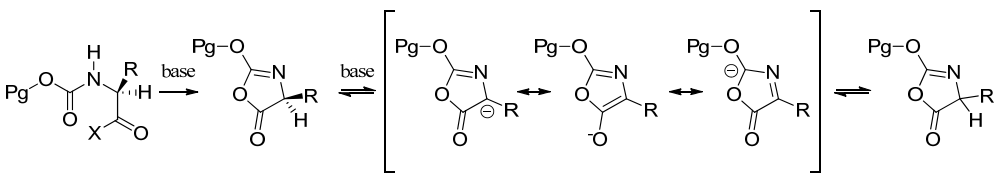

Scheme 3. Illustration of the possible mechanism for racemisation via an oxazolone intermediate. Pg = protective group e.g. *t*Bu, R = amino acid side chain and X = activating group (e.g. active ester).

The choice of coupling reagent, additive, base and protective groups is of great importance since it makes it possible to suppress the undesired racemisation. A few examples of common coupling reagents are shown in **Figure 10**.[61,64,65]

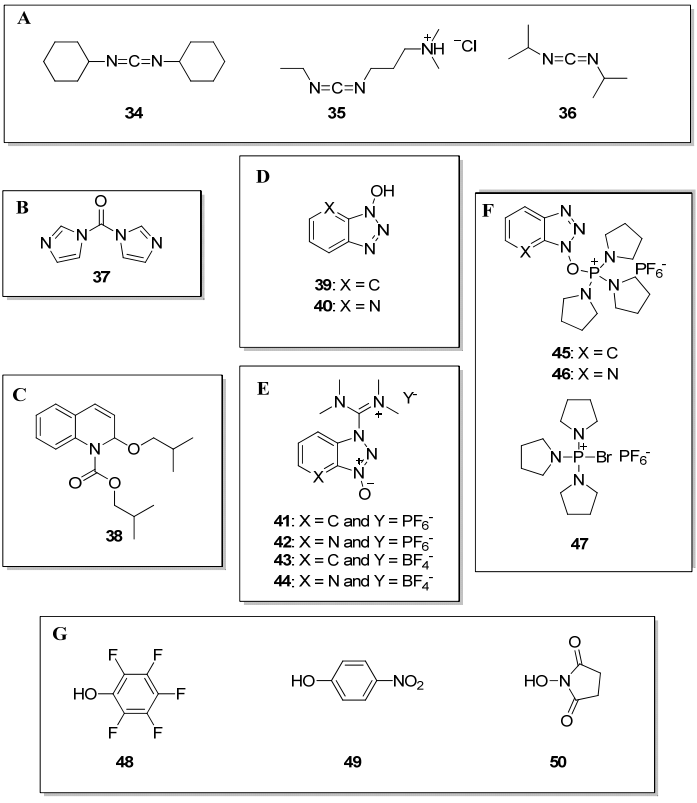

Figure 10. Groups **A** to **G** constitute examples of a small selection of available coupling reagents. Group **A**: carbodiimides DCC (**34**), EDC·HCl (**35**) and DIC (**36**). Group **B**: the imidazolium reagent CDI (**37**). Group **C**: coupling reagent based on mixed anhydride formation, IIDQ (**38**). Group **D**: coupling reagents often used as additives HOBt (**39**) and HOAt (**40**). Group **E**: aminium reagents HBTU (**41**), HATU (**42**), TBTU (**43**) and TATU (**44**). Group **F**: phosphonium reagents PyBOP (**45**), PyAOP (**46**) and PyBrOP (**47**). Group **G**: alcohols/phenols used in amide coupling 2,3,4,5,6-pentafluorophenol (**48**), which gives Pfp-esters, 4-nitrophenol (**49**), which gives Np-esters and *N*-hydroxysuccinimide (**50**), which gives Su-esters.

3.4.1 Carbodiimide Coupling Reagents

Group A in **Figure 10** contains examples of the carbodiimide class of coupling reagents. These were the first coupling reagents to be described and *N*,*N*′-dicyclohexylcarbodiimide (DCC, **34**) was reported by Sheehan already in 1955.[61,64,67] The carbodiimides have been extensively used in peptide bond formation due their moderate reactivity and low price. Typical activation procedure involves pre-mixing of the carboxylic acid and DCC, resulting in *O*-acylisourea formation as the reactive acylating reagent, which then reacts with the amine to form the desired amide bond. Insoluble *N*,*N*′-dicyclohexylurea (DCU) is formed as a by-product and can be filtered off after completion of the reaction.[61,64,67]

3.4.2 Acylimidazoles in Coupling Reactions

Group B contains one example of the imidazolium reagents. Carbonyldiimidazole (CDI, **37**) has been used in large-scale synthesis since it is relatively cheap and its only by-products are carbon dioxide and imidazole.[68] CDI is also useful for one-pot amide formation.[60]

3.4.3 Mixed Anhydrides in Coupling Reactions

The example in group C is *N*-isobutoxycarbonyl-2-isobutoxy-1,2-dihydroquinoline (IIDQ, **38**), a reagent that activates the carboxylic acid by formation of a mixed anhydride. The anhydride is formed very slowly but is rapidly consumed in the aminoacylation process. Thus, the possibility for racemisation is minimised.[61]

3.4.4 Benzotriazole and Azabenzotriazole Coupling Reagents

Many coupling reagents are based on 1-hydroxy-1-*H*-benzotriazole (HOBt, **39**) and 1-hydroxy-7-azabenzotriazole (HOAt, **40**) which are represented in group D (**Figure 10**). These coupling reagents result in activated esters which react with amines under mild conditions. HOBt has been used as an additive to suppress racemisation.[69-72] Examples of coupling reagents based on HOBt and HOAt are the aminium salts and phosphonium salts which are included in groups E and F.

3.4.5 Aminium and Phosphonium Coupling Reagents

The aminium (also referred to as uranium) coupling reagents in groups E and the phosphonium reagents in group F are generally used in one-pot couplings. Common features for these groups are that they provide high reaction rates and usually undergo minimal racemisation. They have also proven to be efficient in sterically demanding aminoacylations.[60,66,73]

3.4.6 Alcohols as Coupling Reagents

The coupling reagents presented in group G represent examples of alcohols used for the formation of activated esters. The active esters can be prepared, isolated and stored over time. Active ester formation results in an increased electrophilicity of the carbonyl centre which facilitates the reaction with amines under mild conditions.[60]

3.5 Solid-Phase Organic Synthesis

Solid-phase organic synthesis (SPOS) has become an important area of research since it was first developed by Merrifield in 1963.[74] Solid-phase synthesis was initially used for peptide synthesis but the methodology has become a useful tool also for the preparation of a large number of structurally diverse compounds.[75] The main advantages of the solid-phase methodology compared to solution-phase synthesis include:[76]

(i) *It is easy to perform reactions on solid-phase.* Only three steps are required, addition of reagents, filtering and washing.

(ii) *Excess reagents can be used to drive reactions to completion.* This is possible since excess reagents are easily washed off after the reaction.

(iii) *Purification after each synthetic transformation in a multi-step synthesis is not necessary.* Purification is only required after cleaving the final product from the solid-phase.

(iv) *The possibility of performing parallel synthesis.* Parallel synthesis of large libraries using solid-phase chemistry becomes practically simple and can be automated.

However, the choice of linker is essential when planning the synthetic route and affects the simplicity of starting material attachment and cleavage. Limitations of SPOS may include that two extra steps are required for starting material attachment to and cleavage from the linker. In addition, development of methodologies compatible with solid-phase synthesis is required since the conditions are generally different from those for solution-phase chemistry (e.g. longer reaction time for reactions performed on solid-phase, in addition the solubility of the reagents in the solvent used is important). Furthermore, the scale could potentially be limited due to the loading level of the solid support (thus expensive) and monitoring of the progress of the reactions using conventional techniques such as thin layer chromatography (TLC), nuclear magnetic resonance (NMR) spectroscopy or liquid chromatography/mass spectrometry (LC/MS) may be difficult.[77-79]

3.5.1 Solid Supports

The success of solid-phase chemistry is strongly dependent on the chemical composition and physical properties of the polymer matrix.[80,81] Although the development of a universal solid support that possesses features ideally suited for all applications is unlikely, many polymers have proven to be effective for specific uses.[76] The first resin used by Merrifield consisted of a chloromethylated nitrated copolymer of styrene and divinylbenzene (DVB).[74] Typical support currently consists of 1–2% DVB cross-linking and polystyrene (PS) (**Figure 11**).[76]

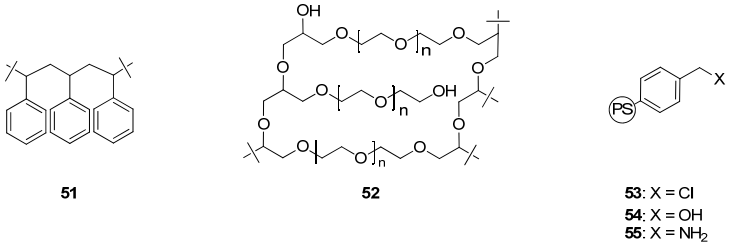

Figure 11. Structure of a polystyrene (PS) matrix (**51**), a poly(ethylene glycol) matrix (**52**) and examples of the three most commonly used PS-supports: chloromethylpolystyrene (X = Cl, **53**), hydroxymethylpolystyrene (X = OH, **54**) and aminomethylpolystyrene (X = NH_2, **55**).

However, the hydrophobicity of PS limits its use for some applications, thus prompting the evaluation of more hydrophilic supports. Several poly(ethylene glycol)-PS (PS-PEG) resins have been developed[82] which provides a combination of a hydrophobic PS core with hydrophilic PEG chains in the same support.[81] More hydrophilic PEG-based resins have also been developed, including the polyamine-containing (PEGA) resin[83] and totally PEG-based resin such as POEPOP[84], SPOCC[85] and ChemMatrix.[86] The amphiphilic nature of PEG ensures that the resin is well solvated in both polar and nonpolar solvents.

3.5.2 Linkers

Solid-phase synthesis is typically performed on linkers attached to the solid support. The linker can be considered as a spacer unit with two handles, one side of which is permanently attached to the solid support and the other side is available for substrate binding. The linker also provides the necessary space between the resin matrix and the chemical modification position.[76,87] There are two different approaches that can be used, either attachment of the substrate to the desired linker (pre-loading method) followed by coupling them both to the solid support. The second approach consists of attaching the desired substrate to the linker already being attached to the solid support (direct loading method).[76] Independent of whether one chooses the pre-loading method or the

direct loading method, the choice of linker is very important since it must be compatible with all the chemical modifications and enable the release of the final product under a defined set of conditions without causing product decomposition.[88] Some examples of linkers are shown in **Figure 12**.

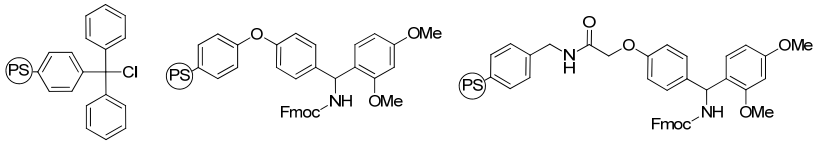

56 **57** **58**

Figure 12. Structures of some common linkers: trityl chloride linker (PS-Tr-Cl, **56**), rink amide linker (PS-Rink, **57**) and rink amide aminomethyl linker (PS-Rink AM, **58**).

The trityl chloride linker (PS-Tr-Cl, **56**) has been used for the attachment of substrates such as alcohols and amines.[89] After synthesis is complete, the product is typically cleaved from the linker using acidic conditions such as 1−50% TFA in DCM.[76] Fmoc-protected rink amide (**57**) and rink amide AM (**58**) are used for the attachment of substrates such as carboxylic acids after the removal of the Fmoc protective group. After synthesis is complete, the product is typically cleaved from the linker using acidic conditions such as 0.1−5% TFA in DCM.[76] Although linkers **57** and **58** are structurally very similar, linker **57** is more acid sensitive than resin **58**.

3.5.3 Polymer Supported Reagents

The use of reagents attached to a polymer support has become of great interest, especially in the field of organic synthesis.[78,90] Compared to what has been described in section *3.5.2*, this strategy relies on having the product in solution and the reagents attached to the polymer support. The advantages of using solid supported reagents (SSR) are: the reactions are often very clean; high yielding (since excess of reagents can be used); and the work up simple as only filtration of the reaction mixture is needed.[78] Resins for organic synthesis include polymer supported coupling reagents such as PS-DCC.[91]

4

Investigation, Optimisation and Synthesis of Sulfamoyloxy-Linked Aminoacyl-AMP Analogues (Paper I)

4.1 Solution-Phase Synthesis of Sulfamoyloxy-Linked Aminoacyl-AMP Analogues

The synthesis of aminoacyl-AMP (aa-AMP) analogues bearing non-hydrolysable phosphate isosteres is of great interest for the development of IBIs as potential anti-infectives (discussed in section *3.1.4*).[15,23-26] Such analogues are also of great value as chemical tools in the study of biological processes, e.g. elucidation of the editing mechanism for aaRSs.[13,92-96] The designs of most of the reported aa-AMP analogues have been based on stable isosteres such as alkyl phosphates, [53,97,98] esters,[99-101] amides,[99] hydroxamates,[99,100] sulfamates,[24,53,102-104] sulfamides, [97] *N*-alkoxysulfamides[48] and *N*-hydroxysulfamides.[48]

This chapter, concerns the development of a novel solution-phase synthetic route towards sulfamoyl-based aa-AMP analogues. These analogues have been difficult to prepare since previously reported methods have relied on the use of acid-labile protective groups. It was envisioned that the developed protocol should be general and applicable to various different amino acids, including those with heteroatoms in the amino acid side chain. The retrosynthetic route for the sulfamoyl-based analogues is outlined in **Scheme 4.**

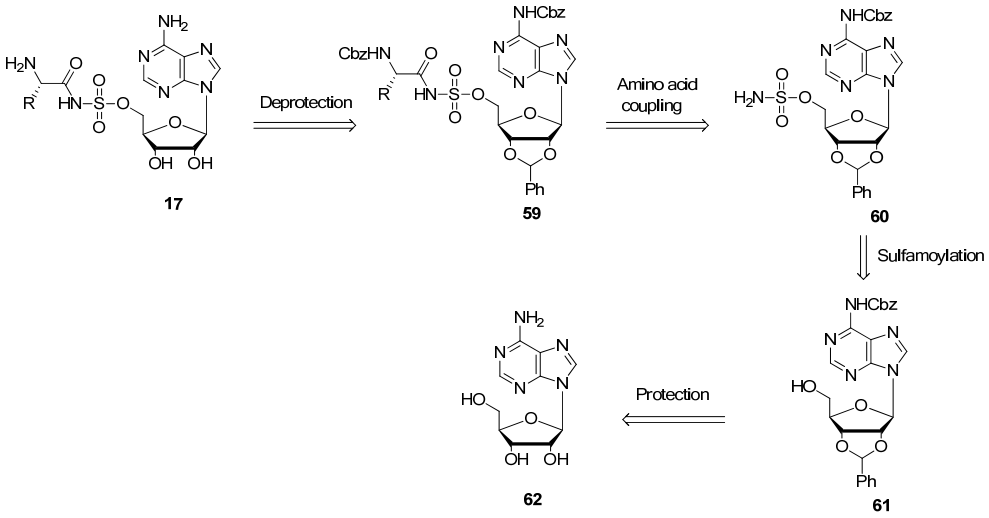

Scheme 4. A retrosynthetic plan for the preparation of sulfamoyl-based aa-AMP analogues. R = amino acid side chain.

4.2 Result and Discussion

4.2.1 Protection of Adenosine

Initial studies for the preparation of *N*-terminally modified sulfamoyl analogues of aaRS (Appendix B) were based on commercially available 2′,3′-*O*-isopropylideneadenosine in analogy with published procedures.[53,97,103,105-108] As discussed in section *3.3.2*, the isopropylidene protective group requires acidic conditions for its hydrolysis and typical conditions are 60–80% aq TFA. According to the literature the products can be obtained in low to good yields[46,97,106-109] which was in accordance with our results (Appendix B). The decreased could be explained by occurrence of side-reactions such as cyclonucleoside formation[109] acylsulfamate bond hydrolysis and/or intramolecular cyclisation[110] (**Scheme 5**).

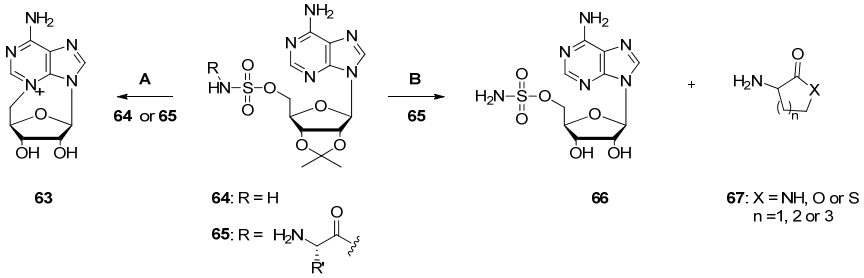

Scheme 5. Side-reactions in the synthesis of aa-AMP analogues contributing to decreased yields. Path **A** shows the assumed side-reaction which results in formation of cyclonucleoside **63**. Path **B** illustrates the possible intramolecular cyclisation reaction that leads to decomposition of the desired products. The side chain of the amino acid in compound **65** should include N, O or S and n should be 1, 2 or 3 for path **B** to be possible.

The side-reactions illustrated in **Scheme 5** are most likely promoted by basic or acidic conditions. Considering these aspects, a protective group strategy that minimises these side-reactions is necessary The new strategy therefore included: i) replacement of the 2′,3′-*O*-isopropylidene acetal with a 2′,3′-*O*-benzylidene acetal; ii) Cbz protection of the exocyclic amino function of the adenine moiety and of the amino function of the amino acids; and iii) a Cbz or benzyl (Bn) protective group of the hetero functionality in the amino acid side chain. The combination of the protective groups would allow global deprotection using catalytic hydrogenation under neutral conditions (**Scheme 6**).

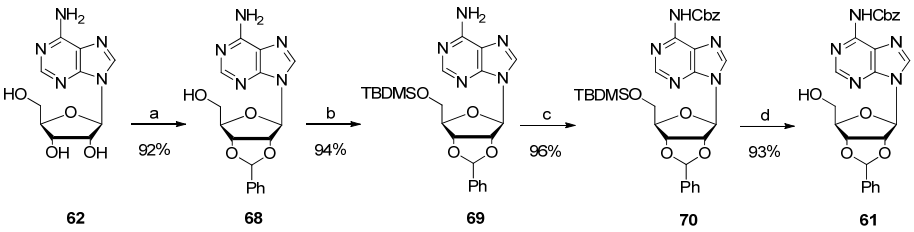

Scheme 6. Protection of adenosine (**62**). Reagents and conditions: a) $ZnCl_2$ (5 equiv), freshly distilled benzaldehyde, rt, N_2, 72 h. b) TBDMS-Cl (3 equiv), imidazole (7 equiv), pyridine, rt, N_2, 24 h then AcOH (80% aq). c) Rapoport's reagent (3.4 equiv), DCM, rt, N_2, 24 h. d) TBAF (4 equiv), THF, rt, N_2, 24 h.

The 5′-hydroxyl moiety of **62** was initially protected as a silyl ether using one equiv of TBDMS-Cl in pyridine and DMF (1:1). The desired 5′-*O*-TBDMS protected adenosine was isolated in a moderate 58% yield. The moderate yield could be due to low selectivity for the desired functional group in the presence of the unprotected secondary alcohols (2′- and 3′-hydroxyls) and the exocyclic amine of the adenine moiety. [111] In a second attempt, the 2′-and 3′-hydroxyls were protected prior to the formation of the 5′-silyl ether. Benzylidene acetal protection of **62** using benzaldehyde dimethyl acetal in the presence of a catalytic amount of TsOH[112] or $ZnCl_2$[113] as a Lewis acid was attempted at various temperatures, but only traces of the desired product **68** could be isolated. The protection was instead performed using freshly distilled benzaldehyde as the solvent and reagent in the presence of $ZnCl_2$ as catalyst. The desired 2′,3′-*O*-benzylideneadenosine (**68**) was isolated in 92% yield after column chromatography.

Compound **68** was then protected as a 5′-*O*-silyl ether using TBDMS-Cl and imidazole in pyridine. The N^6-silyl protected compound was also detected but it could be converted to the desired **69** by stirring the crude mixture in AcOH (80% aq) for 20 min at room temperature, **69** was isolated in 94% yield.[114] Protection of the exocyclic amino group of the adenine component is not required according to previously reported methods, but these compounds are rather polar which makes purification by column chromatography difficult.[105,106,108] Thus, the N^6-amino function of the adenine was therefore Cbz protected. The most common method for introduction of a Cbz group is the use of benzyl chloroformate in the presence of a base such as potassium carbonate. However, it was anticipated that the chloride is not a good enough leaving group for the weakly nucleophilic N^6-amino function. In addition, Cbz protection using Rapoport's reagent (1-benzyloxycarbonyl-3-ethylimidazolium tetrafluoroborate) has been shown to be an active and useful acylating agent for the protection of the N^6-amino function.[114-116] Freshly prepared Rapoport's reagent was added to **69** in DCM and **70** could be isolated in 96% yield. The 5′-*O* -silyl ether in **70** was then removed by treatment with TBAF in THF[117,118] and **61** was obtained in 95% yield after purification by flash chromatography.

4.2.2 Sulfamoylation of N^6-Benzyloxycarbonyl-2',3'-O-benzylideneadenosine

Several different experimental procedures for the sulfamoylation of the 5′-hydroxyl moiety have been reported in the literature including the use of sulfamoyl chloride as reagent in the presence of bases such as TEA, NaH or DBU.[97,106,119-124] A set of different reagents, solvents and reaction conditions was evaluated to identify the optimal system for the formation of **60** (**Table 1).**

Table 1. Optimisation of the sulfamoylation of compound **61** [a]

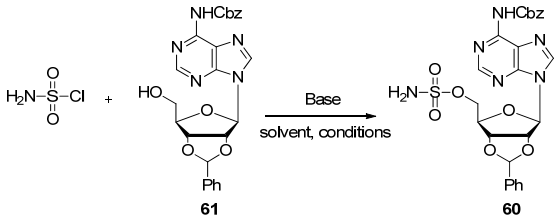

Entry	Base	Solvent	Reaction conditions[a] temp (°C), time (h)	Yield (%)[b]
1	NaH	DMF	0→rt, 4	13
2	DBU	DCM	0→rt, 4	17
3	TEA	DCM	0→rt, 4	—
4	DIPEA	DCM	0→rt, 4	—
5	—	DMA	0→rt, 4	41
6	DMAP[c]	DCM	0→rt, 4	96

[a]Reaction conditions: **61** (0.15 mmol), sulfamoyl chloride (1 equiv), DCM, 4 h, rt, N_2. [b]Isolated yields. [c]Sulfamoyl chloride (2.2 equiv), DMAP (2.3 equiv), 0 °C, 4 h, N_2.

Different bases were tested with varying strengths and sterical hindrances. Strong bases such as NaH (Entry 1) and DBU (Entry 2) gave low yields of **60**, presumably due to the decomposition of sulfamoyl chloride.[121-123] When sterically hindered amine bases were used (Entries 3 and 4) only trace amounts of **60** were formed. When DMA was used without the addition of any base (Entry 5) compound **60** was obtained in 41% yield.[121] The best yield of **60** (96%) was obtained when DMAP was employed as the base (Entry 6). The idea of using DMAP in the sulfamoylation reaction came from its properties in acyl, alkyl [125,126] or sulfonyl transfer[127] reactions,[128] which allow the sulfamoylation to occur under very mild conditions.

4.2.3 Amino Acid Coupling to N^6-Benzyloxycarbonyl-2',3'-O-benzylidene-5'-sulfamoyladenosine

The most frequently reported literature method for the formation of acylsulfamates is the use of *N*-Boc protected succinimide (Su) activated amino acids in the presence of DBU.[46,53,102,105-108] However, not all amino acids are commercially available as Su-activated esters and their preparation is not always straightforward. Thus, a range of different coupling reagents, including those that can be used for *in situ* generation of the required active ester were evaluated as shown in **Table 2**.

Table 2. Investigation of the optimal coupling conditions for acylsulfamate bond formation.[a]

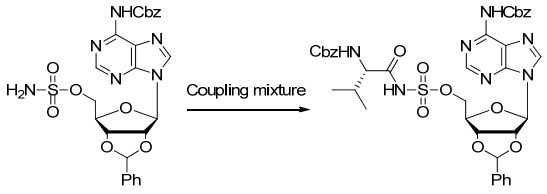

Entry	Coupling mixture	Conversion[c]
1	aa-OSu/DBU	Moderate
2	aa-Pfp/HOBt	Low
3	aa-OH/TBTU/HOBt	Low
4	aa-OH/PyBrOP	Low
5	aa-OH/HATU/DIPEA	Moderate
6	aa-OH/EDC/HOBt	Moderate
7	aa-OH/DCC/DMAP	High
8	aa-OH/PS-DCC/DMAP[b]	High
9	aa-OH/PS-EDC/HOBt[b]	Moderate
10	aa-OH/PS-IDDQ[b]	Moderate

[a]Reaction conditions: **60** (0.15 mmol), *N*-Cbz-L-valine (1 equiv), DMF, overnight, rt, N_2.
[b]Coupling agent polymer-bound to PS.[c]Determined by LC/MS. Low = 10–40%; Moderate = 40–65%; High = 65–99%.

N-Cbz-L-valine was coupled to acylsulfamate **60** using different coupling reagents, the product formation was monitored by LC/MS. Since the sulfamoyl group in **60** is not as nucleophilic as the amino groups in amino acids, it is difficult to predict the outcome based on the use of coupling reagents designed for amide bond formation. When Su-activated valine was used in the presence of DBU, moderate product formation could be detected (Entry 1). Pentafluorophenol (Pfp) activated valine in combination with HOBt resulted in low conversion of **60** to the desired product **59a** (Entry 2). The coupling mixtures in Entries 3–5 are described as being very efficient reagents for the formation of the desired activated esters, but prolonged reaction times can lead to degradation of the activated ester.[60] The acylation of sulfamate **60** using TBTU/HOBt (Entry 3), PyBrOP (Entry 4) and HATU/DIPEA (Entry 5) resulted in low to moderate conversion to the desired **59a**. The use of the carbodiimides (Entries 6–7) gave the best result among the tested coupling methods. Although the combination of DCC/DMAP (Entry 7) resulted in high conversion of the starting material to the product, it also resulted in the formation of

dicyclohexylurea (DCU). The DCU, which partially precipitated could be filtered off but traces could still be detected by ^{1}H–NMR spectroscopy even after purification using column chromatography. This problem was solved using polymer supported DCC in combination with DMAP (Entry 8), which enables filtration of the resin-bound DCU. The use of other polymer supported reagents, namely PS-EDC in combination with HOBt and PS-IDDQ (Entries 9–10) was also evaluated and moderate conversion of **60** to product **59a** was detected.

Having investigated the coupling conditions for the acylsulfamate formation, compounds **59a–h** were synthesised using the PS-DCC/DMAP protocol (**Scheme 7**).

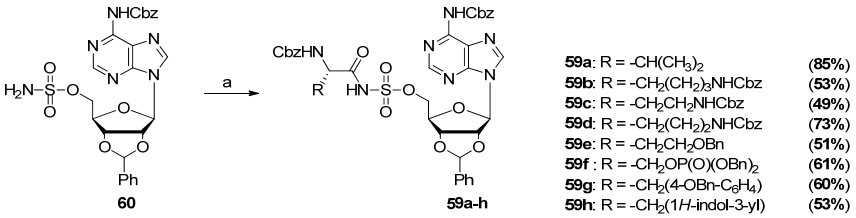

Scheme 7. The acylation of sulfamate **60** using different amino acids. Reaction conditions: a) **60** (0.35 mmol, 1 equiv), amino acid (3 equiv), PS-DCC (4 equiv), DMAP (3 equiv) DCM, 24 h, rt, N_2, 49–85% yields.

Acylsulfamates **59a**–**h** were purified using column chromatography and reverse-phase HPLC and were isolated in 49–85% yield. No racemisation could be detected probably due to the mild coupling conditions.[64,65] Doubled signals were observed in the ^{1}H- and ^{13}C-NMR spectra and from variable temperature ^{1}H-NMR experiments, it could be concluded that products **59a**–**h** adopt two different conformations with a high activation energy barrier for the interconversion (**Figure 13**).[129]

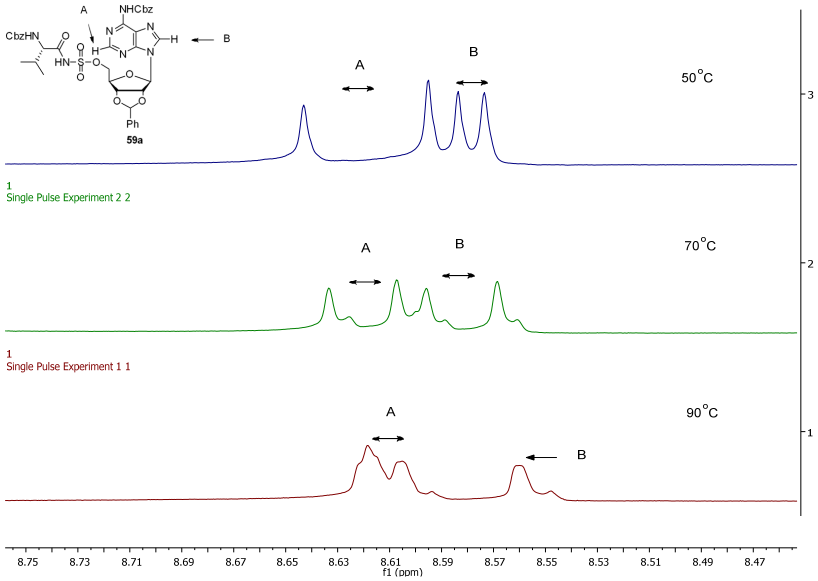

Figure 13. Variable temperature ^{1}H-NMR spectra (400 MHz, acetonitrile-d_3) showing the H-A and H-B signals of compound **59a**.

It was clearly observed that the protons of the two conformers merge with increased temperatures, and at 90 °C, the peaks for the A and B protons had almost merged. Experiments at higher temperatures and prolonged heating led to the decomposition of **59a**.

4.2.4 Deprotection of N^6-Benzyloxycarbonyl-2',3'-O-benzylidene-5'-O-[N-(aminoacyl)-sulfamoyl] adenosines

The last step in the synthesis consisted of global deprotection of compounds **59a–h** using catalytic hydrogenation under neutral conditions. Compound **59a** was used as a test compound for investigation of the required reaction conditions for complete protective group removal. A continuous flow H-Cube® instrument which easily allows testing of different types of catalysts, temperatures, solvents and applied pressures was used (**Table 3**)

Table 3. Different conditions for the deprotection of **59a** (0.015 mmol) using catalytic hydrogenation.

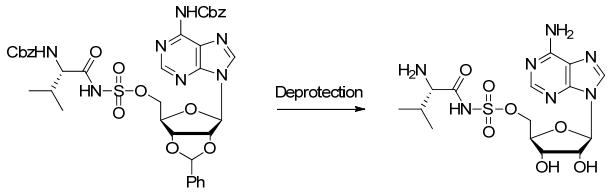

59a **17a**

Entry	Catalyst	Solvent	Pressure (bar)	Temp (°C)	Time (min)	Conversion[a] 59a→17a
1	5% Pd/C	MeOH	1	rt	40	Low
2	10% Pd/C	EtOH	1	rt	40	Low
3	10% Pd/C	EtOH	1	rt	80	Low
4	10% Pd/C	EtOH	10	rt	40	Low
5	10% Pd/C	EtOH[b]	30	30	40	Moderate
6	10% Pd/C	EtOH[b]	50	50	80	Moderate
7	10% Pd/C	*i*-PrOH[b]	50	50	80	Moderate
8	10% Pd/C	*i*-PrOH[b]	50	70	120	High
9	10% Pd/C	*t*-BuOH[b]	50	70	120	Low
10	20% $Pd(OH)_2$/C	*i*-PrOH[b]	50	70	120	Moderate

[a] Determined by LC/MS. Low = 10–40; Moderate = 40–65%; High = 65–99%.
[b] With 5% water present.

In the first experiment, compound **59a** (0.015 mmol) was dissolved in MeOH (**Table 3**) and looped in the H-Cube® using 5% Pd/C (wt/wt), 1 bar and rt for 40 min (Entry 1). The conversion of **59a** to the desired product **17a** was determined to be 10–20% using LC/MS. The major product was **71a** (50%) and traces (<5%) of product **71a** with a mass corresponding to removal of one of the two Cbz groups was also detected (**Figure 14**).

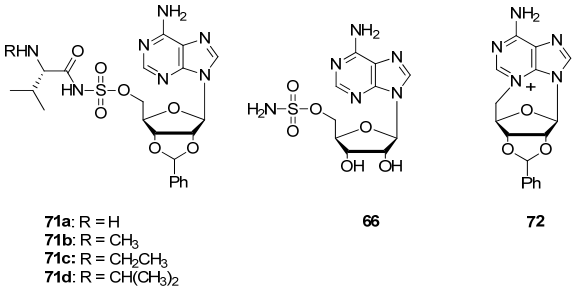

Figure 14. By-products obtained in the deprotection reaction.

These initial observations (Entry 1) resulted in changing the catalyst from 5% Pd/C to 10% Pd/C to expedite the reaction, and the use of EtOH instead of MeOH to increase the solubility of **59a**. Using the new conditions (Entry 2), the desired product **17a** was formed in 25-35% yield, **71a** in 65% yield in addition to <5% of the same by-product as for Entry 1 (one of the two Cbz groups removed) according to LC/MS. Furthermore, the temperature, time and applied pressure were increased to improve the conversion of **59a** to **17a** (Entries 3–6). Unfortunately, increased pressure, temperature and prolonged reaction time led to the formation of an additional by-product **71c**.[130] This by-product is formed as a result of the oxidation of ethanol to acetaldehyde (atmospheric air not excluded from H-Cube®), which reacts with the deprotected amino group and results in Schiff base formation. The Schiff base is readily hydrogenated to the *N*-alkylated by-product **71c**. The corresponding *N*-methylated by-product **71b** was also detected with increased pressure, temperature and prolonged reaction times when MeOH was used as solvent (data not shown). Ethanol containing 5% water (v/v) was used as solvent in an attempt to suppress the undesired formation of by-product **71c** but trace amounts (<5%) could still be detected by LC/MS (Entries 5). Increasing the temperature to 50 °C, the pressure to 50 bar and the reaction time to 80 min (Entry 6) led to the formation of additional by-products (**66** and **72**, <20%). To reduce the formation of by-product **71c**, *i*-PrOH and *t*-BuOH were used as solvents which resulted in trace amounts (<2%) of **71d** in *i*-PrOH as solvent (Entry 7) and low conversion (approximately 30%) of the starting material in *t*-BuOH (Entry 9). The use of other catalysts such as 20% $Pd(OH)_2/C$ (Entry 10) or Raney nickel (data not shown) resulted in much slower conversion of **59a**.

The screening for optimal reaction conditions resulted in concluding that catalytic hydrogenation in *i*-PrOH as solvent at 50 bar, 70 °C for 120 min resulted in full conversion of the starting material with minimal by-product formation (Entry 8). Deprotection of compounds **59a**–**h** was performed using the conditions of Entry 8, and the yields obtained of **17a**–**h** are summarized in **Scheme 8**.

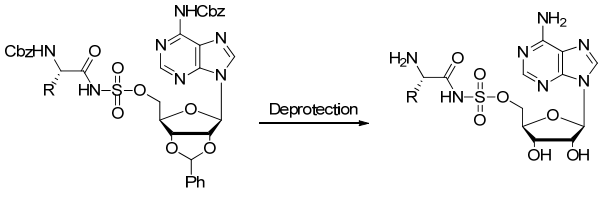

59a-h 17a-h

59a: R = -CH(CH$_3$)$_2$	**17a**: R = -CH(CH$_3$)$_2$	(58%)
59b: R = -CH$_2$(CH$_2$)$_3$NHCbz	**17b**: R = -CH$_2$(CH$_2$)$_3$NH$_2$	(36%)
59c: R = -CH$_2$CH$_2$NHCbz	**17c**: R = -CH$_2$CH$_2$NH$_2$	(78%)
59d: R = -CH$_2$(CH$_2$)$_2$NHCbz	**17d**: R = -CH$_2$(CH$_2$)$_2$NH$_2$	(21%)
59e: R = -CH$_2$CH$_2$OBn	**17e**: R = -CH$_2$CH$_2$OH	(39%)
59f : R = -CH$_2$OP(O)(OBn)$_2$	**17f**: R = -CH$_2$OP(O)(OH)$_2$	(77%)
59g: R = -CH$_2$(4-OBn-C$_6$H$_4$)	**17g**: R = -CH$_2$(4-OH-C$_6$H$_4$)	(66%)
59h: R = -CH$_2$(1*H*-indol-3-yl)	**17h**: R = -CH$_2$(1*H*-indol-3-yl)	(60%)

Scheme 8. Deprotection of compounds **59a**–**h** using continuous flow hydrogenation, flow rate 1 mL/min, 10% Pd/C CatCart 30 × 4 mm, 50 bar, 70 °C, 120 min, water:*i*-PrOH (5:95 v/v), isolated in 21–78% yields.

Deprotection of **59a**, **c**, **f**, **g** and **h** resulted in isolation of **17a** in 58%, **17c** in 78%, **17f** in 77%, **17g** in 66% and **17h** in 60% yields together with trace amounts of **71d**, **66**, **72** and **62** (adenosine). In contrast, deprotection of **59b**, **d** and **e** resulted in isolation of **17b** in 36%, **17d** in 21% and **17e** in 39% yields. The lower yields were probably due to the amino acid side chains having favourable lengths to perform the undesired intramolecular cyclisation leading to **66** and **67** as by-products (path B in **Scheme 5**).

4.3 Conclusion

In summary, this chapter described a general and efficient synthetic procedure which resulted in non-hydrolysable sulfamoyl aminoacyl-AMP analogues. The synthetic procedure included a convenient and convergent protective group strategy that allowed global deprotection using catalytic hydrogenation under neutral conditions with minimal by-product formation. Moreover, the selected protective groups could be incorporated in high yields and were stable under the performed chemical transformations. A thorough investigation of optimal conditions for the sulfamoylation reaction was performed which resulted in a protocol useful for incorporation of

the sulfamoyl group in high yield under mild reaction conditions. Several different coupling reagents were evaluated for the formation of the aminoacyl sulfamate bond which resulted in the development of a general method that allowed incorporation of amino acids with different functionalities in the amino acid side chains.

In addition to the sulfamoyl aa-AMP analogues described in this chapter, two *N*-terminally modified aa-AMP analogues have also been synthesised (**Figure 15**), they have been used by collaborators in crystallographic studies for investigation of the editing mechanism for aaRSs (unpublished results; see Appendix B for the synthetic procedures and the characterisation of the compounds).

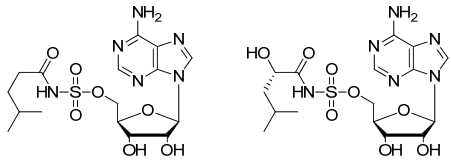

73 **74**

Figure 15. Sulfamoyloxy-linked *N*-terminally modified aa-AMP analogues.

5

Development of a Solid-Phase Method for the Synthesis of 5′-*O*-[*N*-(Acyl)sulfamoyl]Adenosine Derivatives (Paper II)

5.1 Solid-Phase Synthesis of Sulfamoyloxy-Linked Acyl-AMP Analogues

This chapter, concerns the development of a solid-phase synthetic route leading to sulfamoyl analogues of the acyl-AMP.[15,23-26,131-133] As outlined in section *3.5*, solid-phase synthesis allows the parallel generation of structurally diverse combinatorial as well as focused compound libraries.[75,76,78] In the present project it was envisioned that a solid-phase method would be particularly useful for the synthesis of structurally diverse 5′-*O*-[*N*-(acyl)sulfamoyl]adenosine analogues including amino acids, dipeptides, salicylic acid and fatty acids in quantities sufficient for biological screening. Three different solid-phase approaches were investigated in which the strategies differed in the positioning of the attachment point of the substrate to the solid support. The retrosynthetic plan is illustrated in **Scheme 9**.

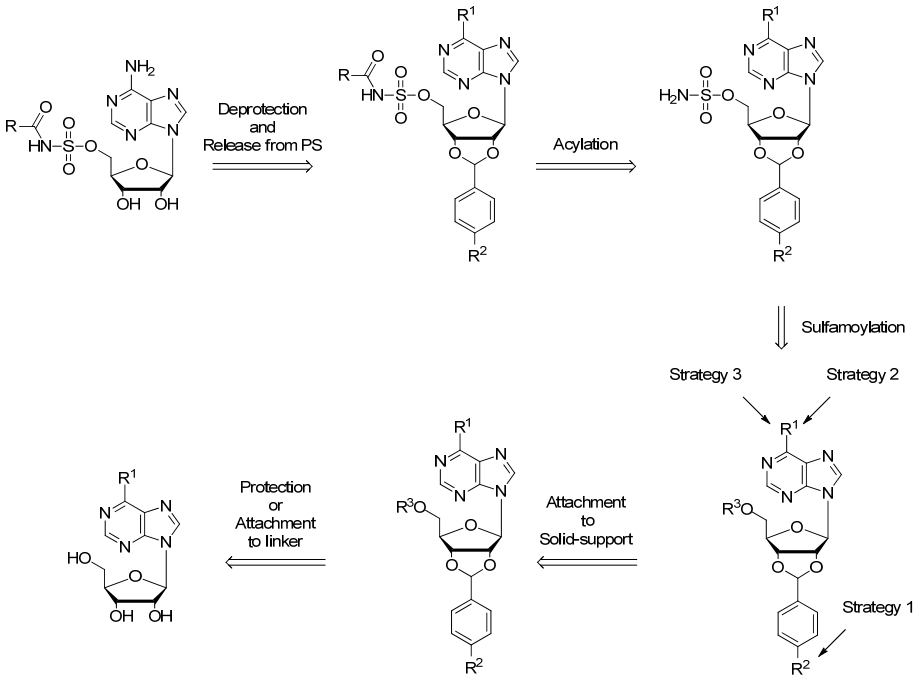

Scheme 9. A retrosynthetic plan for the solid-phase preparation 5′-*O*-[*N*-(acyl)sulfamoyl] adenosines. R = acyl, $R^1 = NH_2$ for strategies 1 and 2, R^1 = Cl for strategy 3. R^2 = linker for strategy; 1 and R^2 = H for strategies 2 and 3. R^3 = H for strategies 1 and 3 and R^3 = TBDMS for strategy 2.

5.1.1 Yields Quantification using HPLC

There are two different approaches that can be employed for the analysis of the outcome of solid-phase reactions: the analysis of the resin-bound intermediate using non-destructive techniques or the analytical liquid phase techniques, which require cleavage of the resin-bound substrate.[134] The methods used for monitoring resin-bound substrates include colorimetric tests such as the Kaiser test for amines,[135] Ellman's reagent for thiols,[136] the Fmoc reading test,[134] NMR spectroscopy,[79] infrared (IR) monitoring[79] and combustion elemental analysis.[137] The most commonly used method for monitoring and quantifying solid-phase reactions is small-scale cleavage followed by solution-state analysis using conventional techniques such as TLC and LC/MS. For our purpose, it was decided to develop a reverse-phase (C18) HPLC method using toluene as an internal standard (ISTD) that would require small-scale cleavage and allow both monitoring and quantification of each reaction step. Toluene was chosen as the internal standard based on its UV activity in the range of 200-400 nm and due to its retention time not coinciding with the reference compounds. The reference compounds corresponded to the products that would be cleaved off from the solid support after each reaction step. An HPLC elution method which allowed the

separation of all reference compounds (**60** without the N^6- protective groups (Cbz), **62**, **68** and **69**), without toluene interference was initially identified. Standard curves were derived for the reference compounds and for toluene by plotting the absorbance for each compound vs. the known concentration (e.g. five different concentrations) to form a linear correlation. The ratio between the analysed compound and the internal standard can be described as the k-value which was derived from **Equation 1**.

Equation 1 $$\frac{A_{prod}}{A_{Tol}} = k\frac{C_{prod}}{C_{Tol}}$$

Where A_{prod} = area for product, A_{Tol} = area for toluene, k = constant describing the relationship between the extinction coefficients of the product and the internal standard at the studied wavelength, C_{prod} = product concentration and C_{Tol} = toluene concentration.[138]
Using the derived HPLC method, the reactions were monitored and quantified by the addition of a known amount of internal standard calculated by **Equations 2a** and **2b**.

Equation 2a $$n_{Tol} = \frac{n_{max\ loading} \times k}{2}$$ **Equation 2b** $$V_{ISTD} = \frac{n_{Tol}}{C_{ISTD}}$$

Where n_{Tol} = moles of toluene, $n_{max\ loading}$ = theoretical maximum loading for a known amount of resin. V_{ISTD} = volume internal standard and C_{ISTD} = concentration of internal standard. The yields were quantified using **Equation 3**.

Equation 3 $$\frac{A_{prod}}{A_{Tol}} = k\frac{C_{prod}}{C_{Tol}} \Longrightarrow \frac{A_{prod}}{A_{Tol}} = k\frac{n_{prod}}{n_{Tol}} \Longrightarrow n_{prod} = \frac{A_{prod} \times n_{Tol}}{A_{Tol} \times k}$$

Where n_{prod} = moles of product.

5.2 Results and Discussion

5.2.1 Strategy 1

In Strategy 1, the 2′,3′-hydroxyl groups of the ribose subunit serves as the attachment point to the solid support via an acetal linker.[139] The advantage gained from attaching the nucleoside onto the linker prior to attachment to the solid support is the possibility for purification of intermediate **82**. The synthetic path is illustrated in **Scheme 10**.

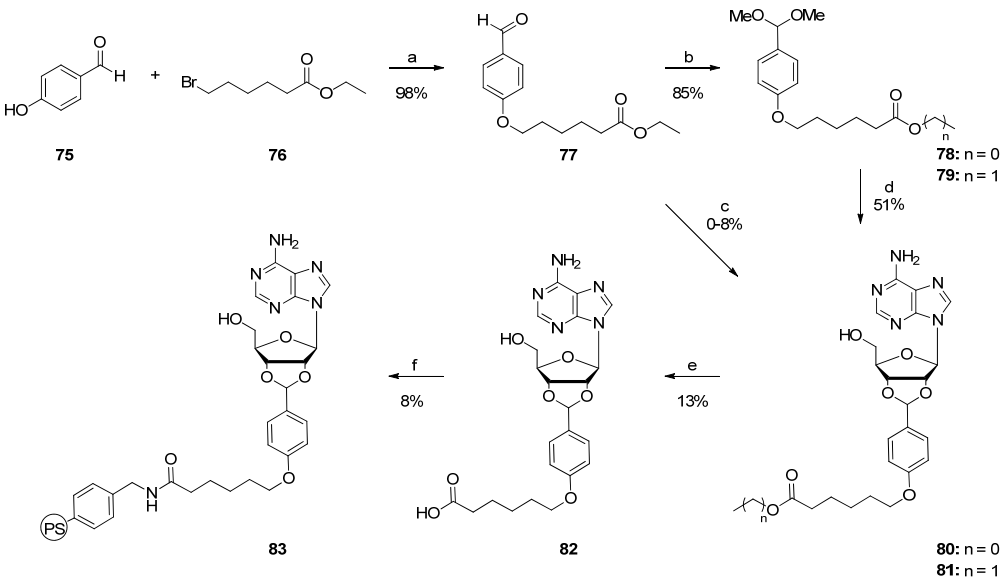

Scheme 10. Attachment of adenosine (**62**) to a solid support. Reagents and conditions: a) K_2CO_3 (2 equiv), DMF, 50 °C, N_2, 20 h. b) TMOF (2 equiv), TsOH (0.05 equiv), MeOH, MW, 150 °C, 4 min. c) i. **62** (2 equiv), $ZnCl_2$ (1 equiv), DMF, rt, 15 h or ii. **62** (0.2 equiv), $ZnCl_2$ (5.1 equiv), a few drops of DMSO, 35 °C, 72 h. d) **62** (1 equiv), TsOH (0.1 equiv), DMF, 50 °C, 70 mbar, 15 h. e) LiOH (2 equiv, 2M aq soln). f) aminomethylpolystyrene (**55**, 0.2 equiv, loading ~0.90 mmol/g), HATU (5 equiv), DIPEA (10 equiv), DMF, rt, 6 h.

Compound **77** was synthesised using previously described procedure.[139] The aldehyde **77** was then treated with trimethylortoformate (TMOF) in MeOH resulting in a mixture of **78** and **79**. The attachment of **62** to the linker via path c in **Scheme 10** was attempted using two different sets of conditions giving **80** and **81** at the best in 8% combined yield. Compounds **80** and **81** were instead obtained by reacting **62** with the mixture of **78** and **79** under acidic conditions. The last step in solution prior to the attachment to the solid support consisted of an ester hydrolysis using aq LiOH and the reaction was monitored by LC/MS and **82** was obtained in 13% isolated yield.

The low yield was due to cleavage of **62** from the linker under the given reaction conditions and the loss of the glue-like crude product during work-up and purification. Attachment of crude **82** to aminomethylpolystyrene (**55**) was performed in DCM using HATU as a coupling reagent in the presence of DIPEA to afford resin-bound **83** in 8% yield. The disappointing yield obtained in the attachment to the solid support could be due to the poor solubility of **82** in DCM. The yield of the attachment of **82** to the solid support was calculated by cleaving adenosine from the linker using 5% TFA and 5% H_2O in dioxane and heating at 50 °C for 18 h followed by quantification using the derived HPLC method with toluene as an internal standard. Strategy 1 was not further investigated due to the low yield obtained in the attachment of **82** to the solid support and due to the possible decomposition of the final products (acyl sulfamates) using the cleavage conditions described above.

5.2.2 Strategy 2

In Strategy 2, the 6-amino function of the adenine moiety in **69** served as the attachment point to the solid support (synthesis of **69** described in section *4.2.1*). The trityl resin (PS-Tr) was selected due to its stability in the planned synthetic route (sulfamoylation and acylation) and due to the mild conditions required for the cleavage of the attached substrates from the solid support (typically1–5% TFA in DCM).[88] In addition, the trityl group has been used as a protective group for the N^6-amino function.[140] The reaction conditions required for the attachment of compound **69** were investigated and included different bases (DMAP, DBU, BEMP, TEA and DIPEA), temperatures (rt to 60 °C using both conventional and microwave (MW) assisted heating), reaction time (0.5–48 h) and solvent (pyridine, THF, DCE and DMF) (**Scheme 11**).

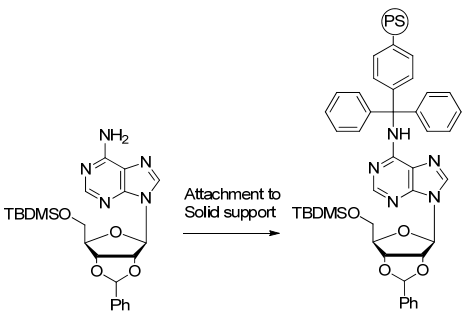

69 **84**

Scheme 11. Investigation of the optimal conditions for the attachment of compound **69** to PS-Tr-Cl (**56**).

Unfortunately, none of the attempts resulted in the desired solid supported **84**. Furthermore, it was also attempted to pre-form the resin-bound trityl carbocation using triethyloxonium tetrafluoroborate (TEOTFB, 2 equiv) prior to the addition of **69** (5 equiv) which resulted in 7% yield of **84** quantified using the derived HPLC method. The developed Ps-Tr-Cl (**56**) activation method using TEOTFB has proven to be useful in the attachment of substrates such as alcohols and anilines and will be described further in Chapter 8.

5.2.3 Strategy 3

In Strategy 3, attachment of the purine subunit via a 6-chloro function to PS-Rink AM resin (**58**) was investigated due to the presumed stability of the linker during the planned synthetic route (**Scheme 12**). Cleavage of the substrate from PS-Rink AM after completing the synthesis would result in the desired 6-amino function.

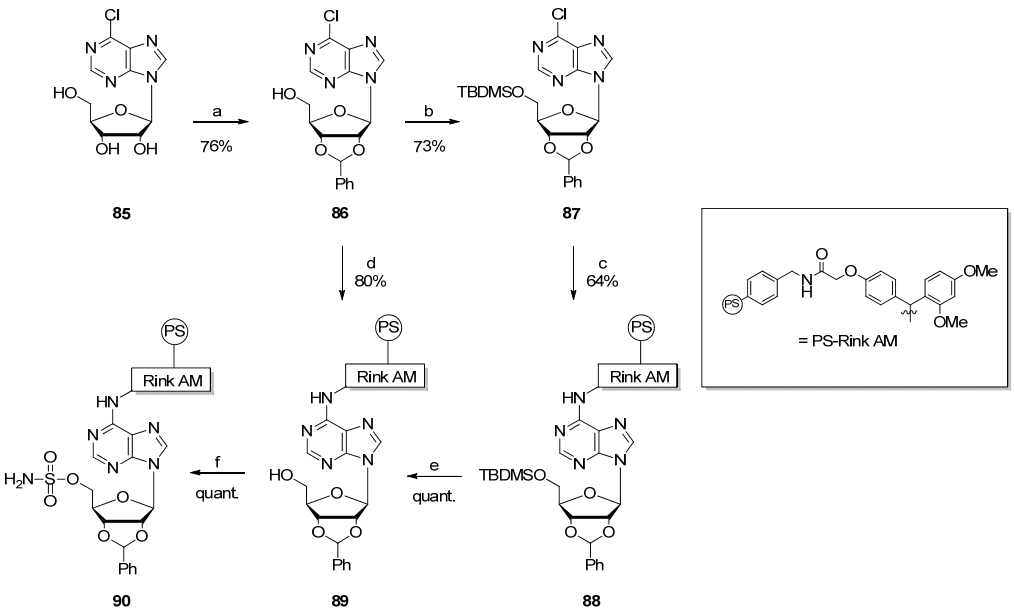

Scheme 12. Synthetic procedure used in Strategy 3. Reagents and conditions: a) $ZnCl_2$ (5 equiv), freshly distilled benzaldehyde, rt, N_2, 72 h. b) TBDMS-Cl (1.2 equiv), imidazole (2.5 equiv), DMF, 0–rt, N_2. c) i. Fmoc cleaved from PS-Rink AM (**58**, 1 equiv, loading ~1.2 mmol/g) using 20% piperidine in DMF and ii. **87** (4 equiv), DBU (4 equiv), BuOH:DMSO (1:1 v/v), MW, 80 °C, 2.5 h. d) i. Fmoc cleaved from PS-Rink AM (**58**, 1 equiv, loading ~1.2 mmol/g) using 20% piperidine in DMF and ii. **86** (4 equiv), DBU (4 equiv), BuOH:DMSO (1:1 v/v), MW, 80 °C, 2.5 h. e) TBAF (1 equiv, 1M in THF). f) sulfamoyl chloride (3 × 3 equiv), DMAP (3 × 3 equiv), DMF, rt. 3 × 1 h, N_2.

In order to block the reactive secondary alcohols, 6-chloropurine riboside (**85**) was protected as the 2′, 3′-*O*-benzylidene acetal using similar reaction conditions as for the benzylidene protection of adenosine to form **68**, **86** was obtained in 76% yield. Prior to the attachment of the substrate, the Fmoc protective group was removed from the rink amide using 20% piperidine in DMF. Various reaction conditions including different amounts of reactants, bases, temperatures (MW and conventional heating) and reaction times (2.5–20 h) were investigated. MW-assisted attachment in the presence of DBU was achieved via the TBDMS protected **87** which was synthesised in 73% yield using TBDMS-Cl and imidazole (path b and c). The final route added two steps (protection and deprotection) to the synthesis and resulted in a 64% combined yield for resin-bound **89**. Attachment to the resin was also performed without the protection of the 5′-hydroxyl moiety by the addition of **86** to PS-Rink AM using MW-assisted heating in the presence of DBU as a base and the yield for **89** was determined to 80% using the derived HPLC method (path d). Unfortunately the loading of different resin batches was not consistent which resulted in large batch-to-batch variations. With the desired resin-bound substrate **89** finally in hand, sulfamoylation could be investigated.

5.2.4 Sulfamoylation of Solid Supported 2',3'-O-Benzylideneadenosine

Sulfamoylation of the 5′-hydroxyl group of the ribose moiety in **89** has been thoroughly investigated and is described in section *4.2.2*. The developed sulfamoylation protocol consisted of treatment of 5′-hydroxyl with sulfamoyl chloride in the presence of DMAP using DCM as solvent. The initial attempts for the sulfamoylation of **89** were performed using DCM as a solvent, but due to the poor solubility of sulfamoyl chloride even in large amounts of solvent (>5 mL), the reaction times were long (>16 h) and often resulted in incomplete reactions. Therefore, DMF was instead used as a solvent which allowed the use of more concentrated solutions. DMF as solvent in the presence of base in the sulfamoylation reaction has been reported to give low yields due to decomposition of the sulfamoyl reagent.[121-123] However, with the use of large excess of the sulfamoyl reagent (3 × 3 equiv) together with DMAP (3 × 3 equiv) dissolved in a minimal amount of DMF (2 mL) the sulfamoylation was achieved in quantitative yields (**Scheme 12**).

5.2.5 Acylation, Cleavage from the Solid Support and Deprotection of 5′-O-[N-(Acyl)sulfamoyl] Adenosines

Optimisation of the aminoacylation of the sulfamate group in solution is discussed in section *4.2.3*. However for the solid-phase synthesis, the use of polymer-bound reagents would not be beneficial since the separation of the two resins (PS-DCC and resin **90**) would be impossible. The

use of non-resin-bound DCC would result in the formation of insoluble DCU which could be difficult to remove after completion of the reaction, since the precipitate would also be able to block the resin pores. Therefore DIC was chosen as the coupling reagent since the soluble DIC urea can easily be removed after completion of the reaction. The synthesis of the target 5′-O-[*N*-(acyl)sulfamoyl] adenosines is illustrated in **Scheme 13**.

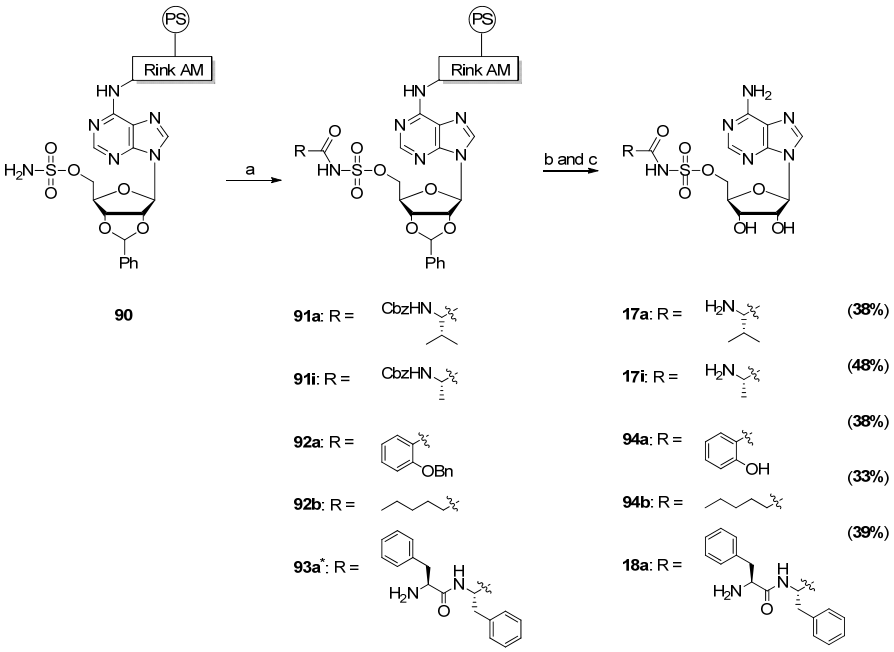

Scheme 13. The acylation, cleavage and deprotection to obtain target compounds **17a**, **i**, **94a**, **b** and **18a**. Reagents and conditions: a) acid (20 equiv), DIC (20 equiv), DMAP (20 equiv), DCM, rt, N_2, 16 h. b) 5% TFA in DCM, 3 x 30 min. c) ammonium formate (5 equiv), 10% Pd/C (10% wt/wt), MeOH, 60 °C, 16 h.* Aminoacylation performed as in a) then 20% piperidine in DMF, 20 min, two times then c) as above.

The acylation of the target compounds was performed in parallel in a Bohdan block, thereby facilitating an effective resin swelling, reagent additions, resin agitation, reagent filtering, resin washing and cleavage of the resin-bound product. The acid, DIC and DMAP were allowed to react for 30 min prior to the addition to the pre-swelled resin **90**. After 16 h agitation, the reagents were removed, the resin was washed thoroughly and the products were cleaved off. The crude 2′,3′-*O*-benzylidene-5′-O-[*N*-(acyl)sulfamoyl] adenosines **91a**, **i**, **92a–b** and **93a** were obtained in 80% purity according to LC/MS analysis. The deprotections were run using ammonium formate in the presence of 10% Pd/C without the isolation of **91a**, **i**, **92a–b** and **93a**. After the removal of

the protective groups, compounds **17a**, **i**, **94a**, **b** and **18a** were purified using preparative HPLC and the combined yields over three (six for **18a)** steps were 33–48% (**Scheme 13**). For the synthesis of **91a** and **i**, the *N*-terminally Cbz-protected amino acids were coupled to the sulfamate **90**, followed by cleavage from the resin and deprotection which resulted in **17a** in 38% and **17i** in 48% isolated yields. Coupling of other *N*-terminally Cbz-protected amino acids than those illustrated in **Scheme 13** have been investigated, including Tyr, Trp and *O*-Cbz-protected homoserine (Hse), and was confirmed using LC/MS (data not shown). The synthesis of **94a** was performed using 2-*O*-benzyl protected salicylic acid which resulted in 38% yield over three steps. Furthermore, coupling of 2-*O*-Fmoc protected salicylic acid, salicylic acid without any protective group on the 2-hydroxyl and various other derivatives of salicylic acid with a Cbz-protected amine, a Cl or F group in the 4-position were unsuccessful due to poor solubility of the substrates. Hexanoic acid was activated using the conditions described above and coupled to sulfamate **90** and after the deprotection **94b** was obtained in 33% yield. In addition to this acid derivative, the coupling of arachidic acid (eicosanoic acid) and lauric acid (dodecanoic acid) was attempted with only trace amounts of product according to LC/MS. The low conversions for these compounds, observed by LC/MS, could be attributed to aggregation of the respective acids. To attain compound **93a**, *N*-terminal Fmoc-Phe was coupled first, followed by Fmoc deprotection using 20% piperidine in DMF. Repeating the procedure resulted in the deprotected dipeptide **93a**, subsequent removal of the 2′,3′-*O*-benzylidene resulted in **18a** in 39% yield over six steps. Coupling of indole-3-acetic acid and biotin was also attempted without any success due to the poor substrate solubility.

5.3 Conclusion

In conclusion, a solid-phase synthetic route leading to sulfamoyl-based acyl-AMP analogues was successfully developed. In addition, a reverse-phase HPLC method was developed to monitor and determine the yield of each of the synthetic transformations performed. To attain the desired resin-bound 2′,3′-*O*-benzylideneadenosine, three different synthetic strategies for the attachment were explored of which only one was successful. With the solid supported starting material in hand, parallel synthesis was facilitated and the resin swelling, reagents additions, agitation of the resin, filtering off the reagents, resin washing and products cleavage were simplified compared to solution-phase parallel synthesis. In Chapter 4, the use of PS-DCC in combination with DMAP was described for coupling of amino acids to **60**, however, for this solid-phase route DIC in combination with DMAP was employed since the formed DIC urea is easily removed after

completion of the reaction. In addition, separation of two PS-supported reagents after the completion of a reaction would be impossible. Another difference to the solution-phase method described in Chapter 4, is that the solid-phase synthesised compounds **91a**, **i**, **92a–b** and **93a** tolerated the use of ammonium formate as the hydrogen source in presence of 10% Pd/C as a catalyst for the deprotection step. This treatment was possible due to the fact that compounds **91a**, **i**, **92a–b** and **93a** lacking the ability to perform the unwanted intramolecular cyclisation described in Chapter 4 which would lead to the formation of **66** and **67** as by-products (path B in **Scheme 5**). In total, five different 5′-O-[*N*-(acyl)sulfamoyl]adenosine derivatives were synthesised in 33–48% yield over three or six steps using the developed solid-phase synthetic route.

6

Identification of the Bioactive Conformation of aa-AMP Derivatives Bound to tRNA Synthetase using X-ray Structures and Conformational Analysis

6.1 Introduction

The aim of this sub-project was to identify the bioactive conformation of aa-AMP derivatives using X-ray crystallography data and conformational analysis and to explore the possibility of employing novel phosphate bioisosteres as aa-AMP analogues that are useful as tRNA synthetase inhibitors. With knowledge of the possible bioactive conformation, molecular modelling can be used as *one* of the tools to evaluate *if* a molecule could be expected to be a potential inhibitor.

6.1.1 Molecular Modelling in Medicinal Chemistry

Molecular modelling comprises the use of computer programs as tools for describing molecules and molecular systems.[141] Computational methods include quantum mechanics and molecular mechanics calculations that are used to perform e.g. energy minimisations and conformational analysis. Computational techniques have become important tools in the field of medicinal chemistry for approaches including hit identification and lead optimisation. Techniques including structure- or ligand-based design and docking of molecules in protein binding sites are also frequently used.[142] Conformational analysis involves the investigation of the preferred three-dimensional structures of compounds, or in other words to identify low-energy conformations of a molecule. The derived molecule can then be used in molecular docking procedures for investigation of the geometric arrangement.[141] Structure-based design involves the use of a protein structure determined by X-ray or NMR techniques for the design of molecules that interact efficiently with the protein.[143] Structure-based drug design involves identification of a molecule that fulfils the geometric constraints defined by the three-dimensional features for a known receptor/enzyme binding site. Another frequently applied modelling technique is ligand-

based drug design.[144] Ligand-based design involves comparison of the structural features of a potential ligand with those of known active and structurally similar inactive ligands.

6.2 Result and discussion

6.2.1 Identification of the Bioactive Conformation

Knowledge about the bioactive conformation of **1** would make it possible to design potential phosphate bioisosteres useful as novel aaRS inhibitors. Compound **1** was simplified into structure **95** since the focus was set on identifying phosphate bioisosteres and minimising the influence of other structural features in **1**. A set of different phosphate bioisosteres was studied using all different combinations of N, O and C atoms in positions X and Y in structures **96** and **97** (**Figure 16)**.

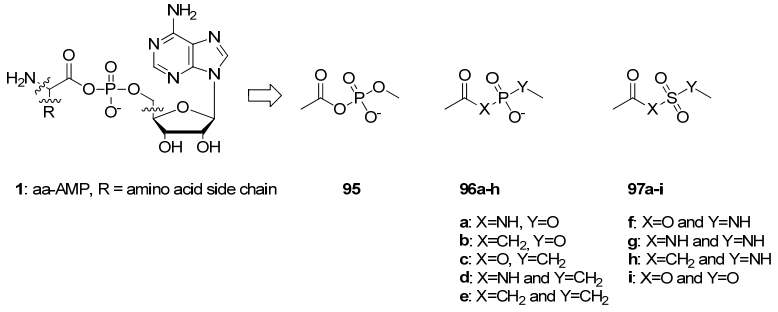

Figure 16. Illustration of the simplified models **95**–**97** that were used for deriving potentially stable analogues of aa-AMP (**1**).

The study was initiated by importing the X-ray structure of lysyl-tRNA synthetase complexed with a lysyl-AMP intermediate (protein data bank (PDB) code: **1e1t**)[145] and the X-ray structure of threonyl-tRNA synthetase complexed with a seryl-AMP analogue (PDB code: **1fyf**),[146] both from *Escherichia coli* (*E. coli*). Conformational analysis of the simplified structure **95** was performed using the systematic torsional sampling (SPMC) method in simulated water and OPLS_2005 as the force field (see **Appendix C**). Nine different low-energy conformations of **95** ($\Delta E < 12$ kJ/mol) were identified.[147,148] The co-crystallised substrates (lysyl-AMP in **1e1t** and seryl-AMP analogue in **1fyf**) were assumed to adopt the bioactive conformation in the X-ray structures. The co-crystallised aa-AMPs (lysyl-AMP and seryl-AMP analogue) were extracted from the X-ray structures above and the nine calculated conformations for **95** were all superimposed with the aa-AMPs (**Figure 17**).

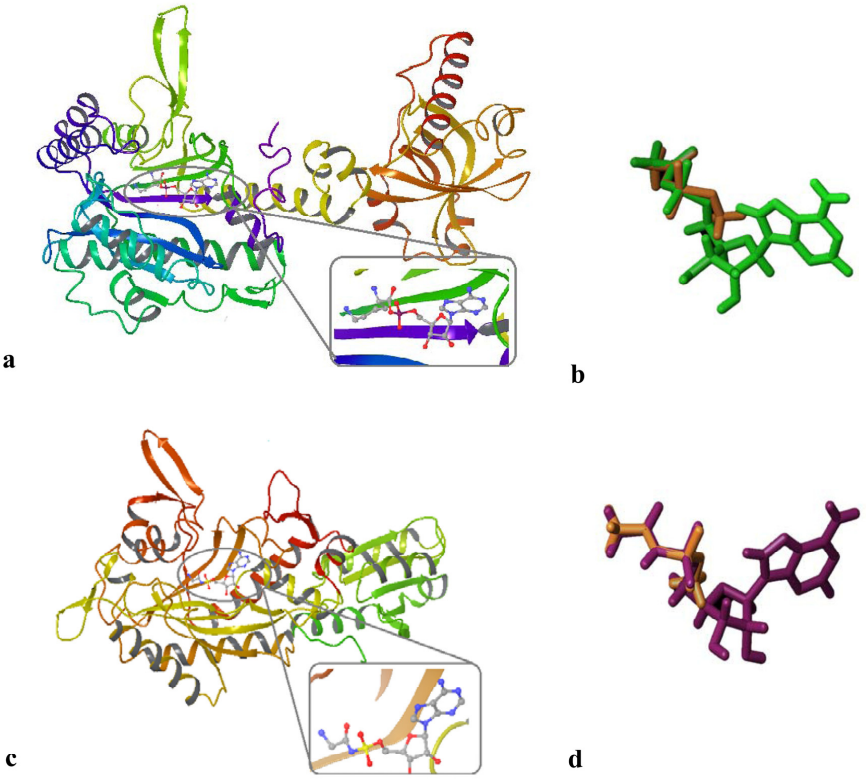

Figure 17a. The crystal structure of lysyl-tRNA synthetase complexed with a lysyl-AMP (PDB code: **1e1t**) and **b.** one low-energy conformation of **95** (orange) superimposed with the co-crystallised substrate (green) imported from the X-ray structure. **c.** The crystal structure of threonyl-tRNA synthetase complexed with a seryl-AMP analogue (PDB code: **1fyf**) and **d.** one low-energy conformation of **95** (orange) superimposed with the co-crystallised substrate (purple) imported from the X-ray structure.

From the superimpositions performed using ligand **95**, a potential bioactive conformation was obtained from the X-ray structures. **Figure 17a** illustrates the X-ray structure of **1e1t** and the derived bioactive conformation superimposed with the lysyl-AMP intermediate (**Figure 17b**) extracted from the X-ray structure, the same potential bioactive conformation could be superimposed with the seryl-AMP analogue (**Figure 17d**) extracted from the X-ray structure of **1fyf** (**Figure 17c**).

6.2.2 Simplified Models of Potential Stable Analogues of aa-AMP

Conformational analysis was performed of analogues **96a–h** and **97a–i** and all identified low-energy conformations were superimposed with the derived bioactive conformation for ligand **95.**

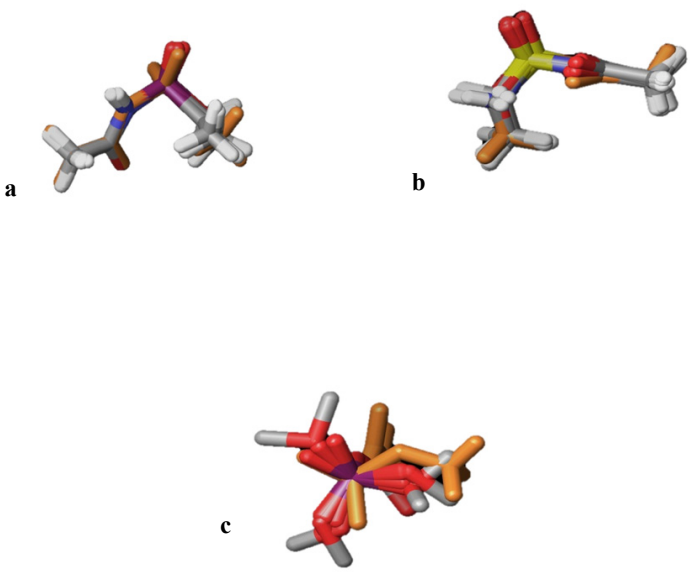

Figure 18a. Superimpositions of the possible bioactive conformation of **95** (orange) and the low-energy conformations of **96a**, **c** and **d**. **b.** Superimpositions of the potential bioactive conformation of **95** (orange) and the low-energy conformations of **97a**, **c**, **d**, **f**, **g** and **i**. **c.** Superimposition of the 20 derived conformations for **97e** with **95** (orange) as an example of a ligand mismatch.

The conformational energy penalties for the model compounds to adopt the bioactive conformation are shown in **Table 4**.[149] Ligands **96a**, **c** and **d** had low-energy conformations which could be superimposed with **95** (**Figure 18a.**). Aminoacyl adenylate analogues having an *N*-acyl phosphoramidate linkage have been synthesised (**96a**, as model ligand) and shown to be promising tRNA synthetase inhibitors.[52,150-152] Type **96b** inhibitors have been studied extensively in the literature but we failed to superimpose any low-energy conformations of **96b** with the derived bioactive conformation.[153,154] A plausible explanation could be that the bioactive conformation does not represent an energy minimum. Since **96b**-type compounds tend to be good inhibitors, a different binding mode should be considered (e.g. the enol form). Also, **96c**-type

compounds have been synthesised but not tested as tRNA synthetases inhibitors.[155,156] Such compounds would be interesting to evaluate as inhibitors, but the stability of the *O*-acyl bond needs to be considered. The **96d**-type compounds are not known in the literature and would be very interesting to synthesise and test for biological activity since the bioactive conformations represents an energy minimum. Ligands **97a**, **c**, **d**, **f**, **g** and **i** adopted low-energy conformations which could be superimposed with the derived bioactive conformation for **95** (**Figure 18b.**). We and others have synthesised several **97a-**type compounds which are good inhibitors of tRNA synthetases.[24,53,102-104] The **97c**, **f** and **i-**type compounds type compounds are not known in the literature, but would probably be hydrolysable analogues of **95**. **97d-**type compounds are not known in the literature, but since the bioactive conformation represents an energy minimum, interesting biological results could be expected with this type of compound. The superimposition of all 20 different low-energy conformations identified for **97e** with **95** are shown in **Figure 18c** as an example of a ligand that did not superimpose well with the bioactive conformation. **97g-**type compounds have been synthesised earlier and according to the literature, are good tRNA synthetase inhibitors.[48]

Table 4. Conformational energy penalties required to attain the bioactive conformation for the ligands showing good structural overlap with **95**.

Ligand	**96a**	**96c**	**96d**	**97a**	**97c**	**97d**	**97f**	**97g**	**97i**
Energy penalty (kJ/mol)	1.66	0	0.40	0	8.33	0	7.72	3.16	4.88

6.3 Conclusion

The study involved the use of molecular modelling techniques for the determination of a possible bioactive conformation of tRNA synthetase inhibitors based on X-ray data. Eighteen different phosphate bioisosteres were selected, a conformational search was performed and low-energy ($\Delta E<12$ kJ/mole) conformations were superimposed onto the derived potential bioactive conformation for a simplified model of **1**. Furthermore, the energy penalties required for all of the model ligands to attain the bioactive conformation were calculated. The model ligands were used in an in-depth literature study that aimed to identify which of the ligands had been synthesised and tested as tRNA synthetase inhibitors. In conclusion, nine different ligands adopted low-energy conformations corresponding to the derived bioactive conformation. The reliability of the derived model was further reinforced since some of the identified ligands that had been

synthesised previously and tested for biological activity showed to be good inhibitors of aaRSs. **96b**-type ligands did not superimpose onto the derived bioactive conformation but have been shown to be good inhibitors of aaRSs and this activity can probably be attributed to a different binding mode (e.g. enol type). Two novel model ligands (**96d**- and **97d**-type) were identified but the synthesis was not carried out. However, the design and synthesis of novel ribose-free bioisosteres as potential aaRS inhibitors has been performed and will be discussed further in Chapter 7.

7

Design, Synthesis and Biological Evaluation of Ribose-Free Isosteres of Aminoacyl-AMP (Paper III)

7.1 Introduction

The isosteres of the aa-AMP intermediate (**1**) discussed in Chapters 4, 5 and 6 have involved modifications on the phosphate subunit of AMP. The synthetic strategies comprised protection and deprotection of the 2′,3′-hydroxyl groups of the ribose subunit which added reaction steps to the synthesis. Extensive purification of the target compounds was required due to the high polarity properties of the molecules, therefore we planned to replace the ribose subunit with an isosteric moiety. The purine subunit is an important structural motif in several projects in our group, such as projects relating to the development of ATP-competitive protein kinase inhibitors.[157,158] This served as the source of inspiration for the development of ribose-free purine-based analogues of aa-AMP. The design of the ribose-free analogues was performed using molecular modelling and the biological evaluation was performed by Prof. Stephen Cusack's lab at the European Molecular Biology Laboratory, Grenoble, France, using isothermal titration calorimetry (ITC).

7.2 Results and Discussion

7.2.1 Design of Ribose-Free Purine-Based Aminoacyl-AMP Analogues

Examination of available protein X-ray structures of aaRSs in complex with ligands lead to the identification of distinct protein folds involved in binding as well as distinct binding conformations. The ligands generally bind in overall extended conformation (**Figure 19**). This binding conformation is observed for both Class I and Class II aaRSs.[5] We envisioned that 1,4-triazoles in the 8-position of the purine scaffold would exhibit similar structural features as those of the ribose unit and serve as suitable linkers capable of positioning the amino acid and purine group in the ribose-free aa-AMP analogues. In analogy, the use of 5-membered rings such as 2,5-

furanyl in the 8-position of purines has been described in the literature as potential bioisosteres to AMP derivatives.[159] The design of ribose-free purine-based aa-AMP analogues comprised the comparison of the spatial similarity between ligands **98** and **99** with sulfamoyl-based aa-AMP analogue **17** (**Figure 19**).

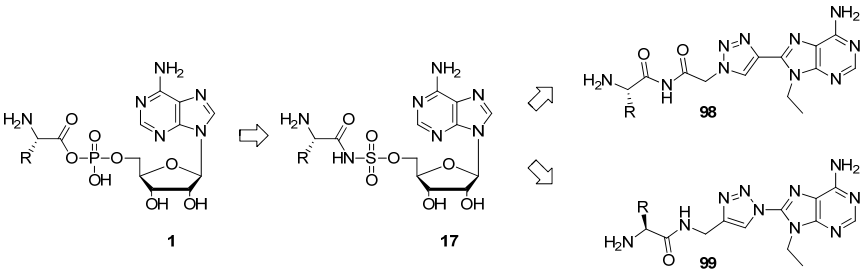

Figure 19. The designed ribose-free purine-based analogues **98** and **99** of aa-AMP **1** and sulfamoyl-based analogue **17**. R = amino acid side chain.

The R groups in structures **17** (**17j**: R = isobutyl group), **98** and **99** were defined as the leucinyl side chain. The superimposition of structures **17j**, **98** and **99** revealed good overlap between the purine ring system and the leucinyl substituent (**Figure 20**).

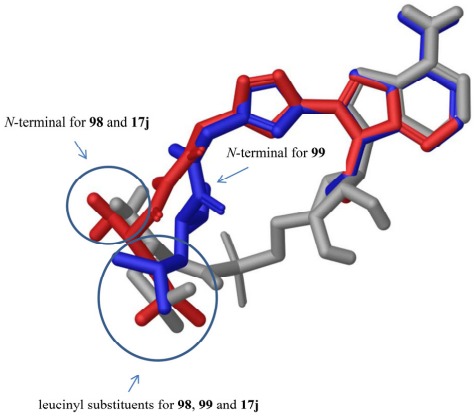

Figure 20. Structures **98** (red) and **99** (blue) superimposed with the sulfamoyl-based aa-AMP analogue **17j** (grey).

The superimpositions indicated that an amino acid protruding from a linker attached to a 1,4-substituted triazole in the 8-position of adenine (**98** in red and **99** in blue) is positioned in a similar manner as the sulfamoyl-based aa-AMP analogue (**17j** in grey). The *N*-terminals for

structures **98** and **17j** point in the same direction while the *N*-terminal for **99** does not adopt the same conformation (**Figure 20**). Furthermore, the designed molecules eliminated the need for ribose as the linker subunit for the amino acid provided that removal of the phosphate and ribose moieties could be compensated by a reduced entropic cost of binding and/or new favourable binding interactions. To further evaluate the design ligands **98** and **99** were docked[160] into the leucinyl-tRNA synthetase structure with **17j** bound in the active site (PDB code: **1H3N**[161]) (**Figure 21**).

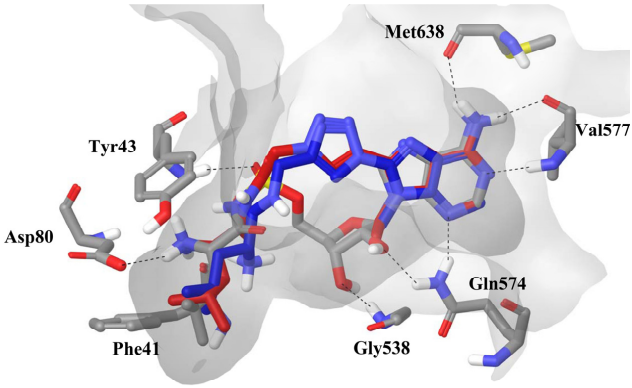

Figure 21. Compound **98** (red) and compound **99** (blue) docked into the X-ray structure of leucinyl tRNA synthetase co-crystallised with sulfamoyl-based analogue **17j** (grey) of aa-AMP (**1**).

The docking study indicated that the leucinyl substituents of **98** (red) and **99** (blue) are positioned within the same area as the leucinyl side chain of the substrate **17j** (grey). Detailed analysis of the interactions formed by **17j** suggests that hydrogen bonds are formed with amino acids in the binding site (**Figure 21**; Tyr43, Asp80, Gly538, Gln574, Val577 and Met638). Compound **98** retains all the hydrogen bonding interactions stated above except those formed with Gly538 and Gln574 (hydrogen bonding interactions with amino acids in the binding site formed by the 2′,3′-hydroxyls of the ribose subunit). Compound **99** retains all the hydrogen bonding interactions formed by the purine in **17j** (Gln574, Val577 and Met638). The possibility for the interaction with Asp80 (*N*-terminal*)* is not present, however it forms an additional favourable interaction with Phe41 (**Figure 21**). These results suggests that **98** and **99** exhibit similar structural features as **17j** and that the designed ligands serve as potential linkers between the amino acid and the purine group in the ribose-free aa-AMP analogues.

7.2.2 Synthesis of Ribose-free 8-Triazolyladenine-Based Analogues of Aminoacyl-AMP

The retrosynthetic plan for the preparation of the ribose-free purine-based inhibitors **98** and **99** is outlined in **Figure 22**. The planned route for acquiring **98** was based on the deprotection of **100** that was obtained from the aminoacylation of **101**. The strategy for obtaining **101** included the use of a 1,4-regioselective copper-catalysed azide/alkyne 1,3-cycloaddition (CuAAC) reaction (**102** where R^1 corresponds to an ethynyl group in the 8-position).[162,163] Starting from **104**, the introduction of the alkyne in the 8-position was planned to be performed using Sonogashira cross-coupling conditions. **104** was intended to be achieved by bromination of **105** which could be obtained by *N*-alkylation of commercially available adenine **106** (**Figure 19**). The strategy which would lead to **99** included deprotection of **107**. Compound **107** was planned to be synthesised using a one-pot two-step CuAAC reaction (**108** where R^1 corresponds to an azide). The azide could be introduced by substituting the bromide in **104** with an azide.

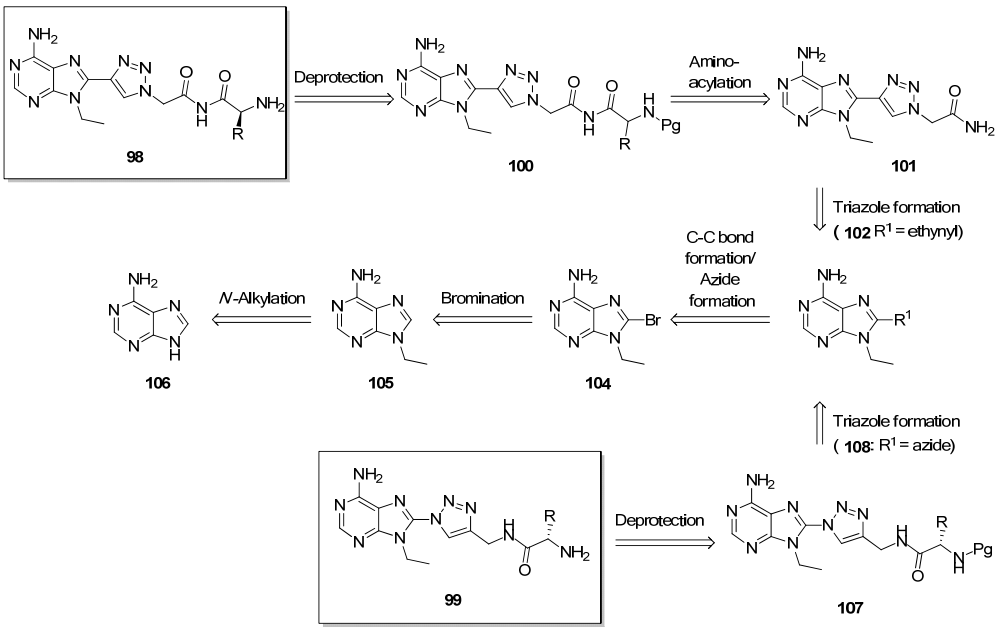

Figure 22. A retrosynthetic plan for the preparation of ribose-free analogues **98** and **99** of aa-AMP. R = amino acid side chain.

Starting from commercially available adenine (**106**), **104** was obtained in two steps using modified literature procedures (**Scheme 14**).[164,165] Compound **104** served as the divergence point

in the synthesis and was used as the starting material for the synthesis of both types of ribose-free purine-based analogues **98** and **99**.

For the synthesis of **98**-type compounds, a Sonogashira cross-coupling was performed to introduce a TIPS-acetylene in the 8-position of **104** using $Pd(PPh_3)_2Cl_2$ (5 mol%) and CuI (20 mol%) as catalysts and amberlite IRA-67 as a base, **103** was obtained in 84% isolated yield. Desilylation of the TIPS-acetylene using polymer supported fluoride afforded **102** in 83% yield. Step e in **Scheme 14** comprised a one-pot two-step synthesis where 2-bromoacetamide was first transformed *in situ* into 2-azidoacetamide using NaN_3 followed by cyclisation with **102**, leading to the triazole formation that afforded **101** in 78% isolated yield.

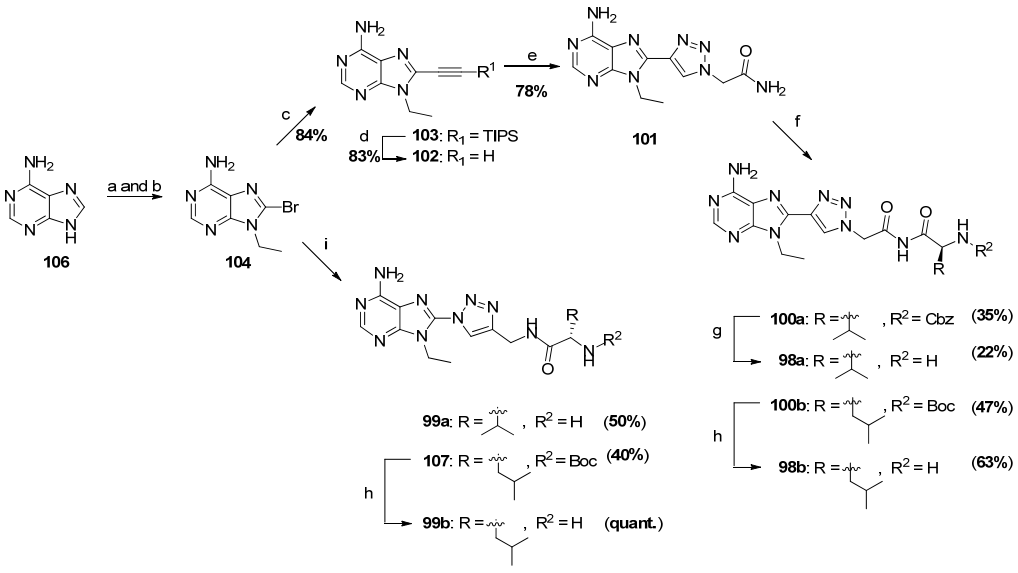

Scheme 14. Synthesis of **98** and **99**. Reagents and conditions: a) ethyl iodide (1.2 equiv), Cs_2CO_3 (1.2 equiv), DMF, 60 °C, 7 h, N_2, 66%. b) Br_2 (8.2 equiv), HOAc buffer (pH ~4), THF, MeOH, rt, 24 h, 67%. c) $Pd(PPh_3)_2Cl_2$ (5 mol%), CuI (20 mol%), amberlite IRA-67 (5 equiv), ethynyltriisopropylsilane (3.3 equiv), THF, MW, 120 °C, 30 min. d) PS-fluoride (2.4–3.6 equiv, 2–3 mmol/g loading), THF, rt, N_2, 24 h. e) one-pot two-step: 1. NaN_3 (1.2 equiv), 2-bromoacetamide (1.1 equiv), DMF, MW, 80 °C, 20 min. 2. **102** (1.0 equiv), NaAscorbate (0.6 equiv), CuI (0.2 equiv), *N*,*N*′-dimethylenediamine (0.3 equiv), MW, 80 °C, 2 h. f) NaH (2.0 equiv), R^2-amino acid-ONp (1.1 equiv), THF, 0 °C 15 min then at rt 3–5 h. g) H-cube® (10% Pd/C wt/wt CatCart, 30x4 mm, 21 °C, 25 min, MeOH, flow rate:1 mL/min). h) 50% TFA in DCM, 1–1.5 h. i) one-pot two-step: 1. NaN_3 (1.8 equiv), DMF, 90 °C, 22 h, dark. 2. Protected propargylamide amino acid derivative (1.4 equiv), NaAscorbate (0.4 equiv), CuI (20 mol%), *N*,*N*′-dimethylenediamine (0.3 equiv), rt, 24 h, dark.

The initial attempts for the acylation of **101** using the activated ester Cbz-Val-ONp and BuLi as base for the formation of imide **100a** failed.[166] The acylation of **101** was instead achieved by the addition of Cbz-Val-ONp (**100a** obtained in 35% yield) or Boc-Leu-ONp (**100b** obtained in 47% yield) in the presence of NaH as a base. Deprotection of **100a** was performed with catalytic hydrogenation using the H-cube® (10% Pd/C as catalyst) in MeOH and resulted in 22% yield of **98a**. The low yield could be attributed to the formation of a by-product corresponding to the methyl ester of **101**, which was detected by LC/MS. The Boc protective group in **100b** was removed under acidic conditions using 50% TFA in DCM and resulted in 63% yield of **98b**. The utilisation of Boc-Leu-ONp for the acylation eliminated the formation of the undesired by-product (methyl ester of **101**) since the use of MeOH (used as solvent for the removal of the Cbz) could be evaded.

The synthesis of **99**-type compounds consisted of a one-pot two-step synthesis (step i in **Scheme 14**) where **104** was first converted to the azide using NaN_3 followed by Cu-catalysed cyclisation with *N*-protected amino acid derivatives bearing an alkyne at the *C*-terminal. The Cbz-Val propargylamide and the Boc-Leu propargylamide used in step i were synthesised following previously described procedures.[167,168] The cyclisation reaction with Cbz-Val propargylamide in step i resulted in *in situ* deprotection of the Cbz protective group and product **99a** was obtained in 50% isolated yield. At first, Cbz-Leu propargylamide was used in the cyclisation reaction step (data not shown), which also resulted in deprotection, however **99b** was only isolated in 4% yield after extensive purification. Performing the cyclisation using Boc-Leu propargylamide resulted in isolation of **107** in 40% yield. Deprotection of **107** using 50% TFA in DCM yielded the TFA salt of **99b** in quantitative yield.

7.2.3 Isothermal Titration Calorimetry

Isothermal titration calorimetry (ITC) is a common technique that is used to measure the binding affinity of a ligand to a specific interaction site (e.g. a binding site in a protein).[169] ITC measures the energy change associated with stepwise addition of a known concentration of a ligand to a protein (see **Appendix D**). The interaction between the ligand and the protein, which results from each addition either releases or absorbs a certain amount of heat (Q) proportional to the amount of ligand that binds to the protein in a particular injection. As the system reaches saturation, the heat signal diminishes until only the heats of dilution are observed. The ITC instruments operate on the heat compensation principle, meaning that the power (μcal/sec) required for maintaining a constant temperature is the measured signal and the heat after each injection is obtained by

calculating the area under each peak. The measurement of heat allows determination of the binding or dissociation equilibrium constant (K_{eq}), reaction stoichiometry (n) and changes in enthalpy (ΔH), entropy (ΔS) and free energy (ΔG) of the ligand association.[170]

7.2.4 Biological Evaluation of Ribose-Free Purine-Based Analogues

Biological evaluation of compounds **98b** and **99b** was performed using ITC to measure the strength of the ligand–protein interaction. The protein used for the experiments was leucinyl-tRNA synthetase (LeuRS) isolated from *E. coli*. The heat produced by the binding interaction between the ligands and the enzyme was measured, Part **A** of **Figure 23** illustrates the calorimetric titration of LeuRS with ligand **99b**. Part **B** of **Figure 23** shows the ligand concentration dependence of the heat released upon binding (circles) together with the best fit (line). Unfortunately, ligand **98b** did not bind to the LeuRS probably due to a presumed stability problems.

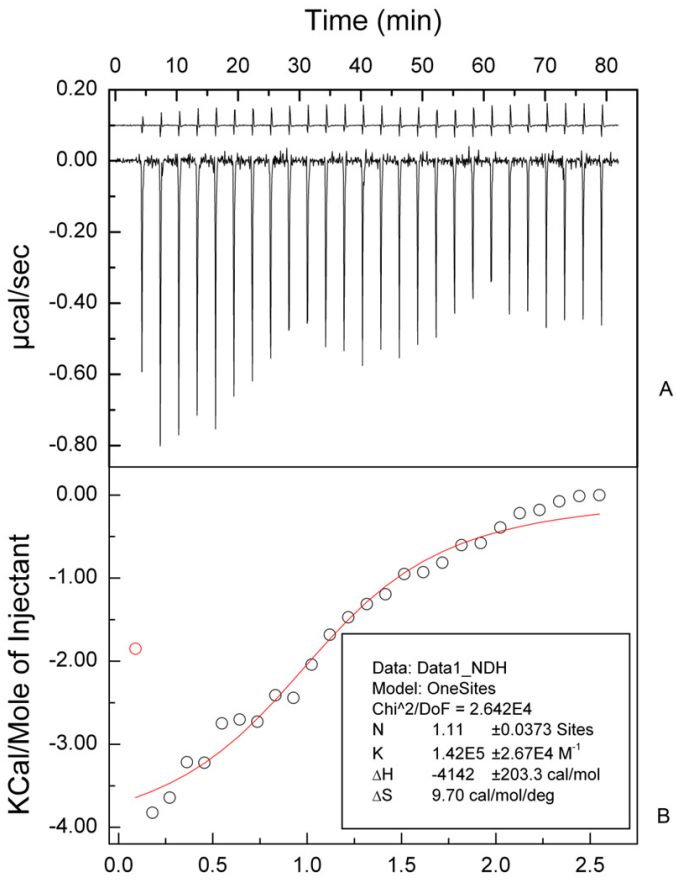

Figure 23. Biological evaluation of ligand **99b**. **A** shows the heat effects associated with the ITC of the leucyl-tRNA synthetase (LeuRS) from *E. coli* with ligand **99b**. **B** shows the corresponding ligand concentration dependence of the heat released upon binding together with the best fit.

The stoichiometry of binding for ligand **99b** was determined to be one (N value approximately 1 in **Figure 23**), corresponding to one binding site for each LeuRS. The negative enthalpy (approximately -4 kcal/mol or -17 kJ/mol) obtained from the ITC experiment was low to moderate compared to other inhibitors of LeuRS (personal communication) and corresponds to polar interactions (hydrogen bonds, electrostatic or van der Waals interactions) formed upon binding (**Figure 23**). The entropy value obtained for the binding of **99b** (9.70 cal/mol/deg) was positive, which is a good indication of a release of water from the binding site of LeuRS as a result of binding of ligand **99b**.

7.3 Conclusion

This study comprised the design of two types of ribose-free purine-based analogues of aminoacyl-AMP **1**. The designed analogues **98** and **99** were docked into the X-ray structure of LeuRS and revealed promising geometries compared to the sulfamoyl-based co-crystallised substrate **17j**. The designed ligands were synthesised and compared to compounds **17**, fewer reaction steps were required to reach the target compounds and extensive purification was not required. In total, four novel ribose-free purine-based analogues of **1** were synthesised and isolated in yields varying from 22% to quantitative yields for the final deprotection step. Furthermore, the synthesised analogues **98b** and **99b** were evaluated using ITC which quantified the ligand binding in LeuRS isolated from *E. coli*. Unfortunately, no conclusions could be made about the binding of **98b** to LeuRS due to a presumed stability problem of the ligand. Ligand **99b** exhibited low to moderate binding to LeuRS compared to other LeuRS inhibitors (personal communication). Comparing the structures of **17j** and **99b**, the moderate binding of **99b** could be attributed to the absence of the ribose and sulfamoyl groups.

8

A Mild and Efficient Method for Activation and Recycling of Trityl Resin

(Paper IV)

8.1 Introduction

In Chapter 5 (section *5.2.2*), the use of TEOTFB in order to pre-form a resin-bound triphenylmethyl (trityl, Tr) carbocation prior to the attachment of 2′,3′-*O*-benzylideneadenosine (**69**) was performed. Even though the desired attachment was only achieved in 7% yield, discovery of the possibility of activating of PS-Tr-Cl was intriguing. This chapter describes a rapid and mild strategy for the attachment of alcohols and anilines to a tritylated polystyrene resin followed by the regeneration of the resin used in the reaction. The trityl group is widely used as a protective group for hydroxyl and amino functions since it is easily introduced and highly acid labile and therefore easily removed using dilute acid.[55,171] Since mild acidic conditions can be employed for the removal of the trityl moiety, protective groups (such as the Boc group) which require stronger acidic conditions for their removal can remain intact.[172] Therefore the simultaneous use of trityl resin as a protective group and linker would be beneficial. Literature procedures which describe the formation of trityl ethers have limitations mainly due to the long reaction times, or the harsh and/or basic reaction conditions that are required.[173] Silver triflate-assisted anchoring of alcohols to PS-Tr-Cl has recently been described, but the formation of an insoluble precipitate of silver chloride on the resin and the partial degradation of acid-sensitive alcohols can be problematic using the reported procedure.[174] In addition, activation of PS-Tr-OH using excess acetyl bromide for the preparation of PS-Tr-Br has also been reported.[175]

To the best of our knowledge, very few methods for recycling of the recovered trityl resin can be found in the literature. The reaction conditions reported for the regeneration of PS-Tr-Cl from PS-Tr-OH include the use of trimethylsilyl chloride as a reagent and refluxing for 10 h,[176] use of excess acetyl chloride as reagent and refluxing overnight,[177] or treatment with thionyl chloride at room temperature for one hour.[178] Although the use of solid-phase methodologies is common in

organic synthesis, the price of solid-phase materials is still relatively high thus, recycling of the recovered resin after completing a reaction cycle would be environmentally friendly and cost efficient. In addition to the cost savings, a fast recycling process that would be compatible with existing methods and instrumentation and allow *in situ* processing of the support without requiring removal from the synthesis column or synthesiser would be beneficial. In the present study procedures for the use of a tritylated polystyrene resin as a protecting group of alcohols and amines during synthetic manipulations were developed. A retrosynthetic plan for an efficient attachment of alcohols and amines to the resin was developed as illustrated in **Scheme 15**. A procedure for recycling of the resin after use was also developed.

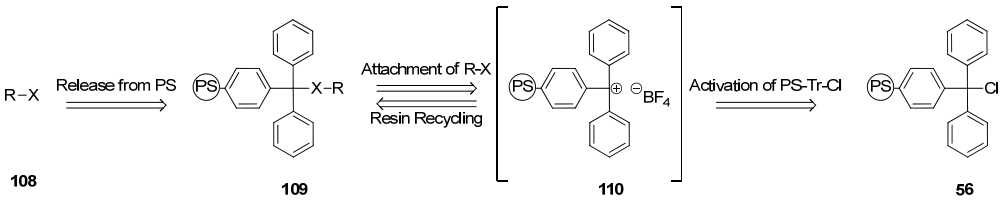

Scheme 15. A retrosynthetic plan for the attachment of alcohols (R-X = R-OH) and anilines (R-X = Ar-NH_2)

8.2 Results and Discussion

8.2.1 Development of an Efficient Method for Trityl Resin Activation

Tritylation of alcohols is typically performed by exposing the alcohol to trityl chloride using pyridine as a solvent at room temperature.[179,180] There are two different mechanisms suggested in the literature (**Scheme 16**). One suggests that pyridine is involved by reacting with the hydrogen chloride (HCl) that is released as a result of the dissociation of trityl chloride and the incorporation of the alcohol (via reaction intermediate **111**).[181] The other suggestion is that the reaction occurs via a tritylpyridinium chloride intermediate (**112**) and that the formation of **112** is the rate determining step.[173]

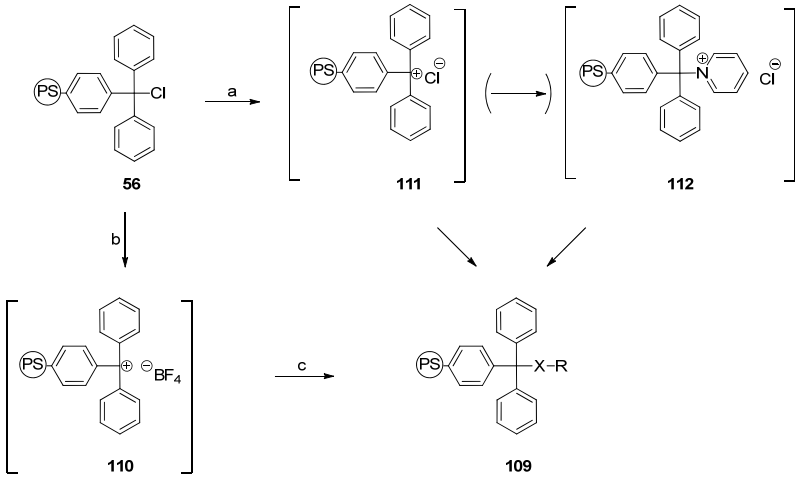

Scheme 16. Loading of alcohols to a PS-trityl resin resulting in **109** where R-X = R-OH. Reagents and conditions: a) R-X (R-X = MeOH), pyridine, rt, 2 d. b) TEOTFB (3 equiv, 0.35 M in DCM), rt, N_2, 15 min. Followed by thorough washing with DCM. c) Alcohol (3 equiv, R-X = R-OH), DIPEA (3 equiv), rt, N_2, 16 h.

An alternative method for the activation of PS-Tr-Cl (**56**) was performed in the present study using triethyloxonium tetrafluoroborate (TEOTFB) that was proposed to result in the formation of a reactive trityl cation intermediate (**110**). The mild[182,183] method comprised the treatment of resin **56** with TEOTFB (**Scheme 16**, path b), which resulted in a deep red coloured resin. After standing for 15 min, the activated resin **110** was washed thoroughly with DCM, followed by the addition of the alcohol and DIPEA that resulted in an instant colour change (from a deep red to light yellow resin). The optimal reaction conditions for the trityl ether formation via intermediate **110** were investigated (**Table 5**). The binding and cleavage of 2,2-diphenylethanol was studied as a model system.

Table 5. Investigation of the reaction conditions for the attachment of 2,2-diphenylethanol (**108a**) to resin **56**.[a]

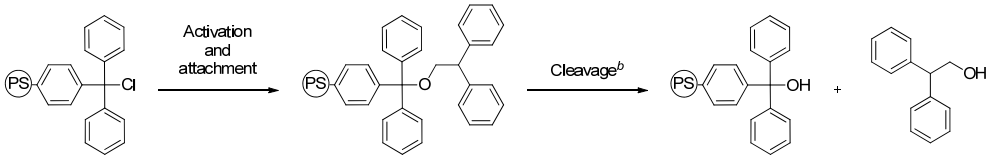

Entry	TEOTFB[b] (equiv)	Activation (min)	108a (equiv)	DIPEA (equiv)	Loading (min)	Loading[c] (%)
1	3	15	3	3	10	86
2	3	15	3	3	60	84
3	3	15	3	3	180	89
4	3	30	3	3	60	86
5	3	15	3	3	960	89
6	5	15	3	3	60	86
7	5	15	5	5	60	84

[a]**56** (300 mg, loading ~1.7 mmol/g) in DCM.

[b]A solution of TEOTFB in DCM was used (0.35 M).

[c]The loading was calculated by recovered weight of **108a** after cleavage from the resin using 5% TFA in DCM and the loading specified by the supplier.

The investigated parameters included the amount of TEOTFB, activation time, amount of substrate (2,2-diphenylethanol, **108a**), amount of DIPEA and reaction time. The results summarised in **Table 5** indicated that variation of the amount of TEOTFB, activation time, amount of **108a**, amount of DIPEA and loading time had no or very little influence on the acquired yields of the alcohol after cleavage. The developed activation method of resin **56** using TEOTFB was applied on a variety of different substrates such as primary alcohols, secondary alcohols and different anilines (**Scheme 17**).

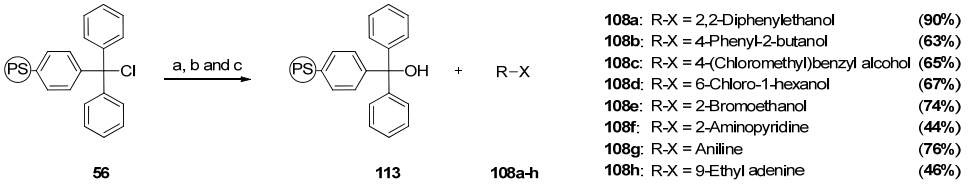

Scheme 17. PS-Tr-Cl (**56**) activation, attachment of alcohol (R-X = R-OH) or aniline (R-X = Ar-NH_2) and cleavage of alcohol (R-X = R-OH) or aniline (R-X = Ar-NH_2). Reagents and conditions: a) TEOTFB (3 equiv, 0.35M in DCM), rt, N_2, 15 min, followed by thorough washing with DCM. b) alcohol (3 equiv, R-X = R-OH) or aniline (3 equiv, R-X = Ar-NH_2), DIPEA (3 equiv), rt, N_2, 16 h. c) 2 × 5% TFA in DCM, rt, N_2, 25 min total. The recovered yield was quantified by weight after cleavage of substrates **108a–h** using the resin loading specified by the supplier.

The attachment of compounds **108a**–**h** using the developed activation method was achieved in 44–90% isolated yields as determined by the recovery of the alcohols/anilines after resin cleavage. The yields obtained using TEOTFB activation are comparable with those of other procedures.[174] Halogen-containing alcohols **108c**, **d** and **e** were included to demonstrate the scope of the method. To the best of our knowledge, very few methods can be found in the literature that describes the loading of aromatic amines (e.g. **108f**, **g** and **h**) to a trityl resin. These relatively poor nucleophiles require excess of a base (i.e. 10 equiv DIPEA) and/or long reaction times for the attachment to proceed in high yields.[184] The yields obtained for the attachment of **108f**, **g** and **h** using TEOTFB activation in the presence of DIPEA (3 equiv) ranges between 44–76% (based on the recovered anilines after cleavage). The developed activation method for the attachment of alcohols and anilines is beneficial due to the short activation time, small amounts of reagents needed, short reaction times, and no formation of precipitates.

8.2.2 Development of an Efficient Method for Trityl Resin Recycling

As discussed in Section *8.1.1*, recycling the resin after completing a reaction cycle would be advantageous, especially for large-scale synthesis on solid-phase. A procedure for activation of the trityl resin, attachment of substrate (**108a**), cleavage of product and recycling of the resin is shown in **Scheme 18**.

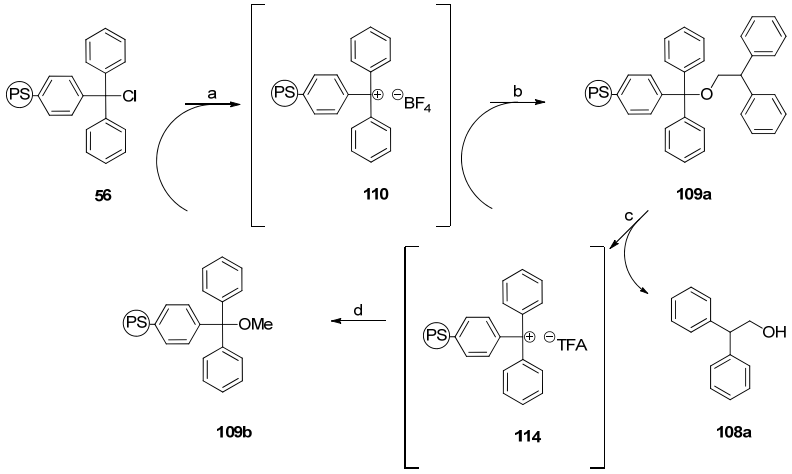

Scheme 18. Activation of PS-Tr-Cl (**56**), attachment and cleavage of **108a** followed by recycling of PS-Tr-OMe (**109b**). Reagents and conditions: a) PS-Tr-Cl, (300 mg, loading ~ 1.7 mmol/g), TEOTFB (3 equiv, 0.35M in DCM), rt, N_2, 15 min. Followed by thorough washing with DCM. b) **108a** (3 equiv), DIPEA (3 equiv), rt, N_2, 16 h. c) 2 × 5% TFA in DCM, rt, N_2, 25 min in total. d) Resin quenched with MeOH.

Resin **56** was activated using the developed TEOTFB method (path a, **Scheme 18**), the attachment and cleavage of alcohol **108a** was performed (paths b and c, **Scheme 18**) and excess anhydrous MeOH was added (path d, **Scheme 18**). Resin **109b** was washed thoroughly with MeOH and DCM then dried under high vacuum before it was re-activated using TEOTFB. The same batch of resin was recycled five times using the method demonstrated in **Scheme 18**. Furthermore, the possibility of recycling directly from resin **114** was investigated. Resin **114** was washed thoroughly with DCM after cleavage of **108a**, and then re-used three times. The yields for both investigated methods are summarised in **Table 6**.

Table 6. Isolated yield for recycling PS-Tr resin starting from **109b** and **114**.

Resin[a]	Cycle 1[b] (%)	Cycle 2[b] (%)	Cycle 3[b] (%)	Cycle 4[b] (%)	Cycle 5[b] (%)
109b	90	58	58	42	20
114	90	58	58	-	-

[a]Resin **56** (300 mg, loading ~ 1.7 mmol/g), the same batch of resin in all cycles.

[b]The yield was calculated by weight of recovered alcohol **108a** after cleavage using the resin loading specified by the supplier.

The yield for recycling resin **109b** and **114** was highest after the first cycle (90%), followed by a radical decrease in yields in the subsequent cycles. The drop in the yields for recycling resin **109b** can be explained by the presence of trace amounts of water during the activation using TEOTFB which results in the formation of ethanol as a by-product. The ethanol can in turn react with intermediate **110** and ethyl trityl ether is obtained. The decrease in yield observed for the recycling of resin **114** can also be explained by the presence of water, which in this case results in formation of resin **113** as a by-product. The decrease in yield will be discussed further below.

8.2.3 Elucidation of the Intermediates Involved in Recycling Trityl Resin

To elucidate the accurate identity of the intermediates, when the trityl resin is recycled using the method described in **Scheme 18** the same reactions were repeated in solution and the isolated products were characterised by NMR spectroscopy (**Scheme 19**). To confirm the hypothesised mechanism for recycling of the resin via **109b**, methyl trityl ether (**116**) was exposed to TEOTFB which led to the observation of a bright yellow reaction mixture (path b, **Scheme 19**). The colour disappeared instantly upon the addition of **108a** and trityl ether **118** was obtained in 20 % isolated yield. The low yield could be caused by the formation the HBF_4 as by-product that due to its acidic properties can hydrolyse the desired product. Increasing the amount of TEOTFB or heating the reaction mixture led to the formation of the ethyl ether of **108a** and triphenylmethane respectively (data not shown). The mechanism involves alkylation of the oxygen atom of **116**, followed by dissociation which results in the formation of **117** and ethyl methyl ether. This suggested mechanism explains the decrease in yield obtained and summarised in **Table 6** when resin recycling was investigated (section *8.2.2*). The formed polymer supported ethyl trityl ether is sterically hindered and therefore the suggested alkylation of the ether oxygen is suppressed.

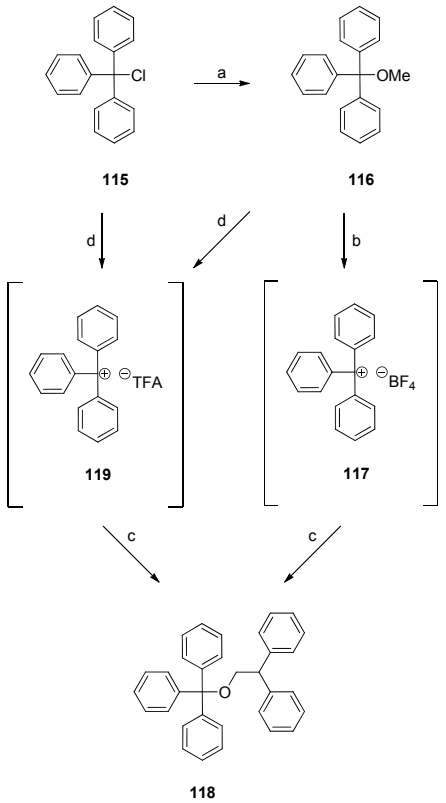

Scheme 19. Reaction pathways for the formation of trityl ether **118**. Reagents and conditions: a) MeOH, reflux, 3 h.[185] b) TEOTFB (0.9 equiv), DCM, rt, 15 min. c) **108a** (1 equiv). d) 5% TFA in DCM, rt, 15 min.

The formation of ether **118** was also confirmed performing the synthesis via intermediate **116** starting from trityl chloride (**115**) and **116** (path d, **Scheme 19**). Starting from **116**, it is assumed that TFA activation contributes to the formation of HCl gas which is released and intermediate **119** is obtained. The suggested mechanism for TFA activation starting from **116** is based on an assumed protonation of the ether oxygen followed by dissociation of methanol which results in **119**. The later mechanistic suggestion implies that the decreased yield for resin recycling using TFA which is summarised in **Table 6** can be explained by the presence of water, which can be assumed to react with resin **114** and result in formation of **113** as by-product.

8.3 Conclusion

This chapter concerned the development of an efficient method for trityl resin activation and recycling. The developed method comprised the use of TEOTFB as a reagent for the desired activation of PS-Tr-Cl which resulted in the formation of a reactive resin-bound intermediate **110**. The attachment of different substrates including primary alcohols, secondary alcohols, halogen-containing alcohols and anilines was performed and the obtained yields after cleavage of the substrates ranged from 44–90%. Furthermore, resin recycling was investigated in parallel using two different methods, one using TEOTFB and the other employing TFA as reagents. The highest yield (90%) was obtained in the first cycle using both methods. The drastic decrease in the yields obtained in the following cycles can be assumed to be a result of water present in the reaction mixtures that causes the regeneration to stop. To confirm the accurate identity of the hypothesised intermediates in the suggested reactions steps, reactions were performed in solution and the products were characterised by NMR spectroscopy.

9

Concluding Remarks and Future Perspectives

This thesis focused on the design and development of synthetic routes leading to non-hydrolysable analogues of aa-AMP. Aa-AMP is considered to be the key intermediate in the synthesis of aminoacyl-tRNAs which is catalysed by the aaRSs.

Novel solution-phase and solid-phase protocols for the synthesis of sulfamoyl-based analogues of aa-AMP were presented in Chapters 4 and 5. Further development of a protective group strategy that would enable even milder deprotection conditions than those presented here would be advantageous. Docking studies in *Brugia* asparginyl-tRNA synthetase have been performed in collaboration with Prof. Leslie Kuhn's group for the identification of potential lead compounds useful for development of drugs against lymphatic filariasis. The analysis suggests that the introduction of a C2-substituent in the adenine subunit is the best way to gain specificity for the *Brugia* tRNA synthetase. The synthesis of a focused library of follow up compounds and their biological evaluation would be the next logical step in the progression of this project. Potentially useful compounds derived from the follow up study can then be optimised to improve binding, potency, solubility and other pharmacokinetic properties.

Conformational analysis was used to identify the potential bioactive conformation of the aaRS inhibitors. The derived model was used to evaluate existing analogues and to design novel analogues of aa-AMP. Synthesis and biological evaluation of the designed compounds would make an exciting subject of future research.

Novel ribose-free purine-based aa-AMP analogues were designed, synthesised and evaluated in a biological assay. An extended series of compounds will be synthesised in order to study the SAR concerning this type of derivatives.

A mild efficient activation and recycling method for trityl resin was discovered during the experimental work presented in the thesis. Further optimisation of the trityl resin activation and recycling using trimethyloxonium tetrafluoroborate as the activating reagent is needed, for example by exclusion of moisture to eliminate the possibility of the side-reaction discussed in Chapter 8.

A beneficial long-term aim of this thesis project would be the design and synthesis of a potent low molecular weight compound that is selective for *Brugia* tRNA synthetase. The establishment of relevant in-house biological assays for the quick evaluation of synthesised compounds against different aaRSs would be desirable for more efficient development of aaRS inhibitors.

10

Acknowledgements

I would like to express my deepest gratitude to the following people, who have all given me their support, in one way or the other, during these years:

First of all my supervisor, Docent **Morten Grøtli**, for the never-ending stream of advice, encouragement, enthusiasm and support. I would not have chosen anyone else as an advisor for the roller-coaster ride that earning a Ph.D. has involved.

My co-supervisor, Professor **Kristina Luthman**, for the valuable advice, generous support, exceptional guidance and inspiration that have been of great importance to me.

My examiner, Professor **Ann-Therese Karlberg**, for contributing with invaluable criticism on the projects, seeing the overall picture and for providing much knowledge.

Collaborators Professor **Leslie Kuhn**, Professor **Stephen Cusack** and Doctor **Andrés Palencia Carrilero**.

All my colleagues involved in proofreading of the manuscripts and this thesis.

My hardworking and irreplaceable diploma worker **Hanna Jacobson Ingemyr** and colleagues **Thomas Ljungdahl**, **Charlotte Johansson**, **David Bliman**, **Susanne Olsson** and **Christopher Lawson** who have contributed to the projects.

Professor **Per-Ola Norrby**, Associate Professor **Mate Erdelyi** and Professor **Johan Gottfries** for taking time to discuss chemistry problems and providing valuable advices.

Former and present members of the Medicinal Chemistry group, **Fariba Jam**, **Marcus Malo**, **Kristina Berggren**, **Maria Fridén-Saxin**, **Christine Dyrager**, **Tina Seifert**, **Mariell Pettersson** and the list goes on…..

Former and present members of the Organic Chemistry and Dermatochemistry groups (eighth and ninth floors), for providing a friendly, stimulating working environment and letting me use their equipment.

My beloved friends, for their patience, support, encouragement and understanding during the past years.

My family, **Firas**, **Jasmin** and **Adam**, the most supportive and loving parents, **Walid** and **Sahira**, and my brothers and sister **Ibrahim**, **Hadi**, and **Natalie**. None of this could have happened without your constant love, support and everlasting source of joy.

Last but not least, the Department of Chemistry and Molecular Biology at University of Gothenburg, the Swedish Academy of Pharmaceutical Sciences and the Swedish Research Council for financial support.

11. Appendices

Appendix A

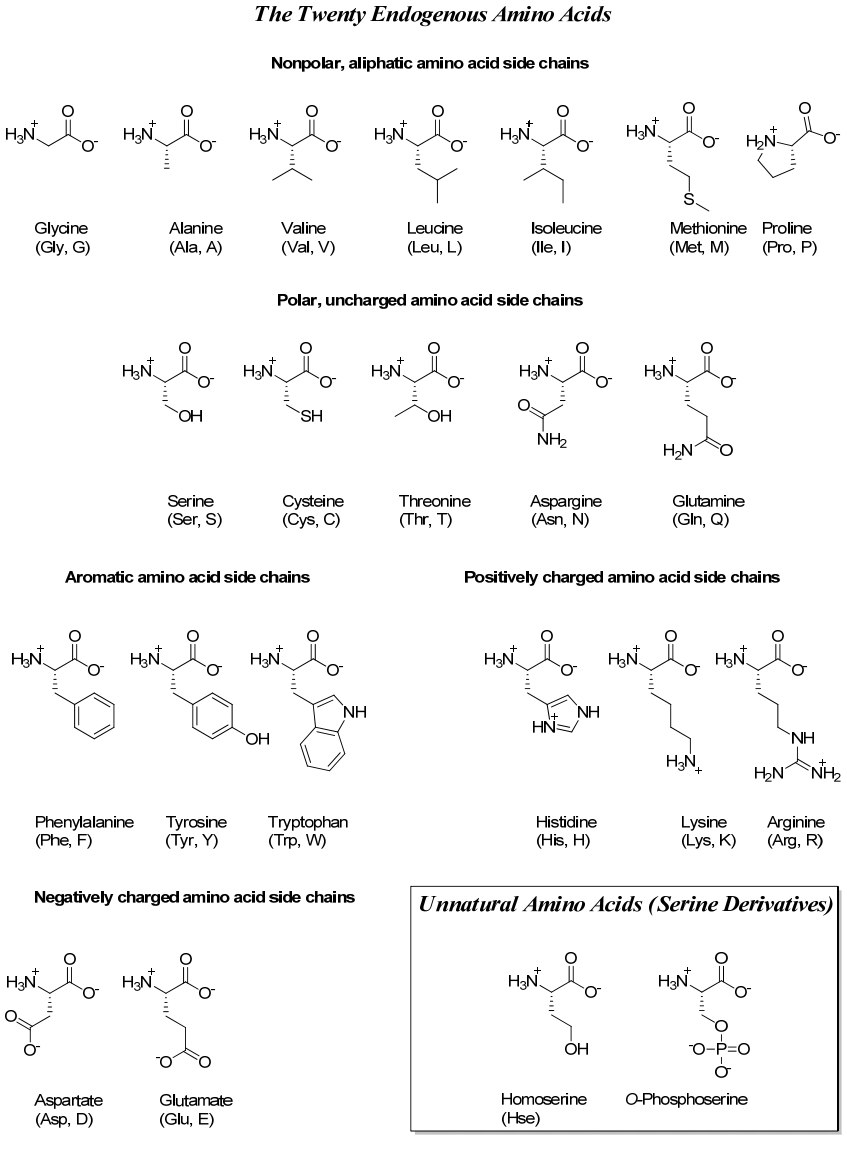

Appendix B

Synthesis of Sulfamoyloxy-Linked N-Terminally Modified Aminoacyl-AMP Analogues

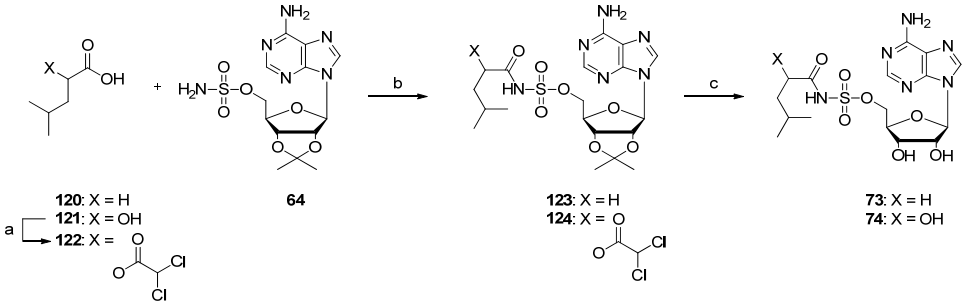

Scheme B1. Synthesis of target compounds **73** and **74**. Reagents: a) Dichloroacetyl chloride (12.5 equiv), 110 °C, 4 h. b) PS-DCC (2 equiv), DMAP (1.5 equiv), rt, 20 h. c) TFA:water (2:4, v/v).

Experimental Procedure

General

All commercial chemicals were used without prior purification. Dichloromethane was distilled from calcium hydride. All reactions were followed by TLC (Merck silica gel 60 F_{254}) and analysed under UV light (254 nm). Column chromatography was performed by manual flash chromatography (wet packed silica, 0.04–0.063 mm) or by automated column chromatography on a Biotage SP-4 instrument using pre-packed columns. Preparative HPLC was carried out on a Waters 600 controller connected to a Waters 2487 Dual λ Absorbance detector using a Atlantis® Prep T3 5 µm C-18 (250 × 19 mm) column. ^{1}H (400 MHz) and ^{13}C (100 MHz) NMR spectra were recorded using a JEOL JNM-EX 400 spectrometer.

(*S*)-2-(2,2-Dichloroacetoxy)-4-methylpentanoic acid (122). (*S*)-2-Hydroxy-4-methylpentanoic acid (0.2 g, 1.6 mmol, **121**) was added to dichloroacetyl chloride (2.0 mL, 20.0 mmol) and heated to 110 °C for 4 h. The excess dichloroacetyl chloride was removed in vacuo. Purification by column chromatography (MeOH:DCM gradient 2-20% v/v) gave compound **122** as a colourless oil (0.3 g, 1.2 mmol, 75%). ^{1}H NMR ($CDCl_3$) 0.98 (s, 3H, C*H*$_3$), 0.99 (s, 3H, C*H*$_3$), 1.79–2.00 (m, 3H, C*H*(CH_3)$_2$ and C*H*$_2$), 5.19 (dd, 1H, *J* = 10.0, 3.6 Hz, C*H*CH_2), 6.01 (s, 1H, C*H*(Cl)$_2$).

2′,3′-Isopropylidene-5′-*O*-sulfamoyladenosine (64). Using a modified literature procedure,[106] water (0.4 mL) was added drop-wise to an ice-cooled solution of chlorosulfonylisocyanate (2.0 mL, 23.0 mmol) in acetonitrile (20 mL). The mixture was allowed to reach room temperature and stirred for 15 min. The solution was concentrated in vacuo by co-distilling with toluene (20 mL) yielding chlorosulfonamide as white crystals (2.6 g, 22. 5 mmol, 98% crude yield). 2′,3′-Isopropylideneadenosine (2.0 g, 6.5 mmol) was suspended in DCM (20mL) and DBU (2.0 mL, 22.5 mmol) was added. Chlorosulfonamide was suspended in DCM (10mL) and added drop-wise to the reaction mixture for 10 min. The solution was stirred for 15 h and the solvent was removed under reduced pressure. Purification by column chromatography (MeOH:ethyl acetate 1:9 v/v) gave the sulfamate **64** as a light yellow-green solid (2.4 g, 6.3 mmol, 97%). NMR data were in agreement with published data.[106]

2′,3′-*O*-Isopropylidene-5′-*O*-[(4-methylpentyl)sulfamoyl]adenosine (123). 4-Methyl pentanoic acid (0.2 mL, 1.5 mmol, **120**) was suspended in DCM (7 mL), PS-DCC (1.3 g, 2 mmol, 1.6 mmol/g) was added and the reaction mixture was agitated gently for 1 h. Sulfamate **64** (0.2 g, 0.5 mmol) and DMAP (0.2 g, 1.5 mmol) were dissolved in DCM/DMF (2 mL, 3:1 v/v) and added drop-wise to the reaction flask. The reaction mixture was agitated at room temperature for 15 h. The resin was filtered off and washed with DCM (3 × 4 mL) and MeOH (3 × 4 mL). The combined filtrate was concentrated in vacuo. Purification by column chromatography (MeOH:DCM gradient 2–20% v/v) gave compound **123** as white crystals (0.2 g, 0.4 mmol, 80%). ^{1}H NMR (DMF-d_7) δ 0.84 (d, 6H, J = 6.59 Hz, $CH_2CH(CH_3)_2$), 1.39–1.57 (m, 3H, $CH_2CH(CH_3)_2$), 1.38 (br s, 3H, CH_3 isopropylidene), 1.58 (s, 3H, CH_3 isopropylidene), 2.10-2.16 (m, 2H, $CH_2CH_2CH(CH_3)_2$), 4.18–4.27 (m, 2H, CH_2-5′), 4.48–4.52 (m, 1H, C*H*-3′), 4.91–4.97 (m, 1H, C*H* $CH_2CH(CH_3)_2$, 5.17 (dd, 1H, J = 2.56, 6.22 Hz, C*H*-4′), 5.48 (dd, 1H, J = 2.93, 5.86 Hz, C*H*-2′), 6.30 (d, 1H, J = 2.93 Hz, C*H*-1′), 8.21 (s, 1H, C*H*-2), 8.54 (s, 1H, C*H*-8). ^{13}C NMR (DMF- d_7) δ 22.2, 24.9, 26.9, 27.8, 37.6, 82.3, 84.4, 84.6, 90.1, 113.6, 119.6, 140.1, 149.7, 153.1, 156.7.

2′,3′-*O*-Isopropylidene-5′-*O*-[(*S*)-2-(2,2-dichloroacetoxy)-4-methylpentyl)sulfamoyl]adenosine (124). Compound **122** (0.3 g, 1.0 mmol) was suspended in DCM (7 mL) and PS-DCC (1.3 g, 2 mmol, 1.6 mmol/g) was added and the reaction mixture was agitated gently for 1 h. 2′,3′-Isopropylidene-5′-*O*-sulfamoyladenosine **64** (0.2 g, 0.5 mmol) and DMAP (0.2 g, 1.5 mmol) were dissolved in DCM/DMF (2 mL, 3:1 v/v) and added drop-wise to the reaction flask. The reaction mixture was agitated at room temperature for 20 h. The resin was filtered off and washed with DCM (3 × 4 mL) and MeOH (3 × 4 mL). The combined filtrate was concentrated in vacuo. Purification by column chromatography (MeOH:DCM gradient 2–20% v/v) gave compound **124** as white crystals (0.2 g, 0.4 mmol, 80%). ^{1}H NMR (DMF-d_7) δ 0.90 (d, 3H, J = 5.86 Hz, $CH_2CH(CH_3)_2$), 0.93 (d, 3H, J = 6.20 Hz, $CH_2CH(CH_3)_2$), 1.38 (s, 3H, CH_3 isopropylidene), 1.58 (s, 3H, CH_3 isopropylidene), 1.70–1.82 (m, 3H, $CH_2CH(CH_3)_2$), 4.19 (d, 2H, J = 4.39 Hz, CH_2-5′), 4.49–4.54 (m, 1H, CH-3′), 4.91–4.97 (m, 1H, CH $CH_2CH(CH_3)_2$, 5.14 (dd, 1H, J = 2.20, 6.22 Hz, CH-4′), 5.41 (dd, 1H, J = 3.30, 5.86 Hz, CH-2′), 6.28 (d, 1H, J = 3.30 Hz, CH-1′), 6.92 (s, 1H, C$H(Cl)_2$), 8.21 (s, 1H, CH-2), 8.57 (s, 1H, CH-8). ^{13}C NMR (DMF-d_7) δ 21.2, 23.0, 24.9. 27.0, 40.1, 40.7, 65.6, 65.7, 75.9, 77.7, 82.4, 84.4, 90.1, 113.5, 139.8, 153.1, 156.7, 164.5, 164.6, 173.3.

(*2RS*)-*5′-O*-[(4-Methylpentyl)sulfamoyl]adenosine (73). Compound **123** (87 mg, 0.2 mmol) was stirred in water/TFA (2 mL, 2:4, v/v) for 60 min at room temperature. The TFA was removed by a stream of nitrogen gas for 15 min. The residual water was removed by freeze drying. The crude product was purified using preparative HPLC (100% A to 100% B in 45 min then 15 min 100% B; A corresponding to 0.1% TFA in MQ water and B corresponding to 0.1% TFA in AcCN, flow rate 14 mL/min) yielding **73** (30 mg, 0.07 mmol, 35%). ^{1}H NMR (DMF-d_7) δ 0.84 (d, 3H, J = 2.20 Hz, $CH_2CH(CH_3)_2$), 0.86 (d, 3H, J = 2.20 Hz, $CH_2CH(CH_3)_2$), 1.42–1.59 (m, 3H, $CH_2CH(CH_3)_2$), 2.37–2.43 (m, 2H, $CH_2CH_2CH(CH_3)_2$), 4.32–4.37 (m, 1H, CH_2-3′), 4.45 (m, 1H, CH-4′), 4.61–4.68 (m, 2H, CH_2-5′) 4.78 (t, 1H, J = 5.13 Hz, CH-2′), 6.14 (d, 1H, J = 5.13 Hz, CH-1′), 8.54 (s, 1H, CH-2), 8.67 (s, 1H, CH-8). ^{13}C NMR (DMF-d_7) δ 21.9, 27.6, 33.6, 33.9, 70.9, 72.0, 74.4, 82.2, 88.8, 119.6, 141.2, 147.7, 149.3, 162.8, 171.9. HRMS m/z $[M + H]^+$ calculated for $C_{16}H_{24}N_6O_7S$: 445.1498. Found: 445.1497.

(*2RS*)-5′-*O*-[((*S*)-2-Hydroxy-4-methylpentyl)sulfamoyl]adenosine (74). Compound **124** (118 mg, 0.2 mmol) was stirred in water/TFA (2 mL, 2:4, v/v) for 60 min at room temperature. The TFA was removed by a stream of nitrogen gas for 15 min. The residual water was removed by freeze drying. The crude product was purified using preparative HPLC (100% A to 100% B in 45 min then 15 min 100% B; A corresponding to 0.1% TFA in MQ water and B corresponding to 0.1% TFA in AcCN, flow 14 mL/min) yielding **74** as white crystals (10 mg, 0.02 mmol, 11%). ^{1}H NMR (DMF-d_7) δ 0.89 (d, 3H, J = 4.03 Hz, $CH_2CH(CH_3)_2$), 0.91 (d, 3H, J = 4.03 Hz, $CH_2CH(CH_3)_2$), 1.37–1.60 (m, 3H, $CH_2CH(CH_3)_2$), 4.19–4.24 (m, 1H, $CHCH_2CH(CH_3)_2$, 4.31-4.35 (m, 1H, C*H*-3′), 4.41–4.46 (m, 1H, CH_2-4′), 4.60–4.69 (m, 2H, CH_2-5′), 4.79 (t, 1H, J = 5.13 Hz, C*H*-2′), 6.12 (d, 1H, J = 5.13 Hz, C*H*-1′), 8.35 (s, 1H, C*H*-2), 8.46 (s, 1H, C*H*-8). ^{13}C NMR (DMF-d_7) δ 21.2, 23.3, 24.4, 44.1, 58.9, 70.1, 70.7, 76.2, 84.4, 94.2, 120.2, 139.9, 140.1, 149.6, 157.4, 162.8. HRMS m/z $[M + H]^+$ calculated for $C_{16}H_{24}N_6O_8S$: 461.1447. Found: 461.1447.

Appendix C

All calculations were performed using Macromodel v.9.1 and all superimpositions were performed using Maestro v. 7.5.[186] The conformational search was performed using the systematic torsional sampling (SPMC) method in simulated water and OPLS_2005 as the force field.[147,148] Two different X-ray structures were imported from PDB: 1. **1e1t-** the crystal structure of lysyl-tRNA synthetase in complex with lysyl-adenylate (**Figure 17a**).[145] 2. **1fyf-** the crystal structure of threonyl-tRNA synthetase in complex with a seryl-adenylate analogue (**Figure 17c**).[146] The X-ray structure of lysyl-tRNA synthetase complexed with lysyl-adenylate intermediate (**1e1t**, resolution 2.10 Å) and the X-ray structure of threonyl-tRNA synthetase complexed with a seryl-adenylate analogue (**1fyf**, resolution 1.65 Å) were both from *Escherichia coli*. The ligands in the imported X-ray structures (lysyl-adenylate intermediate and seryl-adenylate analogue) were simplified by the deletion of the amino acid side chains and *N*-terminals. From ligand **95**, nine different conformations were derived and all of which were superimposed with the substrates from the X-ray structures of **1e1t** and **1fyf** (**Figure 17c**). A putative bioactive conformation was derived from the X-ray structures and the bioactive conformation of **95** was superimposed on all derived conformations of **96a**–**h** and **97a**–**i**.

Appendix D

Thermodynamic ITC Experiments

The ITC experiment measures the heat absorbed or evolved when a bonding interaction occurs between a ligand and a receptor/enzyme. **Figure D1** shows a simulated example of raw data that can be obtained from an ITC experiment.[169]

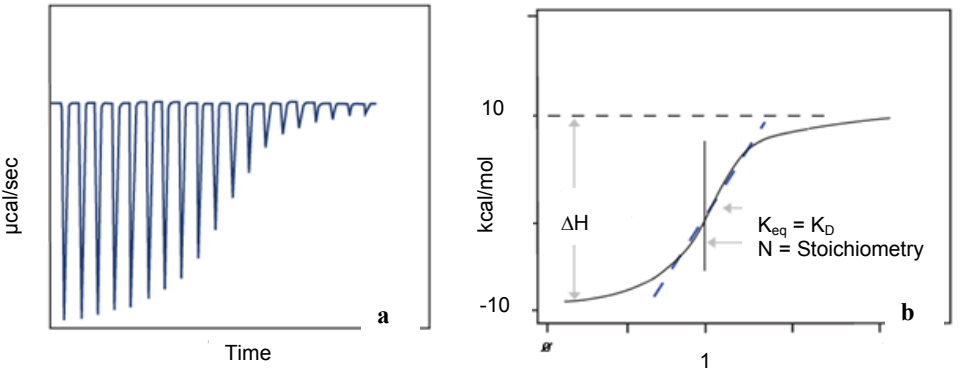

Figure D1a. Simulated raw data and **b**. the theoretical curve fitted to the data (**b**)

The needle shaped peaks in **Figure D1a** correspond to the heat evolved (exothermic interaction) upon the addition of the ligand (known amount and concentration of ligand added in subsequent injections) and each peak represents a single injection. The amount of heat evolved decreases and becomes constant when the receptors are saturated with ligand. The peaks observed after receptor saturation represent the heat of dilution and are subtracted from all peaks before analysis. The corrected area under each peak corresponds to the heat evolved and the amount of heat evolved for the simplest case, in which the protein has one binding site. This can be represented by **Equation D1**.

Equation D1 $$\boldsymbol{Q = V_0 \times \Delta H \times [M]_t \times K_{eq} \times [L]/(1 + K_{eq} \times [L])}$$

Where V_0 = the volume of the cell, ΔH = the enthalpy of binding per mole of ligand, $[M]_t$ = the total protein concentration including bound and free fractions, K_{eq} = the binding constant and $[L]$ = the free ligand concentration.[169,187,188]

Figure D1b shows a simulated example of the integrated data (heat vs. concentration) along with a nonlinear regression fit corresponding to one binding site. The ΔH, K_{eq} and N values can be

determined from the plot. ΔH corresponds to the maximum heat evolved minus the minimum heat evolved. K_{eq} corresponds to the slope of the nonlinear regression fit. The N value corresponds to the theoretical heat produced for the 1:1 complex formation between the ligand and the receptor. A simplified typical interaction between a receptor and ligand is illustrated in **Figure D2**.

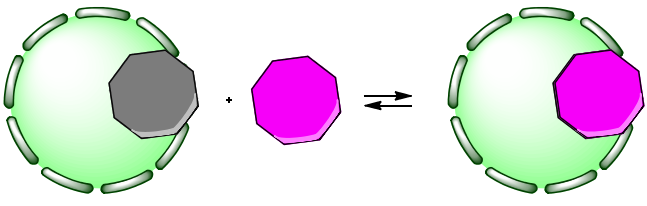

Figure D2. Illustration of a simplified binding interaction between a receptor and a ligand.

There are three entities in equilibrium in solution; free receptor, free ligand and the complex (**Figure D2**). The important thermodynamic relationships are summarised in **EquationD2–4**.

Equation D2 $$\boldsymbol{K_{eq} = \left\{\frac{[Complex]}{[Receptor]} \times [Ligand]\right\}_{equilibrium}}$$

The equilibrium constant K_{eq} corresponds to the relationship calculated using **Equation D2**. The Gibbs free energy change ΔG can be calculated using **Equation D3**.

Equation D3 $$\boldsymbol{\Delta G = -RT \ln K_{eq}}$$

Where R is the universal gas constant, T is the temperature in Kelvin and K_{eq} is derived from **FigureD1b**. The entropy of binding can be derived using **Equation D4**.

Equation D4 $$\boldsymbol{\Delta G = \Delta H - T\Delta S}$$

12. References and Notes

1. Crick, F. H. C. On Protein Synthesis. *Symp. Soc. Exp. Biol.* **1958**, *12,* 138.

2. Doolittle, W. F.; Brown, J. R. Tempo, Mode, the Prognote, and the Universal Root. *Proc. Natl. Acad. Sci.* **1994**, *91,* 6721.

3. Brown, J. R.; Doolittle, W. F. Root of the Universal Tree of Life Based on Ancient Aminoacyl-Transfer-RNA Synthetase Gene Duplications. *Proc. Natl. Acad. Sci.* **1995**, *92,* 2441.

4. Tao, J. S.; Wendler, P.; Connelly, G.; Lim, A.; Zhang, J. S.; King, M.; Li, T. C.; Silverman, J. A.; Schimmel, P. R.; Tally, F. P. Drug Target Validation: Lethal Infection Blocked by Inducible Peptide. *Proc. Natl. Acad. Sci.* **2000**, *97,* 783.

5. Ibba, M.; Soll, D. Aminoacyl-tRNA Synthesis. *Annu. Rev. Biochem.* **2000**, *69,* 617.

6. Park, S. G.; Schimmel, P.; Kim, S. Aminoacyl tRNA Synthetases and their Connections to Disease. *Proc. Natl. Acad. Sci.* **2008**, *105,* 11043.

7. Hausmann, C. D.; Ibba, M. Aminoacyl-tRNA Synthetase Complexes: Molecular Multitasking Revealed. *FEMS Microbiol. Rev.* **2008**, *32,* 705.

8. Schimmel, P. Development of tRNA Synthetases and Connection to Genetic Code and Disease. *Protein Sci.* **2008**, *17,* 1643.

9. Cusack, S.; Berthetcolominas, C.; Hartlein, M.; Nassar, N.; Leberman, R. A 2^{ND} Class of Synthetase Structure Revealed by X-Ray-Analysis of Escherichia-coli Seryl-Transfer RNA-Synthetase at 2.5-Å. *Nature* **1990**, *347,* 249.

10. Eriani, G.; Delarue, M.; Poch, O.; Gangloff, J.; Moras, D. Partition of Transfer-RNA Synthetases into 2 Classes Based on Mutually Exclusive Sets of Sequence Motifs. *Nature* **1990**, *347,* 203.

11. Norris, A. T.; Berg, P. Mechanism of Aminoacyl tRNA Synthesis - Studies with Isolated Aminoacyl Adenylate Complexes of Isoleucyl *t*RNA Synthetase. *Proc. Natl. Acad. Sci.* **1964**, *52,* 330.

12. Baldwin, A. N.; Berg, P. Transfer Ribonucleic Acid-Induced Hydrolysis of Valyladenylate Bound to Isoleucyl Ribonucleic Acid Synthetase. *J. Biol. Chem.* **1966**, *241,* 839.

13. Jakubowski, H.; Goldman, E. Editing of Errors in Selection Amino-Acids for Protein-Synthesis *Microb. Rev.* **1992**, *56,* 412.

14. Rock, F. L.; Mao, W.; Yaremchuk, A.; Tukalo, M.; Crepin, T.; Zhou, H.; Zhang, Y.-K.; Hernandez, V.; Akama, T.; Baker, S. J.; Plattner, J. J.; Shapiro, L.; Martinis, S. A.; Benkovic, S. J.; Cusack, S.; Alley, M. R. K. An Antifungal Agent Inhibits an Aminoacyl-tRNA Synthetase by Trapping tRNA in the Editing Site. *Science* **2007**, *316,* 1759.

15. Schimmel, P.; Tao, J. S.; Hill, J. Aminoacyl tRNA Synthetases as Targets for New Anti-infectives. *FASEB J.* **1998**, *12,* 1599.

16. Kim, S.; You, S.; Hwang, D. Aminoacyl-tRNA Synthetases and Tumorigenesis: More than Housekeeping *Nat. Rev. Cancer* **2011**, *11,* 813.

17. Lee, S. W.; Kang, Y. S.; Kim, S. Multifunctional Proteins in Tumorigenesis: Aminoacyl-tRNA Synthetases and Translational Components. *Curr. Proteomics* **2006**, *3,* 233.

18. Antonellis, A.; Ellsworth, R. E.; Sambuughin, N.; Puls, I.; Abel, A.; Lee-Lin, S. Q.; Jordanova, A.; Kremensky, I.; Christodoulou, K.; Middleton, L. T.; Sivakumar, K.; Ionasescu, V.; Funalot, B.; Vance, J. M.; Goldfarb, L. G.; Fischbeck, K. H.; Green, E. D. Glycyl tRNA Synthetase Mutations in Charcot-Marie-Tooth Disease Type 2D and Distal Spinal Muscular Atrophy Type V. *Am. J. Hum. Genet.* **2003**, *72,* 1293.

19. Nangle, L. A.; Zhang, W.; Xie, W.; Yang, X.-L.; Schimmel, P. Charcot-Marie-Tooth Disease-Associated Mutant tRNA Synthetases Linked to Altered Dimer Interface and Neurite Distribution Defect. *Proc. Natl. Acad. Sci.* **2007**, *104,* 11239.

20. t Hart, L. M.; Hansen, T.; Rietveld, I.; Dekker, J. M.; Nijpels, G.; Janssen, G. M. C.; Arp, P. A.; Uitterlinden, A. G.; Jorgensen, T.; Borch-Johnsen, K.; Pols, H. A. P.; Pedersen, O.; van Duijn, C. M.; Heine, R. J.; Maassen, J. A. Evidence that the Mitochondrial Leucyl tRNA Synthetase (LARS2) Gene Represents a Novel type 2 Diabetes Susceptibility Gene. *Diabetes* **2005**, *54,* 1892.

21. Florentz, C. Molecular Investigations on tRNAs Involved in Human Mitochondrial Disorders. *Biosci. Rep.* **2002**, *22,* 81.

22. Mathews, M. B.; Bernstein, R. M. Myositis Autoantibody Inhibits Histidyl-Transfer RNA-Synthetase- A Model for Autoimmunity *Nature* **1983**, *304,* 177.

23. Hurdle, J. G.; O'Neill, A. J.; Chopra, I. Prospects for Aminoacyl-tRNA Synthetase Inhibitors as New Antimicrobial Agents. *Antimicrob. Agents Chemother.* **2005**, *49,* 4821.

24. Brown, M. J. B.; Mensah, L. M.; Doyle, M. L.; Broom, N. J. P.; Osbourne, N.; Forrest, A. K.; Richardson, C. M.; O'Hanlon, P. J.; Pope, A. J. Rational Design of Femtomolar Inhibitors of Isoleucyl tRNA Synthetase from a Binding Model for Pseudomonic Acid-A. *Biochemistry* **2000**, *39,* 6003.

25. Vondenhoff, G.; Van Aerschot, A. Aminoacyl-tRNA Synthetase Inhibitors as Potential Antibiotics. *Eur. J. Med. Chem.* **2011**, *46,* 5227.

26. Tao, J. S.; Schimmel, P. Inhibitors of Aminoacyl-tRNA Synthetases as Novel Anti-infectives. *Expert Opin. Invest. Drugs* **2000**, *9,* 1767.

27. Kron, M.; Petridis, M.; Milev, Y.; Leykam, J.; Hartlein, M. Expression, Localization and Alternative Function of Cytoplasmic Asparaginyl-tRNA Synthetase in Brugia malayi. *Mol. Biochem. Parasitol.* **2003**, *129,* 33.

28. Organization, W. H. Global Programmeto Eliminate Lymphatic Filariasis: Progress Report on Mass Drug Administration, 2010. *Weekly Epidemiological Record* **2011**, *86,* 377.

29. http://www.who.int/neglected_diseases/NTD_RoadMap_2012_Fullversion.pdf (accessed Mars 22, 2012)

30. Kron, M. A.; Kuhn, L. A.; Sanschagrin, P. C.; Hartlein, M.; Grotli, M.; Cusack, S. Strageis for Antifilarial Drug Development. *J. Parasitol.* **2003**, *89,* 226.

31. Kim, S.; Lee, S. W.; Choi, E. C.; Choi, S. Y. Aminoacyl-tRNA Synthetases and their Inhibitors as a Novel Family of Antibiotics. *Appl. Microbiol. Biotechnol.* **2003**, *61,* 278.

32. Yanagisawa, T.; Lee, J. T.; Wu, H. C.; Kawakami, M. Relationship of Protein Structure of Isoleucyl-tRNA Synthetase with Pseudomonic Acid Resistance of Escherichia coli. A Proposed Mode of Action of Pseudomonic Acid as an Inhibitor of Isoleucyl-tRNA Synthetase. *J. Biol. Chem.* **1994**, *269,* 24304.

33. Werner, R. G.; Thorpe, L. F.; Reuter, W.; Nierhaus, K. H. Indolmycin Inhibits Prokaryotic Tryptophanyl-tRNA Ligase. *Eur. J. Biochem.* **1976**, *68,* 1.

34. Kirillov, S.; Vitali, L. A.; Goldstein, B. P.; Monti, F.; Semenkov, Y.; Makhno, V.; Ripa, S.; Pon, C. L.; Gualerzi, C. O. Purpuromycin: an Antibiotic Inhibiting tRNA Aminoacylation. *RNA* **1997**, *3,* 905.

35. Ogilvie, A.; Wiebauer, K.; Kersten, W. Stringent Control of Ribonucleic-Acid Synthesis in Bacillus-subtilis Treated with Granaticin. *Biochem. J.* **1975**, *152,* 517.

36. Nass, G.; Poralla, K.; Zahner, H. Effect of the Antibiotic Borrelidin on the Regulation of Threonine Biosynthetic Enzymes in E. coli. *Biochem. Biophys. Res. Commun.* **1969**, *34,* 84.

37. Konrad, I.; Roschenthaler, R. Inhibition of Phenylalanine tRNA Synthetase from Bacillus subtilis by Ochratoxin A. *FEBS Lett.* **1977**, *83,* 341.

38. Kohno, T.; Kohda, D.; Haruki, M.; Yokoyama, S.; Miyazawa, T. Nonprotein Amino Acid Furanomycin, Unlike Isoleucine in Chemical Structure, is Changed to Isoleucine tRNA by Isoleucyl-tRNA Synthetase and Incorporated into Protein. *J. Biol. Chem.* **1990**, *265,* 6931.

39. Katagiri, K.; Tori, K.; Kimura, Y.; Yoshida, T.; Nagasaki, T.; Minato, H. A New Antibiotic. Furanomycin, an Isoleucine Antagonist. *J. Med. Chem.* **1967**, *10,* 1149.

40. Capobianco, J. O.; Zakula, D.; Coen, M. L.; Goldman, R. C. Anticandida Activity of Cispentacin - The Active-Transport by Amino-Acid Permeases and Possible Mechanisms of Action *Biochem. Biophys. Res. Commun.* **1993**, *190,* 1037.

41. Isono, K.; Uramoto, M.; Kusakabe, H.; Miyata, N.; Koyama, T.; Ubukata, M.; Sethi, S. K.; McCloskey, J. A. Ascamycin and Dealanylascamycin, Nucleoside Antibiotics from Streptomyces sp. *J. Antibiot.* **1984**, *37,* 670.

42. Ubukata, M.; Osada, H.; Isono, K. Synthesis and Biological Activity of Nucleoside Antibiotics, Ascamycin and its Amino acid Analogs. *Nucleic Acids Symp. Ser.* **1985***,* 81.

43. Farhanullah; Kim, S. Y.; Yoon, E.-J.; Choi, E.-C.; Kim, S.; Kang, T.; Samrin, F.; Puri, S.; Lee, J. Design and Synthesis of Quinolinones as Methionyl-tRNA Synthetase Inhibitors. *Bioorg. Med. Chem.* **2006**, *14,* 7154.

44. Ding, D.; Meng, Q.; Gao, G.; Zhao, Y.; Wang, Q.; Nare, B.; Jacobs, R.; Rock, F.; Alley, M. R. K.; Plattner, J. J.; Chen, G.; Li, D.; Zhou, H. Design, Synthesis, and Structure-Activity Relationship of Trypanosoma brucei Leucyl-tRNA Synthetase Inhibitors as Antitrypanosomal Agents. *J. Med. Chem.* **2011**, *54,* 1276.

45. Xiao, Z.-P.; He, X.-B.; Peng, Z.-Y.; Xiong, T.-J.; Peng, J.; Chen, L.-H.; Zhu, H.-L. Synthesis, Structure, Molecular Docking, and Structure-Activity Relationship Analysis of Enamines: 3-Aryl-4-alkylaminofuran-2(5H)-ones as Potential Antibacterials. *Bioorg. Med. Chem.* **2011**, *19,* 1571.

46. Van de Vijver, P.; Ostrowski, T.; Sproat, B.; Goebels, J.; Rutgeerts, O.; Van Aerschot, A.; Waer, M.; Herdewijn, P. Aminoacyl-tRNA Synthetase Inhibitors as Potent and Synergistic Immunosuppressants. *J. Med. Chem.* **2008**, *51,* 3020.

47. Bernier, S.; Akochy, P.-M.; Lapointe, J.; Chenevert, R. Synthesis and Aminoacyl-*t*RNA Synthetase Inhibitory Activity of Aspartyl Adenylate Analogs. *Bioorg. Med. Chem.* **2004**, *13,* 69.

48. Lee, J.; Kim, S. E.; Lee, J. Y.; Kim, S. Y.; Kang, S. U.; Seo, S. H.; Chun, M. W.; Kang, T.; Choi, S. Y.; Kim, H. O. N-Alkoxysulfamide, N-Hydroxysulfamide, and Sulfamate Analogues of Methionyl and Isoleucyl Adenylates as Inhibitors of Methionyl-tRNA and Isoleucyl-tRNA Synthetases. *Bioorg. Med. Chem. Lett.* **2003**, *13,* 1087.

49. Rye, C. S.; Baell, J. B. Phosphate Isosteres in Medicinal Chemistry. *Curr. Med. Chem.* **2005**, *12,* 3127.

50. Kotoris, C. C.; Chen, M. J.; Taylor, S. D. Novel Phosphate Mimetics for the Design of Non-Peptidyl Inhibitors of Protein Tyrosine Phosphatases. *Bioorg. Med. Chem. Lett.* **1998**, *8,* 3275.

51. Meanwell, N. A. Synopsis of Some Recent Tactical Application of Bioisosteres in Drug Design. *J. Med. Chem.* **2011**, *54,* 2529.

52. Moriguchi, T.; Yanagi, T.; Wada, T.; Sekine, M. Synthesis of New Aminoacyl-Adenylate Analogs having an *N*-Acyl Phosphoramidate Linkage. *Tetrahedron Lett.* **1998**, *39,* 3725.

53. Forrest, A. K.; Jarvest, R. L.; Mensah, L. M.; O'Hanlon, P. J.; Pope, A. J.; Sheppard, R. J. Aminoalkyl Adenylate and Aminoacyl Sulfamate Intermediate Analogues Differing Greatly in Affinity for their Cognate Staphylococcus aureus Aminoacyl tRNA Synthetases. *Bioorg. Med. Chem. Lett.* **2000**, *10,* 1871.

54. Moriguchi, T.; Yanagi, T.; Kunimori, M.; Weda, T.; Sekine, M. Synthesis and Properties of Aminoacylamido-AMP: Chemical Optimization for the Construction of an N-Acyl Phosphoramidate Linkage. *J. Org. Chem.* **2000**, *65,* 8229.

55. Greene, T. X.; Wuts, P. G. M. *Protective Groups in Organic Synthesis*; 3rd ed.; John Wiley & Sons, Inc.: New York, 1999.

56. Carey, F. A.; Sundberg, R. J. *Advanced Organic Chemistry Part B: Reactions and Synthesis*; 3rd ed.; Plenum Press: New York, 1990.

57. Isidro-Llobet, A.; Alvarez, M.; Albericio, F. Amino Acid-Protecting Groups. *Chem. Rev.* **2009**, *109,* 2455.

58. Greenberg, A. *The Amide Linkage: Structural Significance in Chemistry, Biochemistry, and Materials Science*; Wiley-Interscience: New Jersey, 2000.

59. Pattabiraman, V. R.; Bode, J. W. Rethinking Amide Bond Synthesis. *Nature* **2011**, *480,* 471.

60. Montalbetti, C.; Falque, V. Amide Bond Formation and Peptide Coupling. *Tetrahedron* **2005**, *61,* 10827.

61. Valeur, E.; Bradley, M. Amide Bond Formation: Beyond the Myth of Coupling Reagents. *Chem. Soc. Rev.* **2009**, *38,* 606.

62. Roughley, S. D.; Jordan, A. M. The Medicinal Chemist's Toolbox: An Analysis of Reactions used in the Pursuit of Drug Candidates. *J. Med. Chem.* **2011**, *54,* 3451.

63. Clayden, J.; Greeves, N.; Warren, S. *Organic Chemistry*; Oxford University Press: Bristol, 2001.

64. Han, S. Y.; Kim, Y. A. Recent Development of Peptide Coupling Reagents in Organic Synthesis. *Tetrahedron* **2004**, *60,* 2447.

65. Joullie, M. M.; Lassen, K. M. Evolution of Amide Bond Formation. *Arkivoc* **2010**, *viii,* 189.

66. Humphrey, J. M.; Chamberlin, A. R. Chemical Synthesis of Natural Product Peptides: Coupling Methods for the Incorporation of Noncoded Amino Acids into Peptides. *Chem. Rev.* **1997**, *97,* 2243.

67. Sheehan, J. C.; Hess, G. P. A New Method of Forming Peptide Bonds. *J. Am. Chem. Soc.* **1955**, *77,* 1067.

68. Woodman, E. K.; Chaffey, J. G. K.; Hopes, P. A.; Hose, D. R. J.; Gilday, J. P. *N,N* '-Carbonyldiimidazole-Mediated Amide Coupling: Significant Rate Enhancement Achieved by Acid Catalysis with Imidazole center dot HCl. *Org. Process Res. Dev.* **2009**, *13,* 106.

69. Konig, W.; Geiger, R. A New Method for Synthesis of Peptides: Activation of the Carboxyl Group with Dicyclohexylcarbodiimide using 1-Hydroxybenzotriazoles as Additives. *Chem. Ber.* **1970**, *103,* 788.

70. Konig, W.; Geiger, R. Racemization in Peptide Syntheses. *Chem. Ber.* **1970**, *103,* 2024.

71. Carpino, L. A. 1-Hydroxy-7-Azabenzotriazole - An Efficient Peptide Coupling Additive *J. Am. Chem. Soc.* **1993**, *115,* 4397.

72. Carpino, L. A.; Elfaham, A.; Albericio, F. Racemization Studies During Solid-Phae Peptide-Synthesis Using Azabenzotriazole-Based Coupling Reagents *Tetrahedron Lett.* **1994**, *35,* 2279.

73. Albericio, F.; Bofill, J. M.; El-Faham, A.; Kates, S. A. Use of Onium Salt-Based Coupling Reagents in Peptide Synthesis. *J. Org. Chem.* **1998**, *63,* 9678.

74. Merrifield, R. B. Solid Phase Peptide Synthesis 1. Synthesis of a Tetrapeptide. *J. Am. Chem. Soc.* **1963**, *85,* 2149.

75. Bunin, B. A.; Ellman, J. A. A General and Expedient Method for the Solid-Phase Synthesis of 1,4-Benzodiazepine Derivatives. *J. Am. Chem. Soc.* **1992**, *114,* 10997.

76. Guillier, F.; Orain, D.; Bradley, M. Linkers and Cleavage Strategies in Solid-Phase Organic Synthesis and Combinatorial Chemistry. *Chem. Rev.* **2000**, *100,* 2091.

77. Gordon, K.; Balasubramanian, S. Solid Phase Synthesis - Designer Linkers for Combinatorial Chemistry: a Review. *J. Chem. Technol. Biotechnol.* **1999**, *74,* 835.

78. Ley, S. V.; Baxendale, I. R.; Brusotti, G.; Caldarelli, M.; Massi, A.; Nesi, M. Solid-Supported Reagents for Multi-step Organic Synthesis: Preparation and Application. *Farmaco* **2002**, *57,* 321.

79. Scicinski, J. J.; Congreveb, M. S.; Kay, C.; Ley, S. V. Analytical Techniques for Small Molecule Solid Phase Synthesis. *Curr. Med. Chem.* **2002**, *9,* 2103.

80. Hodge, P. C.; Sherrington, D. C. *Polymer-Supported Reactions in Organic Chemistry*; Wiley-Interscience: Chichester, 1988.

81. Meldal, M. *Solid-Phase Peptide Synthesis*; Academic Press: New York, 1997.

82. Bayer, E. Towards the Chemical Synthesis of Proteins. *Angew. Chem., Int. Ed. Engl.* **1991**, *30,* 113.

83. Meldal, M. PEGA - A Flow Stable Polyethylene-Glycol Dimethyl Acrylamide Copolymer for Solid-Phase Synthesis *Tetrahedron Lett.* **1992**, *33,* 3077.

84. Renil, M.; Meldal, M. POEPOP and POEPS: Inert Polyethylene Glycol Crosslinked Polymeric Supports for Solid Synthesis. *Tetrahedron Lett.* **1996**, *37,* 6185.
85. Rademann, J.; Grotli, M.; Meldal, M.; Bock, K. SPOCC: a Resin for Solid-Phase Organic Chemistry and Enzymatic Reactions on Solid Phase. *J. Am. Chem. Soc.* **1999**, *121,* 5459.
86. Garcia-Martin, F.; Quintanar-Audelo, M.; Garcia-Ramos, Y.; Cruz, L. J.; Gravel, C.; Furic, R.; Cote, S.; Tulla-Puche, J.; Albericio, F. ChemMatrix, a Poly(ethylene glycol)-Based Support for the Solid-Phase Synthesis of Complex Peptides. *J. Comb. Chem.* **2006**, *8,* 213.
87. Scott, P. J. H. *Linker Strategies in Solid-Phase Organic Synthesis*; Wiley & Sons Ltd.: Chichester, 2009.
88. Bunin, B. A. *The Combinatorial Index*; Academic Press: San Francisco, 1998.
89. Manku, S.; Laplante, C.; Kopac, D.; Chan, T.; Hall, D. G. A Mild and General Solid-Phase Method for the Synthesis of Chiral Polyamines. Solution Studies on the Cleavage of Borane-Amine Intermediates from the Reduction of Secondary Amides. *J. Org. Chem.* **2001**, *66,* 874.
90. Ley, S. V.; Baxendale, I. R.; Bream, R. N.; Jackson, P. S.; Leach, A. G.; Longbottom, D. A.; Nesi, M.; Scott, J. S.; Storer, R. I.; Taylor, S. J. Multi-Step Organic Synthesis using Solid-Supported Reagents and Scavengers: a New Paradigm in Chemical Library Generation. *J. Chem. Soc., Perkin Trans. 1* **2000**, 3815.
91. Cano, M.; Ladlow, M.; Balasubramanian, S. Practical Synthesis of a Dithiane-Protected 3',5'-Dialkoxybenzoin Photolabile Safety-Catch Linker for Solid-Phase Organic Synthesis. *J. Org. Chem.* **2002**, *67,* 129.
92. Berthet-Colominas, C.; Seignovert, L.; Hartlein, M.; Grotli, M.; Cusack, S.; Leberman, R. The Crystal Structure of Asparaginyl-tRNA Synthetase from Thermus thermophilus and its Complexes with ATP and Asparaginyl-Adenylate: the Mechanism of Discrimination between Asparagine and Aspartic Acid. *EMBO J.* **1998**, *17,* 2947.
93. Dock-Bregeon, A. C.; Sankaranarayanan, R.; Romby, P.; Caillet, J.; Springer, M.; Rees, B.; Francklyn, C. S.; Ehresmann, C.; Moras, D. Transfer RNA-mediated Editing in Threonyl-tRNA Synthetase: The class II Solution to the Double Discrimination Problem. *Cell* **2000**, *103,* 877.
94. Sankaranarayanan, R.; Dock-Bregeon, A. C.; Rees, B.; Bovee, M.; Caillet, J.; Romby, P.; Francklyn, C. S.; Moras, D. Zinc Ion Mediated Amino Acid Discrimination by Threonyl-tRNA Synthetase. *Nat. Struct. Biol.* **2000**, *7,* 461.
95. Lincecum, T. L.; Tukalo, M.; Yaremchuk, A.; Mursinna, R. S.; Williams, A. M.; Sproat, B. S.; Van Den Eynde, W.; Link, A.; Van Calenbergh, S.; Grotli, M.; Martinis, S. A.; Cusack, S. Structural and Mechanistic Basis of Pre- and Posttransfer Editing by Leucyl-tRNA Synthetase. *Mol. Cell* **2003**, *11,* 951.
96. Sukuru, S. C. K.; Crepin, T.; Milev, Y.; Marsh, L. C.; Hill, J. B.; Anderson, R. J.; Morris, J. C.; Rohatgi, A.; O'Mahony, G.; Grotli, M.; Danel, F.; Page, M. G. P.; Hartlein, M.; Cusack, S.; Kron, M. A.; Kuhn, L. A. Discovering New Classes of Brugia Malayi Asparaginyl-tRNA Synthetase Inhibitors and Relating Specificity to Conformational Change. *J. Comput.-Aided Mol. Des.* **2006**, *20,* 159.
97. Brown, P.; Richardson, C. M.; Mensah, L. M.; O'Hanlon, P. J.; Osborne, N. F.; Pope, A. J.; Walker, G. Molecular Recognition of Tyrosinyl Adenylate Analogues by Prokaryotic Tyrosyl tRNA Synthetases. *Bioorg. Med. Chem.* **1999**, *7,* 2473.
98. Bernier, S.; Dubois, D. Y.; Therrien, M.; Lapointe, J.; Chenevert, R. Synthesis of Glutaminyl Adenylate Analogues that are Inhibitors of Glutaminyl-tRNA Synthetase. *Bioorg. Med. Chem. Lett.* **2000**, *10,* 2441.
99. Lee, J.; Kang, S. U.; Kang, M. K.; Chun, M. W.; Jo, Y. J.; Kwak, J. H.; Kim, S. Methionyl Adenylate Analogues as Inhibitors of Methionyl-tRNA Synthetase. *Bioorg. Med. Chem. Lett.* **1999**, *9,* 1365.
100. Lee, J.; Kang, S. U.; Kim, S. Y.; Kim, S. E.; Kang, M. K.; Jo, Y. J.; Kim, S. Ester and Hydroxamate Analogues of Methionyl and Isoleucyl Adenylates as Inhibitors of Methionyl-tRNA and Isoleucyl-tRNA Synthetases. *Bioorg. Med. Chem. Lett.* **2001**, *11,* 961.
101. Lee, J.; Kang, S. U.; Kim, S. Y.; Kim, S. E.; Jo, Y. J.; Kim, S. Vanilloid and Isovanilloid Analogues as Inhibitors of Methionyl-tRNA and Isoleucyl-tRNA Synthetases. *Bioorg. Med. Chem. Lett.* **2001**, *11,* 965.
102. Ueda, H.; Shoku, Y.; Hayashi, N.; Mitsunaga, J.; In, Y.; Doi, M.; Inoue, M.; Ishida, T. X-Ray Crystallographic Conformational Study of 5'-*O*- *N*-(L-Alanyl)-Sulfamoyl Adenosine, a Substrate-Analog for Alanyl Transfer-RNA Synthetase. *Biochim. Biophys. Acta* **1991**, *1080,* 126.
103. Heacock, D.; Forsyth, C. J.; Shiba, K.; Musier-Forsyth, K. Synthesis and Aminoacyl-tRNA Synthetase Inhibitory Activity of Prolyl Adenylate Analogs. *Bioorg. Chem.* **1996**, *24,* 273.
104. Belrhali, H.; Yaremchuk, A.; Tukalo, M.; Larsen, K.; Berthetcolominas, C.; Leberman, R.; Beijer, B.; Sproat, B.; Alsnielsen, J.; Grubel, G.; Legrand, J. F.; Lehmann, M.; Cusack, S. Crystal-Structures at 2.5 Ångstrom Resolution-RNA Synthetase Complexed 2 Analogs of Seryl Adenylate. *Science* **1994**, *263,* 1432.
105. Castro-Pichel, J.; Garcia-Lopez, M. T.; De las Heras, F. G. A Facile Synthesis of Ascamycin and Related Analogs. *Tetrahedron* **1987**, *43,* 383.
106. Tuck, K. L.; Saldanha, S. A.; Birch, L. M.; Smith, A. G.; Abell, C. The Design and Synthesis of Inhibitors of Pantothenate Synthetase. *Org. Biomol. Chem.* **2006**, *4,* 3598.

107. Somu, R. V.; Boshoff, H.; Qiao, C.; Bennett, E. M.; Barry, C. E., III; Aldrich, C. C. Rationally Designed Nucleoside Antibiotics that Inhibit Siderophore Biosynthesis of Mycobacterium tuberculosis. *J. Med. Chem.* **2006**, *49,* 31.

108. Vaughan, M. D.; Sampson, P. B.; Daub, E.; Honek, J. F. Investigation of Bioisosteric Effects on the Interaction of Substrates/Inhibitors with the Methionyl-tRNA Synthetase from Escherichia coli. *Med. Chem.* **2005**, *1,* 227.

109. Peterson, E. M.; Brownell, J.; Vince, R. Synthesis and Biological Evaluation of 5'-Sulfamoylated Purinyl Carbocyclic Nucleosides. *J. Med. Chem.* **1992**, *35,* 3991.

110. Jakubowski, H. Aminoacyl Thioester Chemistry of Class II Aminoacyl-tRNA Synthetases. *Biochemistry* **1997**, *36,* 11077.

111. Ogilvie, K. K.; Beaucage, S. L.; Schifman, A. L.; Theriault, N. Y.; Sadana, K. L. The Synthesis of Digoribonucleotides II. The use of Silyl Protecting Groups in Nucleoside and Nucleotide Chemistry VII. *Can. J. Chem.* **1978**, *56,* 2768.

112. Johansson, R.; Samuelsson, B. Regioselective Reductive Ring-Openinf of 4-Methoxybenzylidene Acetals of Hexopyranosides - Acces to a Novel Protecting-Group Strategy .1. *J. Chem. Soc., Perkin Trans. 1* **1984**, 2371.

113. Baggett, N.; Foster, A. B.; Webber, J. M.; Lipkin, D.; Phillips, B. E. 2,3-*O*-Benzylidene Nucleosides. *Chem. Ind.* **1965**, 136.

114. Watkins, B. E.; Kiely, J. S.; Rapoport, H. Synthesis of Oligodeoxyribonucleotides using *N*-Benzyloxycarbonyl-Blocked Nucleosides. *J. Am. Chem. Soc.* **1982**, *104,* 5702.

115. Watkins, B. E.; Rapoport, H. Synthesis of Benzyl and Benzyloxycarbonyl Base-Blocked 2'-Deoxyribonucleosides. *J. Org. Chem.* **1982**, *47,* 4471.

116. Saha, A. K.; Schultz, P.; Rapoport, H. 1,1'-Carbonylbis(3-Methylimidazolium) Trifalte - An Efficient Reagent for Aminoacylations. *J. Am. Chem. Soc.* **1989**, *111,* 4856.

117. Fujii, N.; Nakai, K.; Habashita, H.; Hotta, Y.; Tamamura, H.; Otaka, A.; Ibuka, T. Synthesis of Optically Pure 2-Aziridinemethanols - Versatile Synthetic Building-Blocks. *Chem. Pharm. Bull.* **1994**, *42,* 2241.

118. Lagisetti, C.; Urbansky, M.; Coates, R. M. The Dioxanone Approach to (*2S,3R*)-2-*C*-Methylerythritol 4-Phosphate and 2,4-Cyclodiphosphate, and Various MEP Analogues. *J. Org. Chem.* **2007**, *72,* 9886.

119. Castro-Pichel, J.; Garcia-Lopez, M. T.; De las Heras, F. G.; Herranz, R.; Perez, C.; Vilas, P. Synthesis and Antiviral Activity of 5'-*O*-(Substituted) Sulfamoylpyrimidine Nucleosides. *Arch. Pharm. (Weinheim, Ger.)* **1989**, *322,* 11.

120. Shuman, D. A.; Robins, M. J.; Robins, R. K. Synthesis of Nucleoside Sulfamates Related to Nucleocidin. *J. Am. Chem. Soc.* **1970**, *92,* 3434.

121. Okada, M.; Iwashita, S.; Koizumi, N. Efficient General Method for Sulfamoylation of a Hydroxyl Group. *Tetrahedron Lett.* **2000**, *41,* 7047.

122. Schwarz, S.; Thieme, I.; Richter, M.; Undeutsch, B.; Henkel, H.; Elger, W. Synthesis of Estrogen Sulfamates: Compounds with a Novel Endocrinological Profile. *Steroids* **1996**, *61,* 710.

123. Farrera-Sinfreu, J.; Albericio, F.; Royo, M. Solid-Phase Synthesis of Sulfamate Peptidomimetics. *J. Comb. Chem.* **2007**, *9,* 501.

124. Jenkins, I. D.; Verheyden, J. P. H.; Moffatt, J. G. 4'-Substituted Nucleosides 2. Synthesis of Nucleoside Antibiotic Nucleocidin. *J. Am. Chem. Soc.* **1976**, *98,* 3346.

125. Scriven, E. F. V. 4-Dialkylaminopyridines: Super Acylation and Alkylation Catalysts. *Chem. Soc. Rev.* **1983**, *12,* 129.

126. Katritzky, A. R.; Burton, R. D.; Shipkova, P. A.; Qi, M. N.; Watson, C. H.; Eyler, J. R. Collisionally Activated Dissociation of *N*-Acylpyridinium Cations. *J. Chem. Soc., Perkin Trans. 2* **1998**, 835.

127. Guibe-Jampel, E.; Wakselman, M.; Raulais, D. Tosylation and Dansylation of Tyrosine Residues of Proteins with 1-Arylsulphonyl-4-Dimethylaminopyridinium Salts. *J. Chem. Soc., Chem. Commun.* **1980**, 993.

128. Winum, J. Y.; Toupet, L.; Barragan, V.; Dewynter, G.; Montero, J. L. N-(*tert*-Butoxycarbonyl)-*N*- 4-(dimethylazaniumylidene)-1,4-dihydropyridin-1-ylsulfonyl azanide: a New Sulfamoylating Agent. Structure and Reactivity Toward Amines. *Org. Lett.* **2001**, *3,* 2241.

129. Mutulis, F.; Erdelyi, M.; Mutule, I.; Kreicberga, J.; Yahorava, S.; Yahorau, A.; Borisova-Jan, L.; Wikberg, J. E. S. 2-(*p*-Hydroxybenzyl)indoles - Side Products Formed Upon Cleavage of Indole Derivatives from Carboxylated Wang Polymer - an NMR Study. *Molecules* **2003**, *8,* 728.

130. Filira, F.; Biondi, L.; Gobbo, M.; Rocchi, R. N-Alkylation of Amino-Acids during Hydrogenolytic Deprotection. *Tetrahedron Lett.* **1991**, *32,* 7463.

131. Van de Vijver, P.; Vondenhoff, G. H.; Denivelle, S.; Rozenski, J.; Verhaegen, J.; Van Aerschot, A.; Herdewijn, P. Antibacterial 5'-O-(N-dipeptidyl)-sulfamoyladenosines. *Bioorg. Med. Chem.* **2009**, *17,* 260.

132. Arora, P.; Goyal, A.; Natarajan, V. T.; Rajakumara, E.; Verma, P.; Gupta, R.; Yousuf, M.; Trivedi, O. A.; Mohanty, D.; Tyagi, A.; Sankaranarayanan, R.; Gokhale, R. S. Mechanistic and Functional Insights Into Fatty Acid Activation in Mycobacterium tuberculosis. *Nat. Chem. Biol.* **2009**, *5,* 166.

133. Qiao, C.; Gupte, A.; Boshoff, H. I.; Wilson, D. J.; Bennett, E. M.; Somu, R. V.; Barry, C. E., III; Aldrich, C. C. 5'-*O*-[(*N*-Acyl)sulfamoyl]adenosines as Antitubercular Agents that Inhibit MbtA: an Adenylation Enzyme Required for Siderophore Biosynthesis of the Mycobactins. *J. Med. Chem.* **2007**, *50,* 6080.

134. Dal Cin, M.; Davalli, S.; Marchioro, C.; Passarini, M.; Perini, O.; Provera, S.; Zaramella, A. Analytical Methods for the Monitoring of Solid Phase Organic Synthesis. *Farmaco* **2002**, *57,* 497.

135. Kaiser, E.; Colescot, R. l.; Bossinge, C. D.; Cook, P. I. Color Test for Detection of Free Terminal Amino Groups in Solid-Phase Synthesis of Peptides. *Anal. Biochem.* **1970**, *34,* 595.

136. Ellman, G. L. Tissue Sulfhydryl Groups. *Arch. Biochem. Biophys.* **1959**, *82,* 70.

137. Yan, B.; Jewell, C. F.; Myers, S. W. Quantitatively Monitoring of Solid-Phase Organic Synthesis by Combustion Elemental Analysis. *Tetrahedron* **1998**, *54,* 11755.

138. Harris, D. C. *Quantitative Chemical Analysis*; 6th ed.; W. H. Freeman & Company: New York, 2003.

139. Epple, R.; Kudirka, R.; Greenberg, W. A. Solid-Phase Synthesis of Nucleoside Analogues. *J. Comb. Chem.* **2003**, *5,* 292.

140. Blank, H. U.; Frahne, D.; Myles, A.; Pfleiderer, W. Nucleosides. IV. Tritylation and Benzylation of Adenosine Derivatives. *Justus Liebigs Ann Chem* **1970**, *742,* 34.

141. Leach, A. R. *Molecular Modeling Principles and Applications*; 2nd ed.; Pearson Education Limited: Harlow, 2001.

142. Kitchen, D. B.; Decornez, H.; Furr, J. R.; Bajorath, J. Docking and Scoring in Virtual Screening for Drug Discovery: Methods and Applications. *Nat. Rev. Drug Discov.* **2004**, *3,* 935.

143. Bissantz, C.; Kuhn, B.; Stahl, M. A Medicinal Chemist's Guide to Molecular Interactions. *J. Med. Chem.* **2010**, *53,* 5061.

144. Nadendla, R. R. Molecular Modeling: a Powerful Fool for Drug Design and Molecular Docking. *Resonance* **2004**, *9,* 51.

145. http://www.rcsb.org/pdb/explore/explore.do?structureId=1E1T (accessed Mars 22, 2012)

146. http://www.rcsb.org/pdb/explore/explore.do?structureId=1FYF (accessed Mars 22, 2012)

147. Goodman, J. M.; Still, W. C. An Unbounded Systematic Search of Conformational Space *J. Comput. Chem.* **1991**, *12,* 1110.

148. Jorgensen, W. L.; Tiradorives, J. The OPLS Potential Functions for Proteins- Energy Minimizations for Crystals of Cyclic-Peptides and Crambin. *J. Am. Chem. Soc.* **1988**, *110,* 1657.

149. Bostrom, J.; Norrby, P. O.; Liljefors, T. Conformational Energy Penalties of Protein-bound Ligands. *J Comput Aided Mol Des* **1998**, *12,* 383.

150. Sekine, M.; Okada, K.; Seio, K.; Kakeya, H.; Osada, H.; Sasaki, T. Structure-Activity Relationship of Phosmidosine: Importance of the 7,8-Dihydro-8-Oxoadenosine Residue for Antitumor Activity. *Bioorg. Med. Chem.* **2004**, *12,* 5193.

151. Metlitskaya, A.; Kazakov, T.; Kommer, A.; Pavlova, O.; Praetorius-Ibba, M.; Ibba, M.; Krasheninnikov, I.; Kolb, V.; Khmel, I.; Severinov, K. Aspartyl-tRNA Synthetase is the Target of Peptide Nucleotide Antibiotic Microcin C. *J. Biol. Chem.* **2006**, *281,* 18033.

152. Ding, Y.; Wang, J.; Schuster, S. M.; Richards, N. G. A Concise Synthesis of Beta-Asparaginyladenylate. *J. Org. Chem.* **2002**, *67,* 4372.

153. Natchev, I. A. Organophosphorous Analogs and Derivatives of Nucleotides.1. Phosphono and Methylphosphino Analogs of Aminoacyl-5'-Adenylic Acid. *Tetrahedron* **1988**, *44,* 6455.

154. Balg, C.; Blais, S. P.; Bernier, S.; Huot, J. L.; Couture, M.; Lapointe, J.; Chenevert, R. Synthesis of Beta-Ketophosphonate Analogs of Glutamyl and Glutaminyl Adenylate, and Selective Inhibition of the Corresponding Bacterial Aminoacyl-tRNA Synthetases. *Bioorg. Med. Chem.* **2007**, *15,* 295.

155. Hampton, A.; Slotin, L. A.; Kappler, F.; Sasaki, T.; Perini, F. Design of Substrate-Site-Directed Inhibitors of Adenylate Kinase and Hexokinase. Effect of Substrate Substituents on Affinity for the Adenine Nucleotide Sites. *J. Med. Chem.* **1976**, *19,* 1371.

156. Hai, T. T.; Picker, D.; Abo, M.; Hampton, A. Species- or Isozyme-Specific Enzyme Inhibitors. 7. Selective Effects in Inhibitions of Rat Adenylate Kinase Isozymes by Adenosine 5'-Phosphate Derivatives. *J. Med. Chem.* **1982**, *25,* 806.

157. Klein, M.; Diner, P.; Dorin-Semblat, D.; Doerig, C.; Grotli, M. Synthesis of 3-(1,2,3-Triazol-1-yl)- and 3-(1,2,3-Triazol-4-yl)-Substituted Pyrazolo[3,4-d]pyrimidin-4-amines via Click Chemistry: Potential Inhibitors of the Plasmodium falciparum PfPK7 Protein Kinase. *Org. Biomol. Chem.* **2009**, *7,* 3421.

158. Klein, M.; Morillas, M.; Vendrell, A.; Brive, L.; Gebbia, M.; Wallace, I. M.; Giaever, G.; Nislow, C.; Posas, F.; Grotli, M. Design, Synthesis and Characterization of a highly Effective Inhibitor for Analog-Sensitive (as) Kinases. *PLoS One* **2011**, *6,* e20789.

159. Erion, M. D.; Dang, Q.; Reddy, M. R.; Kasibhatla, S. R.; Huang, J.; Lipscomb, W. N.; van Poelje, P. D. Structure-Guided Design of AMP Mimics that Inhibit Fuctose-1,6-bisphosphatase with High Affinity and Specificity. *J. Am. Chem. Soc.* **2007**, *129,* 15480.

160. XP docking in Glide version 5.5, Schrödinger, LLC, New York, 2009

161. http://www.rcsb.org/pdb/explore/explore.do?structureId=1H3N (accessed Mars 22, 2012)

162. Dyrager, C.; Borjesson, K.; Diner, P.; Elf, A.; Albinsson, B.; Wilhelmsson, L. M.; Grotli, M. Synthesis and Photophysical Characterisation of Fluorescent 8-(1H-1,2,3-Triazol-4-yl)adenosine Derivatives. *Eur. J. Org. Chem.* **2009***,* 1515.

163. Dierckx, A.; Diner, P.; El-Sagheer, A. H.; Kumar, J. D.; Brown, T.; Grotli, M.; Wilhelmsson, L. M. Characterization of Photophysical and Base-Mimicking Properties of a Novel Fluorescent Adenine Analogue in DNA. *Nucleic Acids Res.* **2011**, *39,* 4513.

164. Zhang, L.; Fan, J.; Vu, K.; Hong, K.; Le Brazidec, J. Y.; Shi, J.; Biamonte, M.; Busch, D. J.; Lough, R. E.; Grecko, R.; Ran, Y.; Sensintaffar, J. L.; Kamal, A.; Lundgren, K.; Burrows, F. J.; Mansfield, R.; Timony, G. A.; Ulm, E. H.; Kasibhatla, S. R.; Boehm, M. F. 7'-Substituted Benzothiazolothio- and Pyridinothiazolothio-Purines as Potent Heat Shock Protein 90 Inhibitors. *J. Med. Chem.* **2006**, *49,* 5352.

165. Minetti, P.; Tinti, M. O.; Carminati, P.; Castorina, M.; Di Cesare, M. A.; Di Serio, S.; Gallo, G.; Ghirardi, O.; Giorgi, F.; Giorgi, L.; Piersanti, G.; Bartoccini, F.; Tarzia, G. 2-n-Butyl-9-methyl-8-[1,2,3]triazol-2-yl-9H-purin-6-ylamine and Analogues as A2A Adenosine Receptor Antagonists. Design, Synthesis, and Pharmacological Characterization. *J. Med. Chem.* **2005**, *48,* 6887.

166. Ke, D.; Zhan, C.; Li, X.; Li, A. D. Q.; Yao, J. A Simple Synthesis of Imide-Dipeptides. *Synlett* **2009***,* 1506.

167. Tran, D. N.; Blaszkiewicz, C.; Menuel, S.; Roucoux, A.; Philippot, K.; Hapiot, F.; Monflier, E. Using Click Chemistry to Access Mono- and Ditopic Beta-Cyclodextrin Hosts Substituted by Chiral Amino Acids. *Carbohydr. Res.* **2011**, *346,* 210.

168. Neres, J.; Labello, N. P.; Somu, R. V.; Boshoff, H. I.; Wilson, D. J.; Vannada, J.; Chen, L.; Barry, C. E.; Bennett, E. M.; Aldrich, C. C. Inhibition of Siderophore Biosynthesis in Mycobacterium tuberculosis with Nucleoside Bisubstrate Analogues: Structure-Activity Relationships of the Nucleobase Domain of 5'-O-[N-(salicyl)sulfamoyl]adenosine. *J. Med. Chem.* **2008**, *51,* 5349.

169. Leavitt, S.; Freire, E. Direct Measurement of Protein Binding Energetics by Isothermal Titration Calorimetry. *Curr. Opin. Struct. Biol.* **2001**, *11,* 560.

170. Weber, P. C.; Salemme, F. R. Applications of Calorimetric Methods to Drug Discovery and the Study of Protein Interactions. *Curr. Opin. Struct. Biol.* **2003**, *13,* 115.

171. Shchepinov, M. S.; Korshun, V. A. Recent Applications of Bifunctional Trityl Groups. *Chem. Soc. Rev.* **2003**, *32,* 170.

172. Rothman, D. M.; Vazquez, M. E.; Vogel, E. M.; Imperiali, B. Caged Phospho-Amino Acid Building Blocks for Solid-Phase Peptide Synthesis. *J. Org. Chem.* **2003**, *68,* 6795.

173. Chaudhary, S. K.; Hernandez, O. A Simplified Procedure for the Preparation of Triphenylmethylethers. *Tetrahedron Lett.* **1979***,* 95.

174. Lundquist, J. T.; Satterfield, A. D.; Pelletier, J. C. Mild and Adaptable Silver Triflate-Assisted Method for Trityl Protection of Alcohols in Solution with Solid-Phase Loading Applications. *Org. Lett.* **2006**, *8,* 3915.

175. Crestey, F.; Ottesen, L. K.; Jaroszewski, J. W.; Franzyk, H. Efficient Loading of Primary Alcohols onto a Solid Phase using a Trityl Bromide Linker. *Tetrahedron Lett.* **2008**, *49,* 5890.

176. Barlos, K.; Gatos, D.; Kallitsis, I.; Papaioannou, D.; Sotiriou, P. Application of 4-Polystyryltriphenylmethyl Chloride to the Syntheses of Peptides and Amino Acid Derivatives. *Liebigs Ann. Chem.* **1988***,* 1079.

177. Fyles, T. M.; Leznoff, C. C. Use of Polymer Supports in Organic Synthesis.5. Preparation of Monoacetates of Symmetrical Diols. *Can. J. Chem.* **1976**, *54,* 935.

178. Harre, M.; Nickisch, K.; Tilstam, U. An Efficient Method for Activation and Recycling of Trityl Resins. *React. Funct. Polym.* **1999**, *41,* 111.

179. Frechet, J. M. J.; Nuyens, L. J. Use of Polymers as Protecting Groups in Organic Synthesis. 3. Selective Functionalization of Polyhodroxy Alcohols. *Can. J. Chem.* **1976**, *54,* 926.

180. Chen, C. X.; Randall, L. A. A.; Miller, R. B.; Jones, A. D.; Kurth, M. J. Analogous Organic Synthesis of Small-Compound Libraries: Validation of Combinatorial Chemistry in Small-Molecule Synthesis *J. Am. Chem. Soc.* **1994**, *116,* 2661.

181. Swain, C. G.; Okamoto, Y. Involvement of a Solute in a Transition State without Any Effect on Rate. The Role of Added Pyridine in Methanolysis of Triphenylmethyl Chloride in Benzene Solution. *J. Am. Chem. Soc.* **1970**, *92,* 3409.

182. Keck, G. E.; McLaws, M. D.; Wager, T. T. A Direct and Mild Conversion of Tertiary Aryl Amides to Methyl Esters using Trimethyloxonium Tetrafluoroborate: a Very Useful Complement to Directed Metalation Reactions. *Tetrahedron* **2000**, *56,* 9875.

183. Urban, F. J.; Anderson, B. G.; Orrill, S. L.; Daniels, P. J. Process Research and Large-Scale Synthesis of a Novel 5,6-Dihydro-(9H)-Pyrazolo 3,4-c -1,2,4-Triazolo 4,3a Pyridine PDE-IV Inhibitor. *Org. Process Res. Dev.* **2001**, *5,* 575.

184. Park, J. G.; Langenwalter, K. J.; Weinbaum, C. A.; Casey, P. J.; Pang, Y. P. Improved Loading and Cleavage Methods for Solid-Phase Synthesis using Chlorotrityl Resins: Synthesis and Testing of a Library of 144 Discrete Chemicals as Potential Farnesyltransferase Inhibitors. *J. Comb. Chem.* **2004**, *6,* 407.

185. Huszthy, P.; Lempert, K.; Simig, G.; Tamas, J. The Reduction of Triarylcarbenium Ions by Alcohols: Simple Hydride Transfer or Concerted Breakdown of Ortho-Adducts? *J. Chem. Soc., Perkin Trans. 2* **1982**, 1671.
186. http://www.schrodinger.com (accessed Mars 22, 2012)
187. Pierce, M. M.; Raman, C. S.; Nall, B. T. Isothermal Titration Calorimetry of Protein-Protein Interactions. *Methods* **1999**, *19,* 213.
188. Freyer, M. W.; Lewis, E. A. Isothermal Titration Calorimetry: Experimental Design, Data Analysis, and Probing Macromolecule/Ligand Binding and Kinetic Interactions. *Methods Cell. Biol.* **2008**, *84,* 79.